UNIVERSITY OF CALIFORNIA, SAN DIEGO

Compartmental Models of Single Cells and Small Networks in the Primary Visual Cortex

of the Cat

A dissertation submitted in partial satisfaction of the requirements for the degree Doctor

of Philosophy

in Neurosciences

by

Paul Bush

Committee in charge:

Professor Terrence J. Sejnowski, Chair

Professor Patricia S. Churchland

Professor Allen Selverston

Professor Thomas D. Albright

Professor Martin I. Sereno

1995

The dissertation of Paul Bush is approved, and it is acceptable in quality and form for

publication on microfilm:

_____

_____

_____

_____

_____

Chair

University of California, San Diego

1995

TABLE OF CONTENTS

LIST OF FIGURES AND TABLES

ACKNOWLEDGEMENTS

Firstly, I wish to thank Terry Sejnowski. He has provided me with six years of continuous support and understanding; people who know me well will appreciate this. With his vast spectrum of knowledge, extremely fast comprehension and insight combined with years of wisdom, Terry's supervision has of course been invaluable during the course of my studies.

I am also grateful to the many members of CNL both past and present. The many lab meetings, journal clubs and discussions I have had with people too numerous to mention individually have lead to direct developments of and improvements to my work, but also, and probably more importantly, the way in which I think about my work has been developed and improved by interactions with the eclectic group of people that is CNL. In addition, I would like to express my gratitude to Rosemary Miller, whose generous help over the years has contributed to making my time at the Salk enjoyable and as stress-free as possible.

Periodic discussions and collaborations with Rodney Douglas and Kevan Martin, my first mentors, have formed an integral part of my thesis work and I look forward to continuing associations in the future. I am indebted to them for advising me to come to San Diego and arranging for me to meet and work for Terry Sejnowski.

Finally, I thank Rita Venturini. Besides enriching my life over the last few years she has provided much appreciated support and encouragement when it was most needed.

VITA

January 2, 1967 Born, Birmingham, England

1988-1989   Research project for M.R.C. A.N.U., Oxford, U.K.

1989   B.A. Neurophysiology & Psychology,

                University College, Oxford, U.K.

1989-1994   Awarded Fulbright Scholarship for

                graduate study in U.S.

1989   Attended 'Methods in Computational Neuroscience'

                MBL course, Wood's Hole, MA.

1989-1995   Neurosciences graduate student, UCSD.

                Advisor: T.J. Sejnowski, Salk Institute.

1992, 1993   Teaching Assistant, Departments of Psychology

                and Biology, UCSD.

1990, 1994   Awarded McDonnell-Pew travel grants for

                research collaboration.

1995   PhD University of California, San Diego.

PUBLICATIONS

Berman, N. J., Bush, P. C. & Douglas, R. J. Adaptation and bursting in neocortical neurons may be controlled by a single fast potassium conductance. *Quarterly Journal of Experimental Physiology.* **74**: 223-226, 1989.

Bush, P. C. and Douglas, R. J. Synchronization of bursting action potential discharge in a model network of neocortical neurons. *Neural Computation.* **3:** 19-30, 1991.

Bush, P. C. and Sejnowski, T. J. Simulations of a reconstructed Cerebellar Purkinje Cell based on simplified channel kinetics. *Neural Computation.* **3:** 299-309, 1991.

Bush, P. C. and Sejnowski, T. J. Reduced compartmental models of neocortical pyramidal cells. *Journal of Neuroscience Methods*. **46**: 159-166, 1993

Bush, P. C. and Sejnowski, T. J. Effects of inhibition and dendritic saturation in simulated neocortical pyramidal cells. *Journal of Neurophysiology*. **71**:6 , 1994.

Bush, P. C. and Sejnowski, T. J. Inhibition synchronizes sparsely connected cortical neurons within and between columns in realistic network models. *Journal of Computational Neuroscience* 1995 (submitted for publication).

ABSTRACTS

Bush, P. C. & Sejnowski, T. J. Large-scale compartment model of a cerebellar Purkinje cell. *Neuroscience Abstracts.* **16**, 1298, 1990.

Bush, P. C., Li, S. & Sejnowski, T. J. Quantal analysis of superimposed EPSPs from multiple synapses. *Neuroscience Abstracts.* **17**, 385, 1991.

Bonds, A. B., Snider, R. K., Kabara. J., Bush, P. and Sejnowski, T. J. On the origins of oscillation in cells of the cat striate cortex.. ARVO. **34/4** 1032. 1993.

Bush, P. C., Gray, C. & Sejnowski, T. J. Realistic simulations of synchronization in networks of layer V neurons in cat primary visual cortex. *Neuroscience Abstracts*.: 1993

INVITED TALKS

The use of reduced compartmental models in cortical network simulations. In: Chicago Workshop on Computational Neuroscience: *Models of Thalamic and Cortical Neurons*.. 1993

BOOK CHAPTERS

Bush, P. C. & Sejnowski, T.J. Simulations of synaptic integration in neocortical pyramidal cells. In:*Computation and Neural Systems.*. Eds. F. H. Eeckman & J. M. Bower. Kluwer, Boston. 1992.

Bush, P. & Sejnowski, T. Models of Cortical Networks. In: *Normal and Pathophysiological Physiology of The Cortical Neuron*. Eds. I. Mody & M. Gutnik. Oxford Univ. Press. 1994.

ABSTRACT OF THE DISSERTATION

Compartmental Models of Single Cells and Small Networks in the Primary Visual Cortex
of the Cat

by

Paul Bush

Doctor of Philosophy in Neurosciences

University of California, San Diego, 1995

Professor Terrence J. Sejnowski, Chair

This thesis has two main themes. Firstly it documents the process of constructing realistic single cell and network models, focusing particularly on how to represent individual neurons in network models consisting of hundreds to thousands of units. In the third chapter a method of drastically reducing the number of compartments in a single cell model is presented. The method is based on conserving the axial resistance of the model neuron and not the surface area. The resulting reduced model neuron displays the same electrotonic characteristics as the original full-size model neuron while taking up a fraction of the memory and computation time. In addition the reduced model neuron retains the spatial dimensions of the full model, an important consideration when attempting to construct spatially accurate models of laminar cortical areas.

Secondly, the subject of cortical inhibition is addressed. In the last few years the perception of the role of inhibition in the neocortex has changed from that of a powerful

antagonist of non-specific excitation to that of a synergistic process helping to shape the excitatory response. The second chapter presents results from a single cell simulation of a recent experiment, showing how excitatory and inhibitory synaptic inputs interact non-linearly in a neuron's dendritic tree. It also demonstrates that while cortical inhibition may be strong enough to suppress even strongly excited cells, it does not do so in the sustained manner necessary to veto non-specific excitation.

The forth and fifth chapters show how strong inhibition can have a role in cortical dynamics when activated transiently by a synchronized burst of pyramidal cell firing. The brief but powerful inhibitory activity serves to truncate and demarcate the burst of firing in the pyramidal cell population. In this manner the inhibition is essential for producing synchronized oscillatory activity in the network. In this system inhibition is maximally active during the period that excitation is greatest, but inhibition and excitation function together rather than in opposition. In addition, the properties and characteristics of synchronized oscillatory activity both within and between cortical columns are analyzed in these chapters.

CHAPTER I

Introduction

The perspective of a computational neuroscientist

What does the neocortex do? We know the answer to this, the neocortex does 'us'. In all probability it is the part of the brain most responsible for generating what we think of as ourselves, our humanness. How does the neocortex function? What are some basic principles of cortical neuronal operation? At the fundamental level of single cells and microcircuits consisting of hundreds to thousands of cells, we really have no answers to these questions at the present time. A significant amount of work has been done at the single cell level discovering and analyzing the cable properties of neurons, characterizing the electrotonic spread of current and documenting a plethora of ligand- and voltage-gated conductances (Rall 1964; Hille 1984; McCormick 1989). The results of this work are of course essential for developing an understanding of, but do not directly address, how single cortical cells operate and what function they are performing. In part this is because it is very difficult if not impossible to determine the function and role of single cells just by studying single cells. After characterizing their basic intrinsic properties the cells must be studied in the context of the circuits that they make up. The functions and principles of

operation of single cortical cells and small networks of such cells will most likely be discovered together. Single cells have features and properties whose purposes will only become clear when considered in their appropriate roles in the network, just as networks of cells will show behaviors and exhibit phenomena that depend on particular characteristics of their component cells.

What is the best way to discover how cortex operates, the fundamental principles? A great deal of experimental work has been done on cortex; anatomy and physiology of networks as well as single cell studies. This work provides constraints within which any comprehensive understanding or theory of cortex must fit. It can also provide some clues as to how the cortex must operate; we now know that all neocortex from primary sensory to frontal 'association' cortex, from rat to human cortex, is organized along similar lines (Martin 1988). Thus, whatever the task, each area of cortex uses the same basic circuit to accomplish it - the biggest difference is the source of the inputs. The following facts are general features of all neocortex: The primary input enters the middle layers, is relayed to the upper layers and then to the deeper layers. The upper layers project to other cortical areas and the lower layers project out of cortex and back to the origin of the inputs. Most cortical neurons are excitatory and are covered in spines, they are the projection neurons of cortex. Approximately 20% of cortical neurons are inhibitory and are not very spiny, they are the interneurons. Recent work shows that the excitatory projection neurons also make significant contributions to the intrinsic circuitry of cortex, and the details of this circuitry are beginning to be mapped out (see Douglas and Martin (1990b) for review).

However, these data, synthesized into principles of organization, are not principles of function. It is unlikely that principles of function at the level of the cortical microcircuit - how a cortical column operates, beginning with its dynamics - can be divined just from consideration of the data. The main reason for this is that cortical circuitry is so complex and consists of many feedback loops. Consider, for example, the first few synapses in the

primary visual cortex of the cat, focusing just on the features that are likely to be general properties of neocortex. The spiny stellate cells in layer 4 receive a numerically small input from the thalamus, a much larger input comes from the neighboring (200 µm) layer 4 spiny stellates in the same column. The thalamic input also activates layer 4 inhibitory cells which contact the spiny stellates. The spiny stellates in turn contact the inhibitory cells, and the inhibitory cells contact each other. However, the largest input to the spiny stellates is from pyramidal cells of layer 6 which contact layer 4 spiny stellates and inhibitory neurons over a wide area (up to 1mm). These layer 6 cells also receive direct input from the thalamus and project back to the precise area from which they receive input. A portion of their dendritic tree arborises over a wide area in layer 4 (~500 µm) where it can receive inputs from spiny stellate cells, inhibitory interneurons, thalamic afferents and possibly other layer 6 cells (Ahmed et al. 1994). A consideration of this anatomy is daunting enough for someone interested in how layer 4 responds to thalamic input, but there is also the physiology to consider. Spiny stellates and layer 6 pyramids fire relatively low frequency adapting trains of action potentials while inhibitory interneurons such as those of layer 4 (clutch cells) have low thresholds and fire high frequency non-adapting trains of short duration spikes (McCormick et al. 1985). Layer 6 cells are particularly sensitive to modulatory neurotransmitters such as noradrenalin and acetylcholine which cause dramatic changes (increases) in response rates (Singer et al. 1976). These modulatory systems are not very active under the anesthetized conditions of most *in vivo* experiments. In order to understand exactly how layer 4 (the gateway to cortex) functions, all these facts must be considered together.

Consider just the case of an excitatory projection that terminates on both excitatory and inhibitory neurons in its target area, a common feature of neocortex. What is the function of this projection? Is it excitatory or inhibitory? A definitive answer cannot be given without knowing the intrinsic properties of the input and target cells as well as,

and this is crucial, the current state of the network. If the target cells are relatively hyperpolarized then the lower threshold inhibitory neurons will fire first and prevent any activity building up in the excitatory cells. If the target cells are depolarized by other synaptic activity then the excitatory cells, containing sub-threshold voltage-dependent conductances activated by depolarization, will fire in response to the input and activity will begin to build up in the target population (Hirsch and Gilbert 1991).

So the state of all of the components of the cortical circuit at any time is a major determinant of its response to input. Returning to the case of layer 4 we see that it is difficult if not impossible to say what the output will be to any input just by considering the (extremely complex) anatomy and physiology. Somehow we need to incorporate all that data and at the same time keep track of the state of all the components in the circuit as the response develops. The most effective way of doing this at present is with computer simulation. All the anatomical data and intrinsic physiological properties can be included in accurate representations of neurons and their synaptic connections. The states of every component are updated as the simulation is numerically integrated. Ideally, one can just watch the results appear - if your model is accurate you discover how layer 4 responds to input just by watching the simulation progress.

Of course in practice things are not so simple. Firstly, the simulation is completely dependent on the data put into it. There must be enough reliable data to constrain the model, if any parameters have to be estimated then it must be shown that the results of the simulation are not affected by variations in these parameters. Constraining simulations with experimental data is the biggest problem to overcome when doing realistic models of the brain. Many brains systems cannot yet be realistically modeled because sufficient data does not yet exist. Only in the last few years has sufficient data become available (and computers become powerful enough) to attempt realistic cellular models of primary visual cortex.

Secondly, the model neurons and synapses must be accurate representations of the known experimental data. Fortunately cable theory (Rall 1964) and Hodgkin Huxley voltage-dependent conductance dynamics (Hodgkin and Huxley 1952) have been proven to provide robust descriptions of single neuron synaptic integration and active responses. These systems of equations have been incorporated into a simulation package known as NEURON (Hines 1989), which through its various incarnations has been the simulator I have used for most the simulations presented in this thesis. Beyond the single neuron level there are other issues of accuracy in representation to be considered. Once such issue, forced on us by the limits of computer power, is how to represent single cells in network simulations containing hundreds or thousands of units. The large compartmental models used for single cell studies take up too much memory and run too slowly, as well as being simply to unwieldy for convenient use in network simulations. The third chapter in this thesis addresses this issue, introducing a technique to drastically reduce the complexity of compartmental neuron representations while preserving their essential electrotonic properties.

The common theme running through the other three chapters (I have to thank my supervisor, Terry Sejnowski, for steering me in this direction) is the role of inhibition in cortex. The prevalent view of the role of cortical inhibition until very recently was as a negator or veto of inappropriate, broadly tuned excitation (Martin 1988). As well as seeming intuitively quite reasonable, this theory appeared to be supported by strong experimental evidence (Sillito 1975). However, later experimental and theoretical work challenged the assumption that cortical stimulus selectivity is based on strong inhibition of inappropriate excitation (Douglas et al. 1988; Koch et al. 1990; Ferster 1986) and even suggested that inhibition in cortex is not strong enough to suppress neurons receiving strong excitatory input (Douglas and Martin 1990a). In Chapter 2 the effect and strength of inhibition is assessed in single cell simulations based on experiment. It is shown that

although strong and effective inhibition can be evoked during physiological synaptic stimulation, such inhibition must be transient and not responsible for sustained inhibition of excitatory input. Chapters 3 and 4 investigate a paradigm in which such strong, transient inhibition not only occurs but creates the characteristic network dynamics. This paradigm is synchronized oscillatory activity, a phenomenon observed in a wide range of experimental preparations (Singer 1993) and the subject of significant speculation as to its role (Crick and Koch 1990).

The work presented here is a beginning in the field of realistic modeling of cortical microcircuitry. It has involved itself in one of the fundamental principles of cortical circuitry operation; the role of inhibition. However, it is only a starting point, and even a full model of a cortical column of this type would not provide all the answers as to how a canonical cortical microcircuit functions. This is because the type of model I have worked on to date does not include learning or plasticity. Cortical circuitry is not static, the synaptic strengths and perhaps the physical connections constantly change as the cortex does its job. Once the basic properties of a cortical microcircuit have been established it is most likely that the circuit will have to be considered in the context of learning and change in order for us to be able to fully understand its function. Studying the static circuit is equivalent to studying the single cell in isolation - an essential step but it cannot lead to a comprehensive theory of cortex.

References

Ahmed, B., Anderson, J. C., Douglas, R. J., Martin, K. A. C., and Nelson, C. J. Polyneuronal innervation of spiny stellate neurons in cat visual cortex. (1994) *J. Comp. Neurol.*, **341**: 39-49.

Crick, F., and Koch, C. Towards a neurobiological theory of consciousness. (1990) *Sem. Neurosci.*, **2**: 263-275.

Douglas, R. J., and Martin, K. A. C. Control of neuronal output by inhibition at the axon initial segment. (1990a) *Neural Comp.*, **2**: 283-292.

Douglas, R. J., and Martin, K. A. C. (1990b) Neocortex. In: *Synaptic Organization of the Brain* G. Shepherd (Ed.), New York: Oxford University Press. p. 220-248.

Douglas, R. J., Martin, K. A. C., and Whitteridge, D. Selective responses of visual cortical cells do not depend on shunting inhibition. (1988) *Nature*, **332**: 642-644.

Ferster, D. Orientation selectivity of synaptic potentials in neurons of cat primary visual cortex. (1986) *J. Neurosci.*, **6**: 1284-1301.

Hille, B. (1984) Ionic Channels of Excitable Membranes. Sunderland, MA: Sinauer Associates, Inc.

Hines, M. L. A program for simulation of nerve equations with branching geometries. (1989) *Int. J. Biomed. Comp.*, **24**: 55-68.

Hirsch, J. A., and Gilbert, C. D. Synaptic physiology of horizontal connections in the cat's visual cortex. (1991) *J. Neurosci.*, **11**: 1800-1809.

Hodgkin, A. L., and Huxley, A. F. A quantitative description of membrane current and its application to conduction and excitation in nerve. (1952) *J. Physiol.*, **117**: 500-544.

Koch, C., Douglas, R., and Wehmeier, U. Visibility of synaptically induced conductance changes: theory and simulations of anatomically characterized cortical pyramidal cells. (1990) *J. Neurosci.*, **10**: 1728-1744.

Martin, K. A. C. From single cells to simple circuits in the cerebral cortex. (1988) *Q. J. Exp. Physiol.*, **73**: 637-702.

McCormick, D. A. GABA as an inhibitory neurotransmitter in human cerebral cortex. (1989) *J. Neurophysiol.*, **62**: 1018-1027.

McCormick, D. A., Connors, B. W., Lighthall, J. W., and Prince, D. A. Comparative electrophysiology of pyramidal and sparsely spiny stellate neurons of the neocortex. (1985) *J. Neurophysiol.*, **54**: 782-806.

Rall, W. (1964) Theoretical significance of dendritic trees for neuronal input-output relations. In: *Neural Theory and Modeling* R. Reiss (Ed.), Stanford: Stanford University Press. p. 73-97.

Sillito, A. M. The contribution of inhibitory mechanisms to the receptive field properties of neurones in the striate cortex of the cat. (1975) *J. Physiol.*, **250**: 305-329.

Singer, W. Synchronization of cortical activity and its putative role in information processing and learning. (1993) *Ann. Rev. Physiol.*, **55**: 349-374.

Singer, W., Tretter, F., and Cynader, M. The effect of reticular stimulation on spontaneous and evoked activity in the cat visual cortex. (1976) *Brain. Res.*, **102**: 71-90.

CHAPTER II

Effects of Inhibition and Dendritic Saturation in

Simulated Neocortical Pyramidal Cells

Summary and Conclusions

1. We have used compartmental models of reconstructed pyramidal neurons from layers 2 and 5 of cat visual cortex to investigate the nonlinear summation of excitatory synaptic input and the effectiveness of inhibitory input in countering this excitation.

2. In simulations that match the conditions of a recent experiment (Ferster & Jagadeesh, 1992), dendritic saturation was significant for physiological levels of synaptic activation: A compound excitatory postsynaptic potential (EPSP) electrically evoked during a depolarization caused by physiological synaptic activation was decreased by up to 80% compared to an EPSP evoked at rest.

3. Synaptic inhibition must be coactivated with excitation to quantitatively match the experimental results. The experimentally observed coactivation of inhibition with excitation produced additional current shunts that amplified the decrease in test EPSP amplitude. About 30% of the experimentally-observed decrease in EPSP amplitude was

caused by decreases in input resistance (R_{in}) due to synaptic conductance changes; a reduced driving force accounted for the remaining decrease.

4. The amount of inhibition was then increased by nearly an order of magnitude, to about 10% of the total number of inhibitory synapses on a typical cortical pyramidal cell. The sustained firing of this many inhibitory inputs was sufficient to completely suppress the firing of a neuron receiving strong excitatory input. However, this level of inhibition produced a very large reduction in R_{in}. Such large reductions in R_{in} have not been observed experimentally, suggesting that inhibition in cortex does not act to veto (shunt) strong, *sustained* excitatory input (of order 100 ms).

5. We propose instead that strong, *transient* activation (< 10 ms) of a neuron's inhibitory inputs, sufficient to briefly prevent firing, is used to shape the temporal structure of the cell's output spike train. Specifically, cortical inhibition may serve to synchronize the firing of groups of pyramidal cells during optimal stimulation.

Introduction

The traditional function assigned to inhibition in cortex is to oppose excitation, acting to veto or shape the response of cortical cells by negating inappropriate excitation (Koch et al., 1987). Evidence for this view was provided by blocking inhibition with bicuculine and observing a decrease in the response selectivity of cortical neurons (Sillito, 1975). However, theoretical studies (Koch et al., 1990) have shown that inhibition strong enough to veto (shunt) significant amounts of excitatory current should produce measurable decreases in R_{in} of the neuron in question. Such decreases in R_{in} have never been seen *in vivo* when cortical neurons do not respond to non-preferred stimuli (Berman et al., 1991; Douglas et al., 1988), and electrically-evoked thalamocortical EPSPs are not

reduced in amplitude during visual stimulation at the nonpreferred orientation (Ferster & Jagadeesh, 1992). These results have led to the conclusion that cortical neurons receive neither excitatory nor inhibitory input in response to non-preferred stimuli (Berman et al., 1991). This conclusion is supported by results showing that both the excitation and the inhibition that a cortical neuron receives are tuned to the preferred orientation (Ferster, 1986).

Thus it is becoming clear that the role of cortical inhibition is more complex than a veto of sustained, untuned excitation. A number of other functions for inhibition have been proposed: Recent physiological experiments using dual gratings (Bonds, 1989) have suggested that a general, non-selective inhibition acts as to normalize cortical responses. This idea receives direct anatomical support from the recent demonstration that large basket cells send (inhibitory) inputs to regions representing all orientaions, not just iso- or cross-orientations (Kisvardy & Eysel, 1993). Douglas and Martin have proposed that cortical inhibition acts to increase the threshold of target neurons and gate intracortical re-excitation (Douglas & Martin, 1992). In order to remain in a state that is sensitive to inputs, the excitation and inhibition to a cortical cell should be balanced (Bell, Mainen & Sejnowski (unpublished data)).

In order to study these issues we have simulated a recent experiment (Ferster and Jagadeesh 1992) that used *in vivo* whole cell patch recording of neocortical neurons to study interactions between synaptic inputs. We have applied a compartmental model to the data of Ferster and Jagadeesh (1992) and shown that they are consistent with nonlinear interactions occurring in dendrites between excitatory inputs alone and between excitatory and inhibitory inputs. The same model was then used to determine conditions under which inhibition can prevent the firing of a neuron receiving synaptic excitation that is strong enough to cause it to discharge at high rates, and how much R_{in} would change under these conditions. Our results, consistent with the experimental data, lead to a hypothesis in

which inhibition is strongly activated during periods of maximum excitation, yet not in a manner that causes a suppression of the firing response.

Methods

Simulations were performed using standard techniques for compartmental models of branching dendritic trees (Rall, 1964); two
digitized HRP-filled pyramidal cells from layers 2 and 5 of cat visual cortex (Koch et al., 1990) were modeled (Fig. 1), each having approximately 400 coupled cylindrical compartments containing only resistive and capacitative elements. The simulator CABLE (Hines, 1989), running on a MIPS Magnum 3000/33, required about 1 minute of computation to simulate 100 ms of real time.

Passive parameters

Appropriate values of the passive parameters (specific membrane resistance, R_m, specific membrane capacitance, C_m, and specific axial resistance, R_i) were selected: C_m for neuronal membrane has a long-established value of 1 $\mu F/cm^2$ (Jack et al., 1975). The accepted value of R_i, at least in the mammalian central nervous system, has recently been revised upwards from its traditional value of about 70 Ωcm for a number of reasons: 1) Voltage responses to brief current pulses could not be modeled accurately with a small R_i (Segev et al., 1992; Shelton, 1985; Stratford et al., 1989). 2) When modeling cerebellar Purkinje cells, a larger R_i was necessary to produce significant attenuation of action potentials as they invade the dendritic tree (Bush & Sejnowski, 1991) 3) A large R_i was needed to explain the observed somatic to dendritic input conductance ratio and steady-

state voltage attenuation of Purkinje cells (for a discussion of this issue see Shelton (1985)). The value chosen for R_i in this study was 200 Ωcm (Bernander et al., 1991; Segev et al., 1992; Shelton, 1985; Stratford et al., 1989).

Once R_i, C_m and the morphology have been fixed, the value chosen for R_m will determine R_{in}, the time constant, τ_m, and the length constant, λ, of the cell. Recent results using whole-cell patch electrodes and Cs^+-filled sharp electrodes have increased the estimate of R_m from its traditional value of 5-10 kΩcm^2 to a value of 50 to 100 kΩcm^2 (Andersen et al., 1990; Major et al., 1990; Spruston & Johnston, 1992; Staley et al., 1992), giving R_{in}'s in the range of a GΩ. However, these results were not obtained *in vivo*, where the effect of background synaptic activity is such that a neuron with a R_m of 100 kΩcm^2 and can have an effective R_{in} as low as 20 MΩ and an effective τ_m of around 20 ms when part of an active *in vivo* circuit (Bernander et al., 1991; Rapp et al., 1992). The background synaptic input decreases the effective average R_m of an *in vivo* neuron in a way that can be accurately taken into account by simply using a lower value for the effective R_m in the model (Barrett & Crill, 1974; Bernander et al., 1991; Holmes & Woody, 1989). A sample of 25 visual cortical neurons recorded using sharp electrodes *in vivo* had R_{in}'s ranging from 10 to 153 MΩ (mean 69 MΩ) (Douglas et al., 1991). Two independent measurements of visual cortical neurons recorded using whole-cell patch electrodes *in vivo* had R_{in}'s ranging from 50 to 200 MΩ (Ferster & Jagadeesh, 1992) and 50 to 150 MΩ (Pei et al., 1991). The range of R_{in} values reported by these studies are similar. Values for R_{in} of 50 to 150 MΩ are closer to values obtained from the best sharp electrode *in vitro* recordings (Tanaka et al., 1991) than to the hundreds of MΩ obtained using whole-cell clamping *in vitro*.

With a C_m of 1 μF/cm^2 and R_i of 200 Ωcm, we found that using a value of 20 kΩcm^2 for R_m produced R_{in}'s for the model layer 5 and layer 2 pyramidal cells of 45 MΩ and 110 MΩ, respectively. The layer 2 cell had a greater R_{in} because it was smaller. With

these parameters (the standard model) both model cells have a dendritic τ_m of 20 ms, which is a typical value for neocortical cells (Bernander et al., 1991).

Though we believe that these values produce an accurate model of the *in vivo* neocortical pyramidal neuron, there is still considerable controversy surrounding "correct" values for the passive parameters R_m and R_i. Consequently, all simulations were repeated using values for R_i of 70, 200 and 500 Ωcm and values for R_m of 5, 20 and 100 kΩcm^2. We focus on results obtained with the standard model (the default for all simulations), which we believe to be the most accurate fit to a functioning pyramidal cell, but we also present and discuss results obtained using the full range of values for R_m and R_i. In general we found only a quantitative, rather than a qualitative, difference between simulations using different parameter values, and none of our conclusions depend on precise values.

Synaptic conductances

EPSPs and inhibitory postsynaptic potentials (IPSPs) in our models were simulated as alpha function conductance changes with a peak amplitude of 0.5 nS and a time to peak of 1 ms. EPSPs had a reversal potential of 0 mV and IPSPs a reversal potential of -70 mV (Connors et al., 1988; McCormick, 1989). These parameters were chosen because they produced EPSPs at the soma with the same time course and amplitude as those observed experimentally (Mason et al., 1991; Thomson et al., 1988). Some simulations were done with synapses on explicitly modeled spines. In these cases we used the same 2-compartment model spine morphology as Qian and Sejnowski (1989), with spine neck dimensions 1 µm x 0.1 µm and head 0.69 µm x 0.3 µm. Trains of EPSPs or IPSPs were modeled according to a Poisson distribution with a mean frequency that is stated for each case. The resting membrane potential was -65 mV.

Active conductances

For some simulations active conductances were placed at the soma to generate adapting trains of action potentials, as observed in regular-firing cortical neurons (McCormick et al., 1985). The action potential was mediated by fast sodium and potassium conductances (g_{Na} + g_{Kd}). A high threshold calcium conductance (g_{Ca}), activated by each spike, introduced calcium into the cell. Intracellular calcium accumulated in the soma compartment and decayed exponentially to its resting value with a time constant of 20 ms (Traub et al., 1991). A slow calcium-sensitive potassium conductance (g_{Kca}) was included to produce the adaptation of firing rate. All the conductances used the Hodgkin-Huxley-like kinetics parameters developed by Borg-Graham (Borg-Graham, 1987), except for g_{Kca} which had an activation rate equal to 200 times the intracellular calcium concentration (in ms^{-1}) and a deactivation rate equal to the reciprocal of the activation rate. The implementation of our kinetic scheme follows that of Lytton and Sejnowski (1991). Briefly, each ionic current, I, was calculated from

$$I = g\ m^n\ h(V - E_r) \qquad\qquad (1)$$

where g is maximal conductance, m is the activation variable, n is the exponent, h is the inactivation variable (g_{Na} only), V is membrane potential and E_r is the reversal potential of the ion concerned. The calcium current was calculated using the Goldman-Hodgkin-Katz equation (Hille, 1984), with g_{Ca} the calcium permeability. The time- and voltage-dependent variable, m, converged on a steady state value, m_{inf}, given by

$$m_{inf} = \alpha_m/(\alpha_m + \beta_m)$$

with a time constant, t_m, given by

$$t_m = 1/(\alpha_m + \beta_m)$$

The rate constants α_m and β_m were defined by the equations

$$\alpha_m = a_0\ exp[zg(V-V_{1/2})F]/RT$$

$$\beta_m = b_0\ exp[-z(1-g)(V-V_{1/2})F]/RT$$

where F is the Faraday constant, R is the gas constant and T is temperature. The kinetics of each channel was determined by the values assigned to the parameters a_0, b_0, z, g and $V_{1/2}$. A similar set of equations governed the inactivation variable, h, and its steady state value, h_{inf}. The values of all the parameters used in the model are shown in Table 1.

Results

Dendritic saturation

Dendrites have a much higher input impedance than the soma (Rinzel & Rall, 1974); thus even single EPSPs can produce significant local depolarization and reduce the driving force on simultaneous and subsequent EPSPs on the same dendritic branch. In addition, synaptic conductances add to the resting membrane conductance of the neuron (Barrett & Crill, 1974; Bernander et al., 1991; Holmes & Woody, 1989; Rapp et al., 1992) (see Methods). This effective decrease in R_m and increase in λ also results in reduced

depolarizations for simultaneous and subsequent EPSPs. We refer to these two phenomena collectively as the dendritic saturation effect, although the term 'saturation' does not necessarily imply that the membrane is at the synaptic reversal potential or that R_m has been effectively reduced to zero.

There is some direct experimental evidence for saturation during synaptic activation under physiological conditions. Ferster and Jagadeesh (1992) have demonstrated that the size of an EPSP evoked in visual cortical cells by electrical stimulation of the LGN was reduced during depolarizations caused by visual stimulation compared to its size at the resting potential. The reduction in EPSP size was proportional to the somatic depolarization caused by the visual stimulation. Thus, an EPSP that peaked at about 6 mV at rest was reduced to less than 1 mV when the cell was depolarized from a resting potential of -60 mV to a potential of -40 mV by visual stimulation (Fig. 3a) (Ferster & Jagadeesh, 1992).

Ferster and Jagadeesh interpreted their results as evidence that the synaptic sites (dendrites) were significantly more depolarized than the soma during synaptic activation of the cell, thus producing saturation by the process described above. We have tested this hypothesis by simulating their experiment, and the results are shown in Figs. 2 and 3. The model layer 2 pyramidal cell was used because its morphology (Fig. 1) is reasonably close to that of the putative layer 4 spiny stellate cells that Ferster and Jagadeesh studied. A constant current of -0.1 nA was injected starting at 30 ms to prevent firing during the synaptic activation, as in the experiments of Ferster and Jagadeesh. Visual stimulation was simulated by 70 excitatory synapses placed randomly on the basal/oblique dendrites, activated by a Poisson process at some mean frequency (for example, 50Hz) starting at 80 ms. 35 additional excitatory synapses were placed on the same dendritic segments as the initial 70, and were given a single simultaneous stimulation at 5 ms and again at 150 ms. The firing of these 35 synapses represented the effects of electrical stimulation of the

LGN: the first stimulation gave a control EPSP, the second, occurring during 'visual stimulation', gave a test EPSP. Different trials using a different seed for the random number generator produced Poisson-distributed trains of EPSPs. One such trial is shown in Fig. 2 (upper trace). The test EPSP was significantly reduced with respect to the control EPSP (by 34% in this case).

Effects of spines

The saturation effect underlying the reduction in EPSP amplitude was dependent on the membrane potential at the synaptic site. Excitatory synapses on real pyramidal cells are made onto spines, not onto dendritic shafts. It was conceivable that the small dimensions, and hence higher input resistance, of a spine head relative to that of a dendritic shaft might lead to greater saturation effects for EPSPs on spines vs. shafts (Segev & Rall, 1988). Consequently, we performed some simulations with excitatory synapses on spine heads rather than dendritic shafts. For a single 0.5 nS EPSP, there was very little difference in the depolarization recorded at the soma for a synapse on the head of a spine vs. on the dendritic shaft; the activation of synapses on spines produced a somatic peak amplitude more than 90% of that from synapses on the shaft. Significant saturation of single EPSPs due to the passive

properties of the spine (Douglas & Martin, 1990b) was only observed if the peak EPSP conductance was increased to several nS. EPSPs produced by these conductance changes were larger than those typically observed in neocortical pyramidal cells (Mason et al., 1991).

To simulate the experiment of Ferster and Jagadeesh with spines explicitly included, 70 spines were placed on the 70 basal dendritic compartments chosen above, then 35 more were added to provide the control and test EPSPs. The result of the

simulation with all excitatory synapses on spines (lower trace, Fig. 2) was not significantly different from that with all excitatory synapses directly on dendritic shafts (upper trace). The presence of spines did not make a difference over the full range of 'visual stimulation' frequencies used. We also found very little difference between simulations using 35 0.2 nS test synapses and those using 14 0.5 nS test synapses.

Although spines may be of great significance in some contexts (Zador et al., 1990), we were only concerned here with ensuring that our results would not be significantly affected by placing all the excitatory synapses on dendritic shafts rather than on spine heads. Fig. 2 shows that this approach is justfied. For this reason, in the remaining simulations spines were not included.

Effect of excitation on saturation

Fig. 3b shows the results of multiple trials at different frequencies of 'visual stimulation'. Higher frequencies of excitatory input produced greater somatic depolarization, as would occur in a cell as the visual stimulus was presented at increasingly optimal values of orientation, velocity and direction. The peak amplitude of the EPSP is plotted against the somatic membrane potential (V_m) just before the EPSP occurs. As in the experimental data (Fig. 3a), the amplitude of the evoked EPSP decreased linearly with V_m. The dendrites were depolarized to between -25 mV and -20 mV during maximal synaptic activation, which means that the EPSP driving force was reduced by about 60%. Since the test EPSP was reduced by about 80% during maximal synaptic activation (Fig. 3b), a reduction in EPSP size of approximately 20% was due to a reduction in R_{in} caused by the excitatory synaptic input. A more detailed, quantitative description of changes in R_{in} during synaptic activation is presented in the last section of the results.

The results shown in Fig. 3b provide a qualitative match to those of Ferster and Jagadeesh, but the difference between the level of somatic and dendritic depolarization in the model was not great. In addition, the slope of the relationship between EPSP height and somatic V_m was not as steep as in the experimental data: the abscissa intercept (EPSP reduced to 0 mV) is about -40 mV in the experimental results (Fig. 3a) and -25 mV in Fig. 3b. Ferster and Jagadeesh report that visual cortical cells cannot be depolarized by more than 20 mV from rest by visual stimulation (Ferster & Jagadeesh, 1992). For our model cell (resting potential -65 mV), this corresponds to complete saturation at a somatic V_m of -45 mV.

Effect of inhibition on saturation

The difference between our simulations of dendritic saturation and the experimental results could be due to the omission of inhibitory input in the simulation. Recent studies (Berman et al., 1991; Douglas et al., 1988; Ferster & Jagadeesh, 1992) have indicated that inhibitory input to visual cortical cells is weak during nonpreferred responses and is strongly correlated with the degree of activation of the excitatory cells (Ferster, 1986; Somers et al., 1993). This fits with anatomical evidence that spiny excitatory cells make direct contacts with inhibitory cells, which then make direct contacts back onto the same excitatory population (Douglas & Martin, 1991). We repeated the simulation described above, this time including 33 inhibitory synapses, 12 on the soma and 21 on the preterminal basal/oblique dendrites. This is the pattern of innervation characteristic of basket cells, the most common inhibitory cell type in cortex (Martin, 1988). Inhibitory (smooth) cells fire at much higher rates than pyramidal cells (McCormick et al., 1985); therefore, inhibitory synapses were activated at a mean frequency twice that of the excitatory synapses. Fig. 3c shows the results of including inhibition in the

simulation. The EPSP/somatic V_m slope is steeper, with an abscissa intercept of about -35 mV. This is much closer to the experimental data of Ferster and Jagadeesh (Fig. 3a). Dendrites were depolarized to about -30 mV during maximal synaptic activation, less than in the excitation-alone case, yet the EPSP/somatic V_m slope is steeper with inhibition. A dendritic depolarization to around -30 mV reduced the EPSP driving force by about 50%. Test EPSPs were reduced in amplitude by up to 80%, so the remaining 30% must be due to decreases in R_{in} caused by the excitatory and inhibitory synaptic conductance changes (see Discussion). There may also be some contribution to the reduction in R_{in} and hence EPSP amplitude from intrinsic sub-threshold voltage-dependent conductances during the experiments of Ferster and Jagadeesh. The simulations of Fig. 3 did not include voltage-dependent conductances, so we cannot evaluate the extent of this contribution, but the simulations of Bernander et al. (1991) indicate that it is likely to be relatively small.

Ferster and Jagadeesh (1992) focused on reduction in driving force as the explanation for the decreases in evoked EPSP amplitude that they observed, but we found that decreases in R_{in} (decrease in effective R_m) due to excitatory inputs made a significant contribution. Furthermore, additional current shunts due to inhibitory synaptic activity must be included to produce an accurate fit to the experimental data. The data in Fig. 3c fall along a straight line because the major component of the saturation effect is due to the linear reduction in driving force. The contribution from increased membrane conductance, which would produce a concave (hyperbolic) curve, is masked by the driving force effect and the variance in the data. When inhibition was included in the simulation the soma could not be depolarized past -45 mV by the firing of the 70 excitatory synapses, which is the limit of depolarization obtainable with optimal visual stimulation reported by Ferster and Jagadeesh (1992).

Fig. 3d shows that the decrease in test EPSP amplitude due to dendritic saturation is stable across a wide range of values for R_m and R_i. The rate of decrease of EPSP amplitude with somatic V_m was constant over the full parameter range.

Fig. 4 displays in higher resolution dendritic (dashed lines) and somatic (solid lines) membrane potentials at the time of the test EPSP (arrow) for synaptic input with (lower traces) and without (upper traces) inhibition. A number of important points are illustrated: Because of a higher R_{in}, the dendrite is more depolarized than the soma (and this dendrite is less depolarized than most), with larger voltage fluctuations due to the influence of individual PSPs. The dendrite is less hyperpolarized than the soma by the inhibition because the inhibitory synapses are proximal and act by shunting current that passes from the dendrites to the soma. The effect of inhibition is to increase the slope of the test EPSP/somatic V_m graph (Fig. 3c), so at the low input rate shown here inhibition causes a small *increase* in the size of the test EPSP by slightly hyperpolarizing the membrane thus increasing the excitatory synaptic driving force. $GABA_A$ inhibition, the type we are modelling here, acts by increasing membrane conductance rather than directly hyperpolarizing the membrane, as its reversal potential is close to the resting membrane potential. The driving force for inhibitory chloride conductance only exists when there is depolarization produced by excitatory synaptic input (silent inhibition). At higher firing rates, when the inhibitory conductance is large, the small increase in excitatory driving force caused by the hyperpolarization, (which is minimised at the site of the excitatory synapses by the spatial separation of the sources of excitatory and inhibitory input, mentioned above) is more than offset by the shunting effect of the inhibition and the test EPSP is decreased in size (Fig. 3c).

The soma could still be depolarized by 20 mV from rest even when the 33 inhibitory synapses are firing at their maximum rate (Fig. 3). This indicates that firing of the postsynaptic cell would persist despite significant inhibition. This seems to support the

conclusion of Douglas and Martin (1990a), who simulated the effect of a maintained inhibitory conductance on the firing rate of a simplified model neuron driven by intrasomatic current injection. They suggested that inhibition in cortex cannot prevent the firing of a neuron receiving strong excitatory input. In contrast, studies *in vitro* indicate that synaptically-evoked GABA$_A$ inhibition is strong enough to briefly suppress the firing of cortical neurons driven by large depolarizing current injections (Connors et al., 1988; McCormick, 1989), although these results must be interpreted with caution given the large difference in GABA$_A$ conductance elicited *in vivo* and *in vitro* (Berman et al., 1989).

Effectiveness of inhibition

Under what conditions could inhibition be strong enough to suppress firing? What is the effect of strong synaptic activation on R_{in} of the target neuron? These have been the subject of previous experimental and theoretical studies (Berman et al., 1991; Douglas et al., 1988; Koch et al., 1990). To address these issues the model layer 2 pyramid was driven by the same concurrently active 70 excitatory and 33 inhibitory synapses as in Fig. 3. Active conductances were added to the model (Table 1) to produce adapting trains of action potentials (Fig. 5a). Fig. 5b shows the firing rate of the model cell as a function of the firing rate of the 70 excitatory synapses. The solid traces are results obtained without any inhibition. The dashed traces are results obtained with the inhibitory firing rate fixed at 100 Hz, which corresponds to the simulations done by Douglas and Martin (1990a). The crosses are the instantaneous firing rate of the model for the first interspike interval. The boxes are the steady-state (adapted) firing rate. In agreement with Douglas and Martin, the effect of the inhibition was to increase the threshold of the neuron and only slightly reduce the firing rate above threshold.

These simulations neglect the observation that inhibition is correlated with excitation (Ferster, 1986), which would occur if the inhibitory cells were being driven by the excitatory cells that they were inhibiting (Douglas & Martin, 1991). It is reasonable to assume that the firing rate of the inhibitory inputs would increase with the firing rate of the pyramidal cell, and hence with the firing rate of the pyramidal cell's excitatory inputs (the 70 excitatory synapses). Therefore, we repeated the above simulations, this time setting the firing rate of the inhibitory synapses to twice that of the excitatory synapses. The results, shown in Fig. 5b (dotted traces), demonstrate that inhibitory input does have the potential to significantly reduce the firing rate of the target cell. However, the firing rate of the pyramidal cell was still substantial: the inhibition produced by 33 synapses is not enough to shut off the target cell.

The simulation was repeated with the 33 somato-dendritic inhibitory synapses replaced by 25 inhibitory synapses on the first 25 µm of an axon initial segment consisting of 7 cylinders whose diameter tapered from 2.5 µm to 0.6 µm. This is the innervation pattern characteristic of chandelier cells, a type of cortical inhibitory interneuron (Farinas & DeFelipe, 1991b). Sodium and potassium spike conductances were included on the first 25 µm at the same density as on the soma (Table 1). The results (not shown) were nearly identical to those shown in Fig. 5. Thus, we found no difference between the effect of basket cell inhibition and that of chandelier cells (see also Lytton and Sejnowski (1991)). Similar results were also obtained when using the layer 5 cell instead of the layer 2 cell (not shown).

Cortical pyramidal cells receive hundreds of inhibitory synaptic contacts on their somata and proximal dendrites (Douglas & Martin, 1990b; Farinas & DeFelipe, 1991a). Therefore, we increased the number of active inhibitory synapses in our simulation. We found that the activity of about 200 somatic inhibitory synapses was sufficient to prevent a cell receiving strong excitation from firing (Fig. 5c). Consequently, strong cortical

inhibition is able to prevent the firing of even strongly driven pyramidal cells, contrary to previous conclusions (Douglas & Martin, 1990a). Firing was completely suppressed by 200 inhibitory inputs whether R_m of the model layer 2 pyramid was 20 or 100 kΩcm^2. When R_m was 5 kΩcm^2, the resting R_{in} of the model cell was so low (about 35 MΩ) that the 70 excitatory inputs did not drive the cell very strongly and the activity of just 33 inhibitory inputs was sufficient to suppress firing.

The inhibition produced by the activity of 200 inhibitory inputs caused a huge decrease in R_{in} of the model neuron. Large decreases in R_{in} were not seen *in vivo* during nonpreferred responses or sustained hyperpolarizations (Berman et al., 1991; Douglas et al., 1988; Ferster & Jagadeesh, 1992). Thus, intracortical inhibition has the potential to shut off the firing of even strongly activated neurons, but this type of (shunting) inhibition has not yet been observed in cortical neurons. A possible reason for this is suggested in the discussion.

Previous simulations have shown that R_{in} of a neuron must decrease by a significant amount in order to prevent the cell from firing (Koch et al., 1990). However, as mentioned above, a number of recent experimental tests have shown that R_{in} shows no significant reduction during the nonpreferred response or even during sustained hyperpolarizations that are part of an optimal response to a visual stimulus (Berman et al., 1991; Douglas et al., 1988; Ferster & Jagadeesh, 1992). Tests of our model show that R_{in} decreased by a significant amount during the synaptic activation used in the above simulations (Fig. 6). Thus, if we consider decrease in R_{in} as an assay for inhibition, the level of inhibition used in the simulations shown in Figs. 3 and 5b was as least as great as the level of inhibition occurring during nonpreferred or hyperpolarizing visual responses. This inhibition was not strong enough to counter significant synaptic excitation (Fig. 5b). This is further evidence that the level of inhibition that occurs during nonpreferred responses is not enough to prevent the cell from firing. It is likely that a lack of excitatory

drive is what prevents the cell from firing during nonpreferred responses (Berman et al., 1991; Ferster, 1986).

Table 2 shows the percentage decrease in R_{in} caused by weak and strong synaptic input. The input firing rate shown is for the 70 excitatory synapses and 33 inhibitory synapses active at twice these rates. The decrease in R_{in} was calculated relative to R_{in} at rest in the steady state as determined by current injections many times τ_m in duration. The decreases in R_{in} produced by even weak synaptic input were above the experimentally detectable threshold (Berman et al., 1991) for all values of R_m and R_i. We found that approximately half of the decrease in R_{in} was due to excitatory, and half to inhibitory, synaptic conductance changes. This is not suprising since the individual synaptic conductances were equal and there were about twice as many excitatory synapses but they fired at half the rate of the inhibitory synapses. As noted above, the simulations of the experiments of Ferster and Jagadeesh (1992) showed that up to 20% of the EPSP reduction was due to decreases in R_{in}, even when no inhibition was present (see Discussion). That excitatory input alone can cause significant decreases in R_{in} is apparent from considering the fact that the peak conductance of just one excitatory input (0.5 nS) is an appreciable fraction of the input conductance of a neuron (which for our model layer 2 pyramid ranged from 1.9 to 34.8 nS, depending on R_m and R_i).

Discussion

Saturation

Recent simulations of reconstructed neocortical pyramidal cells show electrotonic compactness of the basal dendrites and oblique dendrites (lateral branches from the apical

trunk) over a wide range of parameter values (Holmes & Woody, 1989; Stratford et al., 1989). Dendritic branches are quite isolated from each other and have high input impedances relative to the soma (Rinzel & Rall, 1974). Inputs on the same branch may interact nonlinearly because synaptic currents and voltages depend on the local membrane potential and R_{in}, respectively, and these in turn both depend on local synaptic activity (Barrett & Crill, 1974; Rall, 1964; Rall, 1967). Synaptic input could act to reduce the excitatory driving force and R_{in}, leading to a saturation of simultaneous and subsequent excitatory input

In confirmation, our simulations of the experiments of Ferster and Jagadeesh (1992) have provided evidence for two contributions to dendritic saturation: A reduction in driving force and a reduction in R_{in} (shunting). Based on Eq. (1) for the membrane current, applied to voltage-independent synaptic conductances, these two components can be represented analytically in the equation for the peak synaptic potential, ΔV, produced by n synapses each with their own reversal potential, $V_r{}^i$, undergoing conductance change Δg^i on a single compartment with resting membrane potential V_L:

$$\Delta V = \frac{(V_r - V_L)\Delta g}{(g_L + \Delta g)} \tag{2}$$

$$\text{where} \quad V_r = \sum_i^n V_r^i \frac{\Delta g^i}{\Delta g}$$

$$\Delta g = \sum_i^n \Delta g^i$$

and g_L is the leak conductance. The numerator in Eq. (2) represents the driving force and the denominator gives the shunting effect. The composite synaptic event is equivalent to a single synapse with a reversal potential V_r that is a weighted sum of the individual reversal potentials and a conductance equal to the sum of the individual conductances.

All of the results we have described regarding saturation of excitatory input, effectiveness of inhibition and changes in R_{in} were consistent across a wide range of values for R_m and R_i (Table 2, Fig. 3d). The largest value for R_m we considered (100 kΩcm^2) seemed unlikely to occur *in vivo*. This value produced a value for R_{in} of more than 500 MΩ for the model layer 2 pyramidal cell, which is well outside the range reported thus far for *in vivo* cortical neurons (Douglas et al., 1991; Ferster & Jagadeesh, 1992; Pei et al., 1991). This value for R_m also gave a value for τ_m of 100 ms. Such a large time constant seems incompatible with neuronal processes occurring on the time scale of tens of ms (Gray et al., 1992). In performing the simulations shown in Fig. 3, with a τ_m of 100 ms, the relative timing of all events had to be increased several fold because the model neuron took hundreds of ms to reach a steady state in response to any stimulus. If cortical neurons do have a fundamental R_m of 100 kΩcm^2, the effective R_m of *in vivo* neurons is likely to be much lower due to the effect of background synaptic input (Bernander et al., 1991) (see Methods).

A number of simulations were performed with excitatory synaptic inputs on the heads of explicitly modeled spines. The results were not significantly different from those obtained with inputs made directly onto dendritic shafts (Fig. 2). The reason for this is that the spine stem resistance (255 MΩ for our spines) is small compared to the inverse of the peak synaptic conductance (2 GΩ) (Jaslove, 1992), so that nearly all the current entering the spine head flows into the dendritic shaft (the membrane conductance of the spine is negligible). There are, however, circumstances when the differences between spine and shaft synaptic input can become significant (Qian & Sejnowski, 1989; Zador et al., 1990).

Synaptic excitation

Although this study was based on simulations of single neocortical pyramidal neurons, the results can be used to infer some of the principles of operation of the circuits in the neocortex. One such principle, proposed 10 years ago on the basis of physiological evidence, is that a single synapse is ineffective in firing another cell (Abeles, 1982). Since one pyramidal cell makes on average only one or two synaptic contacts onto each of its targets (Braitenberg & Schuz, 1991; Gabbot et al., 1987) and the vast majority of cortical synapses are pyramidal-pyramidal contacts (White, 1989), the effect of a single neocortical pyramid on another is almost negligible — certainly not enough to drive the postsynaptic cell by itself (Abeles, 1982). In our simulations a single synapse firing at a mean frequency of 100 Hz produced a somatic depolarization of less than a millivolt. Maximally activating a whole dendritic segment (depolarizing to 0 mV using current injection) was not enough to drive the cell to fire at the rates observed during visual stimulation.

Thus, there must be convergence of synaptic inputs from many cells to produce significant firing (Douglas & Martin, 1990b). How many? Our model cells required tens of synapses, active within an interval of a few milliseconds, to reach threshold. Firing at the rates observed during visual stimulation required about a hundred synapses active at a few hundred Hz. The saturation demonstrated in Fig. 3 indicates that the additional activation of more synapses has a decreasing effect. Because the maximum firing rates we used for our inputs were at the upper limits of sustained firing rates in cortex, it is likely that maximal firing will require the activity of a few hundred presynaptic cells, as suggested for the hippocampus (Andersen et al., 1990; Miles & Wong, 1986; Sayer et al., 1990), spinal cord (Jack et al., 1981; Walmsley et al., 1987) and cerebellum (Rapp et al., 1992). If the inputs were completely synchronous, a high frequency discharge could be evoked by a few tens of active synapses (Abeles, 1982; Bush & Douglas, 1991). This 'dynamic range' of a few tens to a few hundred active inputs is only a small fraction of the thousands of synapses on a single pyramidal neuron (Douglas & Martin, 1990b). This implies that a

pyramidal cell can be driven by any one of several different groups of presynaptic cells, allowing the same neuron to participate in many (possibly independent) processes.

Assuming passive membrane, a single EPSP with peak conductance 0.5 nS on the model layer 2 cell produced a somatic depolarization with a peak amplitude approximately twice that seen in the layer 5 cell. This is because R_{in} of the layer 2 cell (with the same τ_m) is approximately twice that of the layer 5 cell. We have found that twice as many excitatory synapses were needed to drive the layer 5 cell to fire at the same frequency as the layer 2 cell. This fits with the observation that large layer 5 pyramids have about twice the number of spines as small layer 2 pyramids. However, there is as yet no experimental evidence that single EPSPs are larger in layer 2 cells than in layer 5 cells.

Synaptic inhibition

The 33 inhibitory synapses used in the simulations of Fig. 3c,d are a fraction of the several hundred that exist on the soma and proximal dendrites of each pyramidal cell (Douglas & Martin, 1990b; Farinas & DeFelipe, 1991a). The activity of this small fraction was not sufficient to prevent the firing of a cell receiving strong excitation (Fig. 5b), yet it was enough to reduce R_{in} significantly (Fig. 6, Table 2). Since R_{in} does not decrease during nonpreferred or hyperpolarizing responses to visual stimuli (Berman et al., 1991; Douglas et al., 1988; Ferster & Jagadeesh, 1992), we agree with Berman et al. (1991) that inhibition in the cortex (at least primary visual cortex) does not act to counter sustained (longer than 50-100 ms) excitation.

What then is the role of inhibition? Inhibition is correlated with excitation (Ferster, 1986); thus maximal inhibitory activity is expected during the periods of maximum firing caused by excitatory input. This statement may seem paradoxical, but only if the excitation and inhibition are considered as simultaneous and sustained, without any temporal

structure. However, analysis of inhibitory activity during visual stimulation (Fig. 14 of Lytton and Sejnowski (1991)) reveals that compound IPSPs can occur rhythmically rather than randomly. This might be produced by feedback inhibition generated in response to stimulation by the same excitatory cells that the inhibition targets (Douglas & Martin, 1991). It has been shown that such a system can produce synchronization of excitatory and inhibitory populations and consequent rhythmic IPSPs (Bush & Douglas, 1991). Compound EPSPs are also rhythmic in this model, but are out of phase with the IPSPs. In fact, it is the compound IPSP generated by the compound EPSP that terminates the burst of firing in the pyramidal cells and insures synchronization (Bush & Douglas, 1991).

The activity of hundreds of inhibitory synapses would be required to generate an IPSP capable of shutting off the firing of the pyramidal cells. In our simulations the simultaneous activity of about 200 inhibitory synapses prevented the firing of our model cells despite strong synaptic excitation. Such a compound IPSP would produce a very large decrease in R_{in} of the target cell, but the decrease would be transient (of order 10 ms) because the inhibitory cells stop firing when no longer driven by the pyramids they inhibit. Transient conductance changes cannot be detected by current pulse injection (Berman et al., 1991) but it might be possible to sample the peak slope conductance at different membrane potentials. Thus, we suggest that the role of inhibition is to synchronize the firing of groups of pyramidal cells by rhythmically turning on transiently but powerfully during optimal stimulation (see also Lytton and Sejnowski (1991), who considered the efficacy of lower frequency inhibitory inputs to entrain pyramidal cells). Our proposal reconciles the fact that effective inhibition (preventing firing of target) must cause a large decrease in R_{in} with the fact that such decreases in R_{in} have not been seen *in vivo*.

There has been very little experimental study of changes in R_{in} during the response to optimal stimulation. Such experiments are hard to perform and interpret because of the

large, rapid fluctuations in membrane potential and large supra-threshold intrinsic voltage-dependent conductance changes occurring during these periods. Existing data show input conductance increases of up to 40% during optimal stimulation (Berman et al., 1991). Our results indicate that R_{in} should decrease substantially during optimal stimulation, but, as with inhibition, the detectibility of this decrease using current pulses would depend on how much of the excitatory input is transient and how much is sustained.

The inhibition discussed in the above argument is assumed to be $GABA_A$ inhibition. The slower, hyperpolarizing $GABA_B$ inhibition probably has a different role that could be investigated using a network simulation (for one suggestion see (Abbott, 1991)). In a realistic network the temporal structure of synaptic inputs would be much closer to *in vivo* conditions than the random inputs used here. This would allow better estimates of the numbers of inputs driving a pyramidal cell and a better way to study the role of inhibition.

Our conclusion that inhibition does not act as a veto of sustained excitation is in agreement with Berman et al. (1991). We have also replicated their results showing that a modest level of inhibition does not prevent the firing of its target (Douglas & Martin, 1990a). However, using revised assumptions about the amount of inhibition impacting upon a single pyramidal neuron, we have shown that a stronger level of inhibition can shut off the firing of a strongly driven target cell. We reconcile these results by postulating that such strong inhibition is only activated transiently, during periods of maximum excitatory activity.

Conclusion

Neocortical pyramidal cells do not linearly integrate synaptic input, even in the absence of active membrane properties. Despite the electrotonic compactness of pyramidal

basal/oblique dendritic trees, saturation of excitatory input is a real phenomenon that places a sharp limit on the number of active excitatory inputs that can contribute to the response of a particular pyramidal cell.

Cortical inhibition can in principle suppress the firing of its targets, but a role for inhibition as a negator of inappropriate excitatory input is not consistent with experimental data and theoretical studies. Both data and models lead to the view that excitation and inhibition are a synergistic pair of processes combining coactively to shape the response of cortical neurons to optimal stimuli (Berman et al., 1991; Bush & Douglas, 1991).

References

Abbott, L. (1991). Firing-rate models for neural populations. In *Neural Networks: From Biology to High-Energy Physics. Proceedings*,
edited by O. Benhar, C. Bosio, P. Del Guldie, and E. Taber. Pisa: ETS Edrifice.

Abeles, M. (1982). *Local Cortical Circuits: An Electrophysiological Approach*. Berlin: Springer-Verlag.

Andersen, P., Raastad, M., & Storm, J. F. (1990). Excitatory synaptic integration in hippocampal pyramids and dentate granule cells. *Symp. Quant. Biol.*, **55**, 81-86.

Barrett, J. N., & Crill, W. E. (1974). Influence of dendritic location and membrane properties on the effectiveness of synapses on cat motoneurones. *J. Physiol.*, **293**, 325-345.

Berman, N. J., Douglas, R. J., & Martin, K. A. C. (1989). The conductances associated with inhibitory postsynaptic potentials are larger in visual cortical neurons *in vitro* than in similar neurons in intact, anaesthetized rats. *J. Physiol.*, **418**, 107P.

Berman, N. J., Douglas, R. J., Martin, K. A. C., & Whitteridge, D. (1991). Mechanisms of inhibition in cat visual cortex. *J. Physiol.*, **440**, 697-722.

Bernander, O., Douglas, R. J., Martin, K. A. C., & Koch, C. (1991). Synaptic background activity influences spatiotemporal integration in single pyramidal cells. *Proc. Nat. Acad. Sci.*, **88**, 11569-11573.

Bonds, A. B. (1989). Role of inhibition in the specification of orientation selectivity of cells in the cat striate cortex. *Vis. Neurosci.*, **2**, 41-55.

Borg-Graham, L. J. (1987). *Modeling the somatic electrical response of hippocampal pyramidal neurons*. M.S., MIT.

Braitenberg, V., & Schuz, A. (1991). *Anatomy of the cortex*. Berlin: Springer-Verlag.

Bush, P. C., & Douglas, R. J. (1991). Synchronization of bursting action potential discharge in a model network of neocortical neurons. *Neural Comp.*, **3**, 19-30.

Bush, P. C., & Sejnowski, T. J. (1991). Simulations of a reconstructed Cerebellar Purkinje Cell based on simplified channel kinetics. *Neural Comp.*, **3**, 299-309.

Connors, B. W., Malenka, R. C., & Silva, L. R. (1988). Two inhibitory postsynaptic potentials, and GABAa and GABAb receptor-mediated responses in neocortex of rat and cat. *J. Physiol.*, **406**, 443-468.

Douglas, R. J., & Martin, K. A. C. (1990a). Control of neuronal output by inhibition at the axon initial segment. *Neural Comp.*, **2**, 283-292.

Douglas, R. J., & Martin, K. A. C. (1990b). Neocortex. In G. Shepherd (Ed.), *Synaptic Organization of the Brain* (pp. 220-248). New York: Oxford University Press.

Douglas, R. J., & Martin, K. A. C. (1991). A functional microcircuit for cat visual cortex. *J. Physiol.*, **440**, 735-769.

Douglas, R. J., & Martin, K. A. C. (1992). Exploring cortical microcircuits: A combined anatomical, physiological, and computational approach. In T. McKenna, J. Javis, & S. F. Zornetzer (Eds.), *Single Neuron Computation* San Diego: Academic Press.

Douglas, R. J., Martin, K. A. C., & Whitteridge, D. (1988). Selective responses of visual cortical cells do not depend on shunting inhibition. *Nature*, **332**, 642-644.

Douglas, R. J., Martin, K. A. C., & Whitteridge, D. (1991). An intracellular analysis of the visual responses of neurones in cat visual cortex. *J. Physiol.*, **440**, 659-696.

Farinas, I., & DeFelipe, J. (1991a). Patterns of synaptic input on corticocortical and corticothalamic cells in the cat visual cortex. I. The cell body. *J. Comp. Neurol.*, **304**, 53-69.

Farinas, I., & DeFelipe, J. (1991b). Patterns of synaptic input on corticocortical and corticothalamic cells in the cat visual cortex. II. The axon initial segment. *J. Comp. Neurol.*, **304**, 70-77.

Ferster, D. (1986). Orientation selectivity of synaptic potentials in neurons of cat primary visual cortex. *J. Neurosci.*, **6**, 1284-1301.

Ferster, D., & Jagadeesh, B. (1992). EPSP-IPSP interactions in cat visual cortex studied with *in vivo* whole-cell patch recording. *J. Neurosci.*, **12**, 1262-1274.

Gabbot, P. L. A., Martin, K. A. C., & Whitteridge, D. (1987). Connections between pyramidal neurons in layer 5 of cat visual cortex (area 17). *J. Comp. Neurol.*, **259**, 364-381.

Gray, C. M., Engel, A. K., Koenig, P., & Singer, W. (1992). Synchronization of oscillatory neuronal responses in cat striate cortex: Temporal properties. *Vis. Neurosci.*, **8**, 337-347.

Hille, B. (1984). *Ionic Channels of Excitable Membranes*. Sunderland, MA: Sinauer Associates, Inc.

Hines, M. L. (1989). A program for simulation of nerve equations with branching geometries. *Int. J. Biomed. Comp.*, **24**, 55-68.

Holmes, W. R., & Woody, C. D. (1989). Effects of uniform and non-uniform synaptic 'activation distributions' on the cable properties of modeled cortical pyramidal neurons. *Brain Res.*, **505**, 12-22.

Jack, J. J. B., Noble, D., & Tsien, R. W. (1975). *Electric current flow in excitable cells*. Oxford: Oxford University Press.

Jack, J. J. B., Redman, S. J., & Wong, K. (1981). The components of synaptic potentials evoked in cat spinal motorneuons by impulses in single group 1a afferents. *J. Physiol.*, **321**, 65-96.

Jaslove, S. W. (1992). The integrative properties of spiny distal dendrites. *Neurosci.*, **47**(3), 495-519.

Kisvardy, Z. F., & Eysel, U. T. (1993). Functional and structural topography of horizontal inhibitory connections in cat visual cortex. *Eur. J. Neurosci.*, **5**, 1558-1572.

Koch, C., Douglas, R., & Wehmeier, U. (1990). Visibility of synaptically induced conductance changes: theory and simulations of anatomically characterized cortical pyramidal cells. *J. Neurosci.*, **10**, 1728-1744.

Koch, C., Poggio, T., Edelman, G. M., Gall, W. E., & Cowan, W. M. (1987). Biophysics of computation: Neurons, synapses, and membranes. In G. M. Edelman, W. E. Gall, & W. M. Cowan (Eds.), *Synaptic Function* (pp. 637-698). New York: John Wiley & sons.

Major, G., Larkman, A. U., & Jack, J. J. B. (1990). Constraining non-uniqueness in passive electrical models of cortical pyramidal neurons. *J. Physiol.*, 13P.

Martin, K. A. C. (1988). From single cells to simple circuits in the cerebral cortex. *Q. J. Exp. Physiol.*, **73**, 637-702.

Mason, A., Nicoll, A., & Stratford, K. (1991). Synaptic transmission between individual pyramidal neurons of the rat visual cortex *in vitro*. *J. Neurosci.*, **11**(1), 72-84.

McCormick, D. A. (1989). GABA as an inhibitory neurotransmitter in human cerebral cortex. *J. Neurophysiol.*, **62**, 1018-1027.

McCormick, D. A., Connors, B. W., Lighthall, J. W., & Prince, D. A. (1985). Comparative electrophysiology of pyramidal and sparsely spiny stellate neurons of the neocortex. *J. Neurophysiol.*, **54**, 782-806.

Miles, R., & Wong, R. K. S. (1986). Excitatory synaptic interactions between CA3 neurons in the guinea pig hippocampus. *J. Physiol.*, **373**, 397-418.

Pei, X., Volgushev, M., Vidyasagar, T. R., & Creutzfeldt, O. D. (1991). Whole cell recording and conductance measurements in cat visual cortex *in vivo*. *NeuroReport*, **2**, 485-488.

Qian, N., & Sejnowski, T. J. (1989). An electro-diffusion model for computing membrane potentials and ionic concentrations in branching dendrites, spines and axons. *Biol. Cybern.*, **62**, 1-15.

Rall, W. (1964). Theoretical significance of dendritic trees for neuronal input-output relations. In R. Reiss (Ed.), *Neural Theory and Modeling* (pp. 73-97). Stanford: Stanford University Press.

Rall, W. (1967). Distinguishing theoretical synaptic potentials computed for different soma-dendritic distributions of synaptic input. *J. Neurophysiol.*, **30**, 1138-1168.

Rapp, M., Yarom, Y., & Segev, I. (1992). The impact of parallel fiber background activity on the cable properties of cerebellar Purkinje cells. *Neural Comp.*, **4**(4), 518-533.

Rinzel, J., & Rall, W. (1974). Transient response in a dendritic neuron model for current injected at one branch. *Biophys. J.*, **14**, 759-789.

Sayer, R. J., Friedlander, M. J., & Redman, S. J. (1990). The time course and amplitude of EPSPs evoked at synapses between pairs of CA3/CA1 neurons in the hippocampal slice. *J. Neurosci.*, **10**, 826-836.

Segev, I., & Rall, W. (1988). Computational study of an excitable dendritic spine. *J. Neurophysiol.*, **2**, 499-523.

Segev, I., Rapp, M., Manor, Y., & Yarom, Y. (1992). Analog and digital processing in single nerve cells: dendritic integration and axonal propagation. In T. McKenna, J. Javis, & S. F. Zornetzer (Eds.), *Single Neuron Computation* San Diego: Academic Press.

Shelton, D. P. (1985). Membrane resistivity estimated for the Purkinje neuron by means of a passive computer model. *Neuroscience*, **14**, 111-131.

Sillito, A. M. (1975). The contribution of inhibitory mechanisms to the receptive field properties of neurones in the striate cortex of the cat. *J. Physiol.*, **250**, 305-329.

Somers, D., Nelson, S. B., & Sur, M. (1993). Computational model of the effects of short range excitation and inhibition on orientation selectivity in visual cortex. *Soc. Neurosci. Abstr.*, **19**, 628.

Spruston, N., & Johnston, D. (1992). Perforated patch-clamp analysis of the passive membrane properties of three classes of hippocampal neurons. *J. Neurophysiol.*, **67**(3), 508-528.

Staley, K. J., Thomas, S. O., & Mody, I. (1992). Membrane properties of dentate gyrus granule cells: Comparison of sharp microelectrode and whole-cell recordings. *J. Neurophysiol.*, **67**(5), 1346-1358.

Stratford, K., Mason, A., Larkman, A., Major, G., & Jack, J. (1989). The modelling of pyramidal neurons in the cat visual cortex. In R. Durbin, C. Miall, & G. Mitchison (Eds.), *The Computing Neuron* Wokingham, England: Addison-Wesley.

Tanaka, E., Higashi, H., & Nishi, S. (1991). Membrane properties of guinea pig cingulate cortical neurons in vitro. *J. Neurophysiol.*, **65**, 808-821.

Thomson, A. M., Girdlestone, D., & West, D. C. (1988). Voltage-dependent currents prolong single-axon postsynaptic potentials in layer III pyramidal neurons in rat neocortical slices. *J. Neurophysiol.*, **60**, 1896-1907.

Traub, R. D., Wong, R. K. S., Miles, R., & Michelson, H. (1991). A model of a CA3 hippocampal pyramidal neuron incorporating voltage-clamp data on intrinsic conductances. *J. Neurophysiol.*, **66**, 635-650.

Walmsley, B. F. R., Edwards, F. R., & Tracey, D. J. (1987). The probablistic nature of synaptic transmission at a mammalian central synapse. *J. Neurosci.*, **7**, 1037-1046.

White, E. L. (1989). *Cortical circuits*. Boston: Birkhaeuser.
Zador, A., Koch, C., & Brown, T. H. (1990). Biophysical model of a Hebbian synapse. *Proc. Natl. Acad. Sci.*, **87**, 6718-6722.
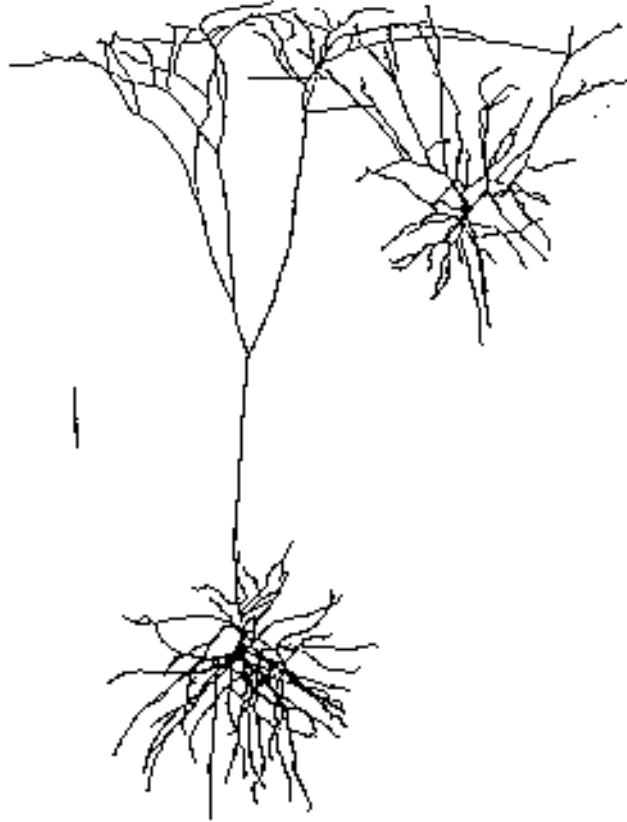
FIG. 1. Drawings of reconstructed HRP-filled layer 2 (right) and layer 5 (left) pyramidal cells. Scale bar 100 um.
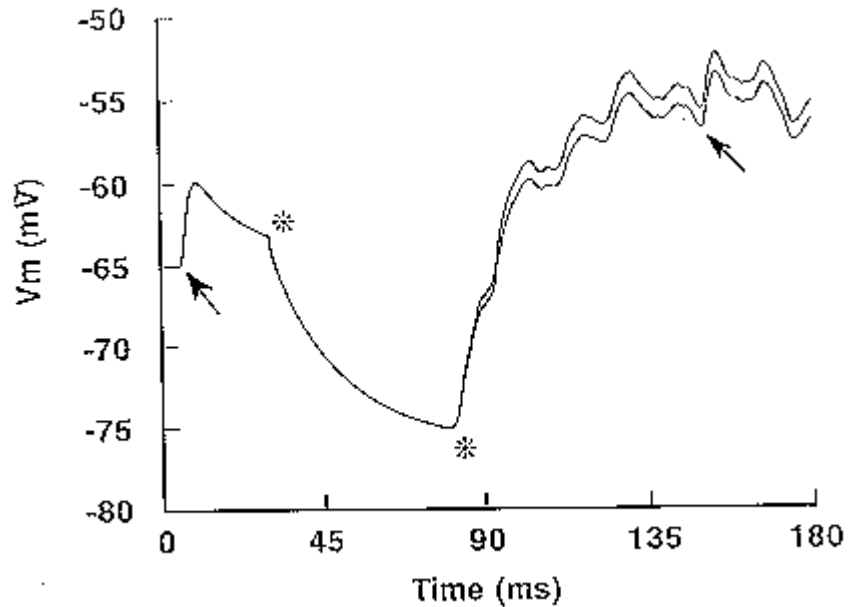
FIG. 2. Simulation of reduction in amplitude of EPSP by synaptic activity. Somatic membrane potential (V_m) during simulation of model layer 2 pyramid. A constant current of -0.1 nA is injected into the soma at t = 30 ms to prevent firing (first asterisk), then 70 excitatory synapses are activated at a mean frequency of 50 Hz to simulate visual stimulation (second asterisk). 35 additional synapses are given a simultaneous stimulus to produce a control (first arrow) and test (second arrow) EPSP. The amplitude of the test EPSP is significantly reduced with respect to the control. Upper trace is result of simulation with all excitatory synapses directly on dendritic shafts, lower trace is result of simulation with all synapses on the heads of dendritic spines (see methods).

FIG. 3. Dendritic saturation during physiological synaptic activation. (A) Experimental data: Peak amplitude of the test EPSP plotted against V_m just before the EPSP occ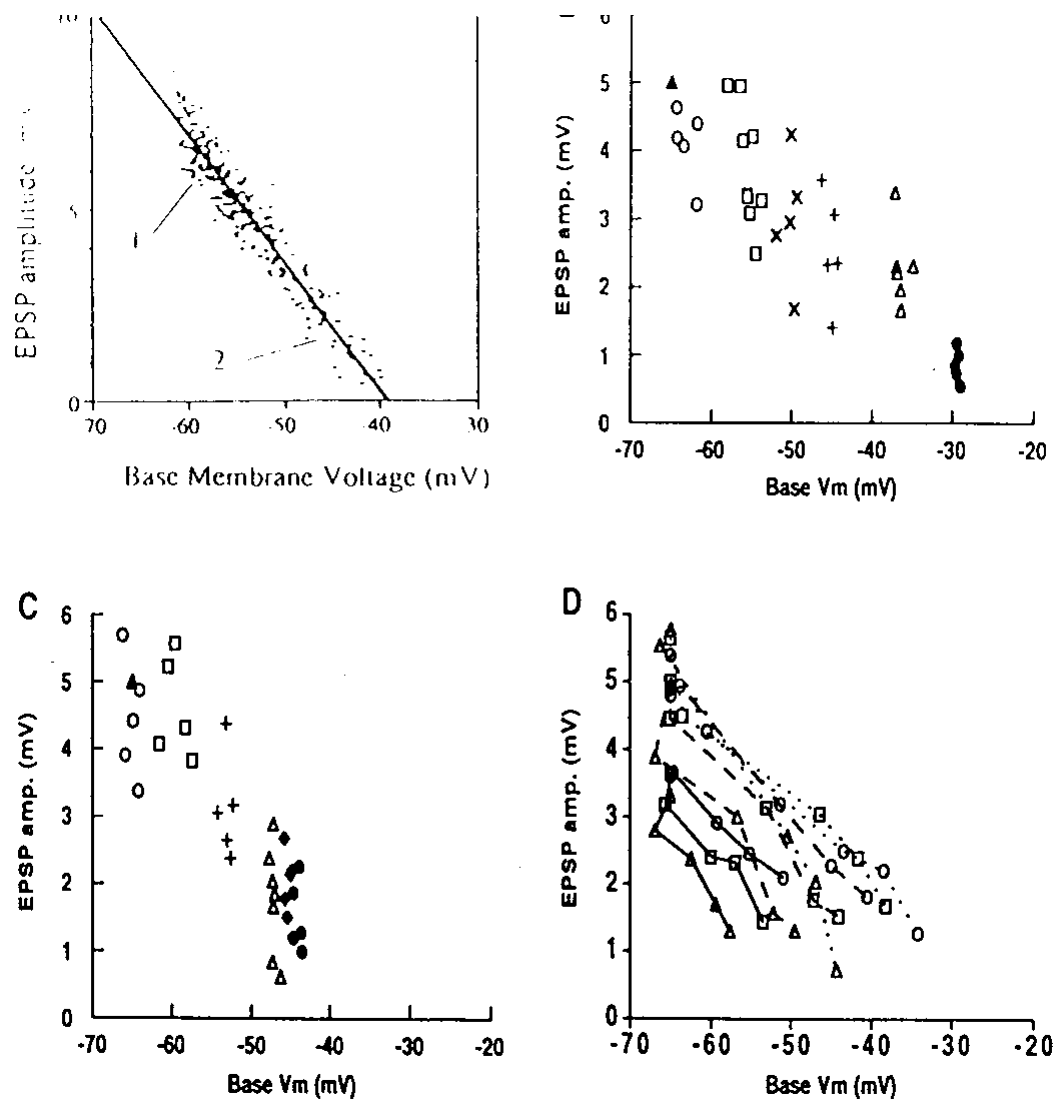urred while the visual stimulus was at the optimal orientation for the cell. Arrow 1 indicates control EPSP (before stimulation), arrow 2 indicates test EPSP (at peak of visual response) (reproduced by permission (Ferster & Jagadeesh, 1992)). (B) Simulation of the experiment in *A*, as detailed in Fig. 2. Peak amplitude of the test EPSP plotted against V_m just before the EPSP occurred, for a variety of firing frequencies of the 70 excitatory synapses; H = 0 Hz, E = 25 Hz, G = 50 Hz, I = 75 Hz, D = 100 Hz, C = 200 Hz, F = 300 Hz, J = 400 Hz. The amplitude of the EPSP decreased linearly with V_m. (C) Concurrent inhibition is included in the simulation (33 inhibitory synapses at twice frequency of excitatory synapses). (D) Simulations in *C* repeated for R_m values of 5 (solid), 20 (dashed) and 100 (dotted traces) $k\Omega cm^2$ and R_i values of 70 (E), 200 (G) and 500 (C) Ωcm. Data plotted for excitatory input frequencies of 0, 25, 100, 200 and 400 Hz. Each point is the average of five trials.
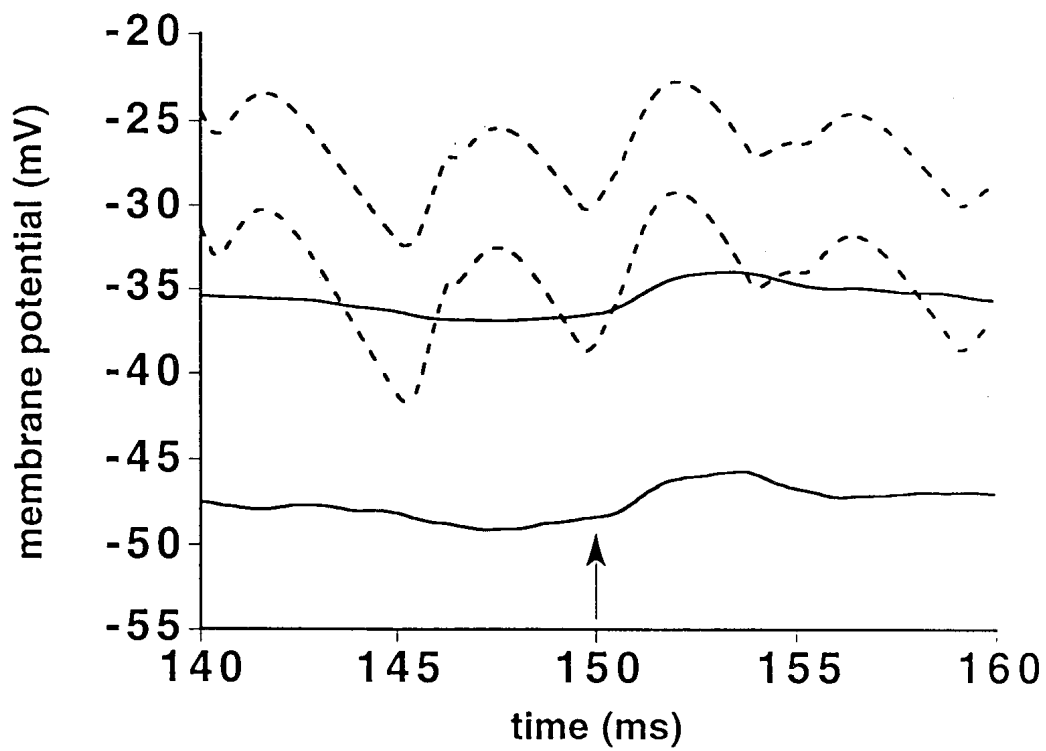
FIG. 4. Effect of inhibition on dendritic saturation at low input rates. Dendritic (dashed lines) and somatic (solid lines) membrane potentials during the application of the test EPSP (arrow) with (lower traces) and without (upper traces) inhibitory input are shown.
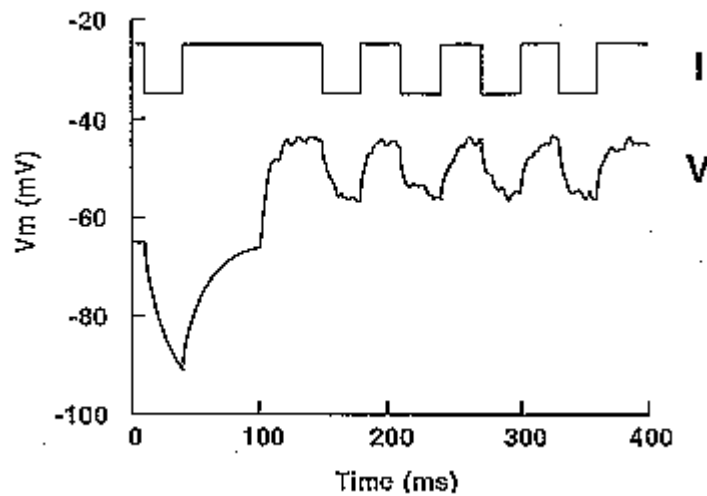
FIG. 5. Effect of inhibition on firing rate of synaptically activated model layer 2 pyramid. (A) Adapting train of action potentials produced by 70 excitatory inputs active at a mean frequency of 200 Hz. (B) Firing rate of model as a function of the firing rate of its 70 excitatory inputs. I = Initial, peak firing rate. G = Steady, adapted firing rate. Solid traces are results without inhibition. Dashed traces are results with 33 additional, inhibitory synapses firing at 100 Hz. This level of inhibition has little effect on the strongly activated pyramid. Dotted traces are results with the firing rate of the inhibitory inputs equal to twice that of the excitatory inputs in each case. This more realistic level of inhibition causes a significant decrease in the firing rate of the pyramid, although firing is not completely suppressed. (C) Firing is completely suppressed when an additional 150 somatic inhibitory inputs, starting firing at a mean frequency of 400 Hz at t = 100 ms, are added to the simulation shown in *A*.
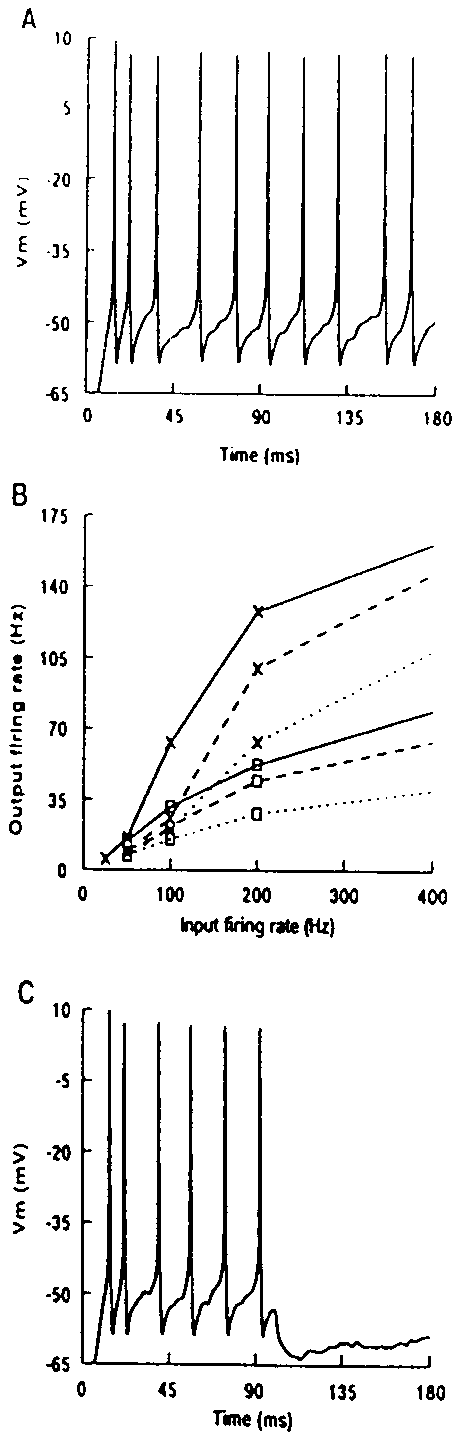
FIG 6. Decrease in input resistance of model layer 2 pyramidal cell during synaptic activation. At 100 ms, 70 excitatory synapses and 33 inhibitory synapses were activated at 200 Hz and 400 Hz, respectively. Upper trace is current injected into model soma (-0.3 nA each 30 ms pulse, to conform with protocol of Berman et al. (1991)), lower trace is

voltage response of model. Size of voltage deflection to each pulse gives measure of input resistance of cell. Voltage deflection is significantly smaller during synaptic activation (last 4 pulses) than at rest (first pulse). Decrease in input resistance is actually larger than measured here, because cell is not fully charged by the pulse at rest but is fully charged by the pulses during synaptic activation. This is due to the cell's smaller time constant during synaptic activation. Data in Table 2 is calculated using the real (steady-state) input resistance of the cell.

TABLE 1 Parameters for active conductances

Channel	E_r (mV)	g (mS/cm^2)	z	g	a_0,b_0	$V_{1/2}$	t_{min} (ms)	T (^{o}C)	n
Na(m)	45	40	4.3	0.7	4.2	-38	0.05	37	3
Na(h)			-6	0.5	0.2	-42	0.5	37	1
Kd	-90	30	3	0.7	0.03	-35	1.0	24	4
Ca	N/A	0.6	6	0.7	1	-15	0.1	37	1
K$_{Ca}$	-90	10				see text			

TABLE 2 Percentage Decrease in R_{in} during concurrent synaptic excitation and inhibition

$R_m(k\Omega cm^2)$		5	5	20	20	100	100
Input rate (Hz)	firing	50	400	50	400	50	400
$R_i(\Omega cm)$							
70		16.0	41.5	42.3	74.2	82.6	94.2
200		15.3	39.2	45.5	72.6	78.1	91.9
500		15.1	37.6	39.5	70.0	80.0	91.8

CHAPTER III

Reduced Compartmental Models of Neocortical Pyramidal Cells

Abstract

Model neurons composed of hundreds of compartments are currently used for studying phenomena at the level of the single cell. Large network simulations require a simplified model of a single neuron that retains the electrotonic and synaptic integrative properties of the real cell. We introduce a method for reducing the number of compartments of neocortical pyramidal neuron models (from 400 to 8-9 compartments) through a simple collapsing method based on conserving the axial resistance rather than the surface area of the dendritic tree. The reduced models retain the general morphology of the pyramidal cells on which they are based, allowing the accurate positioning of synaptic inputs and ionic conductances on individual model cells, as well as the construction of spatially accurate network models. The reduced models run significantly faster than the full models, yet faithfully reproduce their electrical responses.

Introduction

Compartmental computer models have been used to investigate many aspects of single neurons, including passive properties (Rall 1964, Shelton 1985), the role of active conductances in producing observed firing behavior (Yamada et al. 1989, Bush and Sejnowski 1991), and synaptic integration (Rall 1967, Shepherd et al. 1985, Fleshman et al. 1988, Clements and Redman 1989, Bernander et al. 1991, Lytton and Sejnowski 1991, Segev et al. 1992, Bush and Sejnowski 1992). The models used in these studies contain hundreds of compartments and thousands of coupled differential equations must be solved each time step. To speed up simulations, model networks use simplified representations of the single neurons that comprise the network.

Most model neurons composed of just a few compartments have been assigned a somewhat arbitrary geometry, with no systematic testing of the reduced model against the real cell or a more complete model (Wilson and Bower 1989, Traub 1982, Lytton and Sejnowski 1991, Wehmeier et al. 1989). Such models may have the same input resistance (R_{in}) and membrane time constant (τ_m) as the real cell, but typically will not accurately simulate the integration of synaptic inputs in the dendritic compartments and the resulting flow of current into the soma. Recent experimental and theoretical evidence indicates that the electrotonic structure of cortical neurons causes significant nonlinearities in the integration of synaptic input (Ferster and Jagadeesh 1991, Ferster and Jagadeesh 1992, Bush and Sejnowski 1992). It is still an open question as to whether such effects are important at the level of network function, but it would be prudent to ensure that a simplified model neuron destined for network simulation is an as accurate representation of the real cell as possible.

An example of a simplified model neuron that does retain the electrotonic characteristics of the full model is the 'cartoon representation' developed by Stratford et al. (1989). This is a model of a cortical pyramidal cell reduced to 24 compartments by using a

number of mathematical transformations to collapse the basal and apical dendritic trees into equivalent profiles, then collapsing all the oblique dendrites (lateral branches from the apical trunk) that are at the same electrotonic distance from the soma. Stratford et al. demonstrated that the cartoon model is a good fit to the full model in terms of its response to transient current injections at different locations as well as displaying the same R_{in} and τ_m. We have combined this approach with a simpler method to construct an alternative cartoon representation that allowed us to achieve fewer compartments yet retain accurate electrical properties.

Methods

Simulations were performed using standard techniques for compartmental models of branching dendritic trees (Rall 1964); two digitized HRP-filled pyramidal cells from cat visual cortex (layers 2 and 5) (Koch et al. 1990) were modeled, each consisting of coupled cylindrical compartments containing only resistive and capacitative elements. The full models against which the reduced models were tested had approximately 400 compartments (Fig 1A), and have been used in a number of previous studies (Koch et al. 1990, Lytton and Sejnowski 1991, Bernander et al. 1991, Bush and Sejnowski 1992). The simulator CABLE (Hines 1989), running on a MIPS Magnum 3000/33, required about 1 minute of computation to simulate 100 ms of real time for the full models. The reduced models ran approximately 5 times faster in simulations that included a full set of voltage- and ligand-gated conductances.

Model parameters

The choice of values for the passive parameters (specific membrane resistance, R_m, specific membrane capacitance, C_m, and axial resistivity, R_i) for pyramidal cells has recently been discussed (Bush and Sejnowski 1992). Following that study, we used $C_m = 1 \ \mu F/cm^2$ (Jack et al. 1975), $R_i = 200 \ \Omega cm$ (Bernander et al. 1991, Shelton 1985, Stratford et al. 1989, Segev et al. 1992) and $R_m = 20 \ 000 \ \Omega cm^2$. This value for R_m is the effective specific membrane resistance for an *in vivo* neocortical pyramidal neuron receiving background synaptic input from spontaneously active neurons (Barrett and Crill 1974, Bernander et al. 1991). These passive parameters produced R_{in}'s for the model layer 5 and layer 2 pyramidal cells of 45 MΩ and 110 MΩ, respectively and a τ_m of 20 ms. These values are within the range recorded from cells in cat visual cortex *in vivo* (Douglas et al. 1991, Pei et al. 1991, Ferster and Jagadeesh 1992).

The inclusion of spines in a passive model may significantly increase the membrane area of the cell (Stratford et al. 1989, Segev et al. 1992). A recent calculation has shown that the addition of the membrane area of 4000 spines to our layer 5 pyramidal cell increases the area by about 7.5% (Bernander et al. 1992). This can be accounted for in a model by increasing C_m and proportionally decreasing R_m (Holmes 1989). Our values for R_m and C_m are constrained by measurements of R_{in} and τ_m and are not based on direct measurement. Thus, if we assume that adding spines increases the membrane area of our pyramidal cells by, for example, 20%, we revise our estimate of R_m to 24 kΩcm^2 and our estimate of C_m to 0.8 $\mu F/cm^2$. These values are then decreased and increased, respectively, to account for spine membrane, producing the values that we use in our model. We have found very little difference between results obtained with excitatory synaptic inputs on the heads of explicitly modeled spines as opposed to those obtained with inputs made directly onto dendritic shafts (Bush and Sejnowski 1992). Thus, in these simulations synaptic inputs were made directly onto dendritic shafts.

Excitatory and inhibitory postsynaptic potentials (EPSPs and IPSPs) in our models were simulated as alpha function conductance changes with a peak amplitude of 0.5 nS and a time to peak of 1 ms (Rall 1967, Bernander et al. 1991). These parameters were chosen because they produced EPSPs at the soma with the same time course and amplitude as those observed experimentally (Mason et al. 1991, Thomson et al. 1988). The reversal potential for EPSPs was 0 mV and the reversal potential for IPSPs was -70 mV (Connors et al. 1988, McCormick 1989). Trains of EPSPs or IPSPs were modeled according to a Poisson distribution with a fixed mean frequency of activation.

For some simulations, active conductances were placed at the soma to generate adapting trains of action potentials, as observed in regular-firing cortical neurons (McCormick et al. 1985). The conductances followed Hodgkin-Huxley-like kinetics based on parameters developed by Borg-Graham (1987). The implementation was exactly as described in Bush and Sejnowski (1992).

Reduced compartmental models

When reducing a compartmental model to one with fewer compartments, R_m, C_m and R_i should be preserved so that the reduced model will have same the same R_{in}, τ_m and length constant, λ, as the full model. Pyramidal cells do not obey Rall's constraints for collapse into a single equivalent cylinder (Stratford et al. 1989, Douglas and Martin 1991), so other approaches must be tried. Surface area (hence R_m and C_m) can be conserved by constructing an 'equivalent dendritic profile' (Fleshman et al. 1988, Clements and Redman 1989, Stratford et al. 1989, Manor et al. 1991). In this technique the sum of the diameters to the 3/2 power of all the dendrites at regular intervals from the soma are used to compute the diameter of an equivalent dendrite. The length of the equivalent dendrite must also be scaled appropriately. As shown by Stratford et al., the equivalent profile has

the same R_{in} and τ_m as the full model but the degree of attenuation of synaptic input along the length of the apical dendrite is not large enough. This is because the axial resistance of the equivalent profile is not equal to the axial resistance of the apical dendrite, due to the lumping of the oblique dendrites into the profile. The cartoon model developed by Stratford et al. (1989) solved this problem by explicitly representing the oblique dendrites as sidebranches from the apical trunk.

An alternative approach to the cartoon representation is a collapsing technique based on conserving R_i rather than the membrane surface area. This is done by making the cross-sectional area of the equivalent cylinder equal to the sum of the cross-sectional areas of all the dendrites represented by that equivalent cylinder:

$$R = \sqrt{\sum_i r_i^2}$$

(1)

Where R is the radius of the equivalent cylinder and r_i is the radius of dendrite i. The length of the equivalent cylinder is just the average length of all the dendrites represented by the equivalent cylinder.

We have applied this collapsing technique to create a new reduced pyramidal cell model. First, all dendrites with approximately the same origin and (electrotonic) length are collapsed into a single equivalent cable. Thus, all the preterminal basal dendritic segments (Larkman 1991a) were collapsed together into an equivalent cylinder, as were all the terminal basal dendritic segments. The distal apical dendritic aborization was also collapsed together. The main apical dendrite was reduced to 2 or 3 equivalent cylinders. To insure the correct attenuation along the apical dendrite, the oblique dendrites were represented as a single sidebranch from the apical trunk. Some fine tuning of the structure obtained using this method was required; in particular we found it necessary to use two paired basal dendritic compartments rather than one. This was to ensure a large enough

dendritic load on the soma while maintaining the correct attenuation from dendrites to soma: A single large-diameter cylinder does not show great enough attenuation of synaptic input. The somatic compartment had the same dimensions as in the full model.

The surface areas of our reduced models are less than those of the full models. Thus the next step in the reduction was to scale the values used for R_m and C_m appropriately. R_i was conserved, so R_m could be changed until the reduced model had the same R_{in} as the full model. We found that R_m had to be reduced by 2.84 times to match the R_{in} of the reduced layer 5 cell model with that of the full layer 5 cell model. R_m had to be reduced by 2.95 times to match the R_{in} of the reduced layer 2 cell model with that of its full model. C_m must then be multiplied by this scaling factor to match τ_m of the reduced cell to that of the full cell. This procedure is a correction for the reduction in surface area, and indeed if an approximate calculation of the ratio of the areas of the full and reduced layer 5 cell model is made by summing up the areas of all the cylindrical compartments in each model, a value of 2.74 is obtained, which is quite close to the empirical scaling factor of 2.84. The dimensions of the reduced models are given in Table 1.

Our collapsing method is simpler than that of Stratford et al. and allowed us to produce accurate models composed of less than 10 compartments. In addition, the lengths of our equivalent dendrites were equal to the average lengths of the dendrites which they represent. This is important when incorporating these models into spatially accurate networks.

Our method takes advantage of some of the morphological features of neocortical pyramidal cells: All the dendrites collapsed together into an equivalent cylinder have approximately equal lengths and diameters, as well as equivalent electrotonic origins. It should be possible to construct similar models of other types of neurons using our method if their dendritic morphologies display these features.

Results

The geometries of the reduced model layer 2 and layer 5 pyramidal cells are shown in Fig. 1B. Drawings of the HRP-filled pyramidal cells are included for comparison (Fig. 1A). In order to assess the accuracy of the method that produced the reduced models, we compared the responses of the reduced and full models to different types of stimulation. The response of the reduced and the full model layer 5 pyramid to a continuous somatic current injection of -0.7 nA are compared in Fig. 2A. The superposition of the two traces shows that both models have the same R_{in} and τ_m. It is relatively easy to match these parameters by tuning R_m and C_m. Such a match says little about how faithfully the reduced model captures the synaptic integration properties of the full model (Fleshman et al. 1988). The responses of the reduced and the full model layer 2 pyramid to a brief somatic current injection are compared in Fig. 2B (Stratford et al. 1989, Shelton 1985). The response to a transient somatic input is dependent on R_i as well as R_m and C_m, because it is dependent on how fast current moves from the soma into the dendrites. The response of the reduced model is a good fit to that of the full model. The responses of both models to an EPSP on the soma, with 0.5 nS peak conductance are compared in Fig. 2C. This tests essentially the same properties as the brief current pulse; the performance of the reduced model is very close to that of the full model.

Fig. 3A shows the firing of the full 400 compartment layer 5 cell in response to a maintained 1 nA somatic current injection. The
model cell produced an adapting spike train typical of the regular-firing class of cortical pyramidal cells (McCormick et al. 1985). The
conductances underlying this firing behavior, located in the soma only, were put into the 9 compartment model without changing a single parameter. Because both models have the

same somatic dimensions, the same conductance densities were used in both. Fig. 3B shows the firing of the 9 compartment model in response to a 1 nA somatic current injection. The response of the reduced model has the same form as that of the full model — an adapting train of action potentials. The firing frequency of the reduced model was slightly higher, but the small difference was within the limits of uncertainty of the model parameters as well as the variance in response recorded across different pyramidal cells (McCormick et al. 1985, Douglas et al. 1991).

The final test was to compare the response of both models to synaptic input. To produce the same output as the full model, the reduced model must perform the same nonlinear integration of dendritic EPSPs and IPSPs as the full model (Bush and Sejnowski 1992), and display the same dendrites-to-soma transfer characteristics. In other words, the reduced model must have the same input-output function as the full model.

A majority (70-90%) of excitatory inputs to cortical pyramidal cells are made on the basal/oblique dendrites (Larkman 1991b). We distributed synapses on the dendrites and soma to reflect these measurements. Thus, 140 excitatory synapses were placed randomly on the basal and oblique dendrites of the full model and 140 on the 1 oblique and 2 basal equivalent dendrites of the reduced model. In addition, 33 inhibitory synapses were placed on the proximal dendrites and 12 on the soma of each model, a pattern of innervation characteristic of basket cells, the most common inhibitory cell type in cortex (Martin 1988). Inhibitory (smooth) cells fire at much higher rates than pyramidal cells (McCormick et al. 1985), therefore inhibitory synapses were activated at a mean frequency twice that of the excitatory synapses. Fig. 3C shows the responses of the full and reduced models for the peak (initial) and steady-state (adapted) firing rates as a function of the frequency of the excitatory inputs. The fit is close for all input frequencies, demonstrating that the reduced

model shows about the same dendritic integration characteristics and response to inhibition as the full model, despite having an extremely simplified structure.

Discussion

Given current computational limitations, simulation of a large, realistic network requires a model cell with a minimal number of compartments. The reduced pyramidal cell model presented here is a good fit to the full model for a variety of stimuli (Figs. 2 and 3), and is suitable for network simulations involving multiple, spatially-separated synaptic inputs to the neurons.

The R_{in} of an equivalent dendrite of the reduced model is not as large as the R_{in} of one of the dendrites represented by the equivalent dendrite. Hence, a single EPSP on an equivalent dendrite of the reduced model is not equivalent to a single EPSP on a single dendrite of the full model. Rather it would be equivalent to dividing the EPSP and applying one fraction to each of the real dendrites represented by the equivalent dendrite. Thus, the reduced model is not appropriate for studying the effect of single synaptic inputs on single dendritic branches of pyramidal cells or local dendritic processing in general. For example, we would not use this reduced model to investigate clustering of individual synaptic inputs or the inhibitory control of specific dendrites. Such studies must use more detailed models that represent each process of the neuron explicitly. However, we found that the membrane potential of the basal dendrites of the reduced model was equal to the mean potential of the basal dendrites of the full model during multiple synaptic activation (eg. Fig. 3C), giving us some confidence that the voltage-dependent processes (such as NMDA) occurring in the dendrites (as well as the soma) during multiple synaptic activation could be accurately simulated with the reduced model.

References

Barrett, J. N. and Crill, W. E. Influence of dendritic location and membrane properties on the effectiveness of synapses on cat motoneurones. *J. Physiol.* **293:** 325-345, 1974.

Bernander, O., Douglas, R. J. and Koch, C. A model of regular-firing cortical pyramidal neurons (16). California Institute of Technology. 1992.

Bernander, O., Douglas, R. J., Martin, K. A. C. and Koch, C. Synaptic background activity influences spatiotemporal integration in single pyramidal cells. *Proc. Nat. Acad. Sci.* **88:** 11569-11573, 1991.

Borg-Graham, L. J. Modeling the somatic electrical response of hippocampal pyramidal neurons. M.S., MIT, 1987.

Bush, P. C. and Sejnowski, T. J. Simulations of a reconstructed Cerebellar Purkinje Cell based on simplified channel kinetics. *Neural Comp.* **3:** 299-309, 1991.

Bush, P. C. and Sejnowski, T. J. Dendritic saturation and effects of inhibition in simulated neocortical pyramidal cells. *J. Neurophysiol.* Submitted for publication, 1992.

Clements, J. D. and Redman, S. J. Cable properties a of cat spinal motoneurons measured by combining voltage clamp, current clamp and intracellular staining. *J. Physiol.* **409:** 63-87, 1989.

Connors, B. W., Malenka, R. C. and Silva, L. R. Two inhibitory postsynaptic potentials, and GABAa and GABAb receptor-mediated responses in neocortex of rat and cat. *J. Physiol.* **406:** 443-468, 1988.

Douglas, R. J. and Martin, K. A. C. A functional microcircuit for cat visual cortex. *J. Physiol.* **440:** 735-769, 1991.

Douglas, R. J., Martin, K. A. C. and Whitteridge, D. An intracellular analysis of the visual responses of neurones in cat visual cortex. *J. Physiol.* **440:** 659-696, 1991.

Ferster, D. and Jagadeesh, B. An *in vivo* whole-cell patch study of the linearity of IPSP-EPSP interactions in cat visual cortex. *Soc. Neurosci. Abstr.* **17:** 176, 1991.

Ferster, D. and Jagadeesh, B. EPSP-IPSP interactions in cat visual cortex studied with *in vivo* whole-cell patch recording. *J. Neurosci.* **12:** 1262-1274, 1992.

Fleshman, J. W., Segev, I. and Burke, R. E. Electrotonic architecture of type-identified alpha-motoneurons in the cat spinal cord. *J. Neurophysiol.* **60:** 60-85, 1988.

Hines, M. L. A program for simulation of nerve equations with branching geometries. *Int. J. Biomed. Comp.* **24:** 55-68, 1989.

Holmes, W. R. The role of dendritic diameters in maximizing the effectiveness of synaptic inputs. *Brain Res.* **478:** 127-137, 1989.

Jack, J. J. B., Noble, D. and Tsien, R. W. *Electric current flow in excitable cells* . Oxford: Oxford University Press. 1975.

Koch, C., Douglas, R. and Wehmeier, U. Visibility of synaptically induced conductance changes: theory and simulations of anatomically characterized cortical pyramidal cells. *J. Neurosci.* **10:** 1728-1744, 1990.

Larkman, A. U. Dendritic morphology of pyramidal neurons of the visual cortex of the rat: I. Branching patterns. *J. Comp. Neurol.* **306:** 307-319, 1991a.

Larkman, A. U. Dendritic morphology of pyramidal neurons of the visual cortex of the rat: III. Spine distributions. *J. Comp. Neurol.* **306:** 332-343, 1991b.

Lytton, W. W. and Sejnowski, T. J. Simulations of cortical pyramidal neurons synchronized by inhibitory interneurons. *J. Neurophysiol.* **66:** 1059-1079, 1991.

Manor, Y., Gonczarowski, J. and Segev, I. Propagation of action potentials along complex axonal trees. Model and implementation. *Biophys. J.* **60:** 1411-1423, 1991.

Martin, K. A. C. From single cells to simple circuits in the cerebral cortex. *Q. J. Exp. Physiol.* **73:** 637-702, 1988.

Mason, A., Nicoll, A. and Stratford, K. Synaptic transmission between individual pyramidal neurons of the rat visual cortex *in vitro*. *J. Neurosci.* **11:** 72-84, 1991.

McCormick, D. A. GABA as an inhibitory neurotransmitter in human cerebral cortex. *J. Neurophysiol.* **62:** 1018-1027, 1989.

McCormick, D. A., Connors, B. W., Lighthall, J. W. and Prince, D. A. Comparative electrophysiology of pyramidal and sparsely spiny stellate neurons of the neocortex. *J. Neurophysiol.* **54:** 782-806, 1985.

Pei, X., Volgushev, M., Vidyasagar, T. R. and Creutzfeldt, O. D. Whole cell recording and conductance measurements in cat visual cortex *in vivo*. *NeuroReport* **2:** 485-488, 1991.

Rall, W. Theoretical significance of dendritic trees for neuronal input-output relations. In R. Reiss (Ed.), *Neural Theory and Modeling* (pp. 73-97). Stanford: Stanford University Press. 1964.

Rall, W. Distinguishing theoretical synaptic potentials computed for different soma-dendritic distributions of synaptic input. *J. Neurophysiol.* **30:** 1138-1168, 1967.

Segev, I., Rapp, M., Manor, Y. and Yarom, Y. Analog and digital processing in single nerve cells: dendritic integration and axonal propagation. In T. McKenna, J. Javis & S. F. Zornetzer (Ed.), *Single Neuron Computation* San Diego: Academic Press. 1992.

Shelton, D. P. Membrane resistivity estimated for the Purkinje neuron by means of a passive computer model. *Neuroscience* **14:** 111-131, 1985.

Shepherd, G. M., Brayton, R. K., Miller, J. F., Segev, I., Rinzel, J. and Rall, W. Signal enhancement in distal cortical dendrites by means of interactions between active dendritic spines. *Proc. Natl. Acad. Sci. USA* **82:** 2192-2195, 1985.

Stratford, K., Mason, A., Larkman, A., Major, G. and Jack, J. The modelling of pyramidal neurons in the cat visual cortex. In R. Durbin, C. Miall & G. Mitchison (Ed.), *The Computing Neuron* Wokingham, England: Addison-Wesley. 1989.

Thomson, A. M., Girdlestone, D. and West, D. C. Voltage-dependent currents prolong single-axon postsynaptic potentials in layer III pyramidal neurons in rat neocortical slices. *J. Neurophysiol.* **60:** 1896-1907, 1988.

Traub, R. D. Simulation of intrinsic bursting in CA3 hippocampal neurons. *Neuroscience* **7:** 1233-1242, 1982.

Wehmeier, U., Dong, D., Koch, C. and Van Essen, D. • Modeling the mammalian visual system. In C. Koch & I. Segev (Ed.), *Methods in Neuronal Modeling* (pp. 335-359). Cambridge, MA: MIT Press. 1989.

Wilson, M. A. and Bower, J. M. The simulation of large-scale neural networks. In C. Koch & I. Segev (Ed.), *Methods in Neuronal Modeling: From Synapse to Networks* (pp. 291-333). Cambridge, MA: MIT Press. 1989.

Yamada, W. M., Koch, C. and Adams, P. R. Multiple channels and calcium dynamics. In C. Koch & I. Segev (Ed.), *Methods in Neuronal Modeling: From Synapse to Networks* (pp. 97-133). Cambridge, MA: MIT Press. 1989.
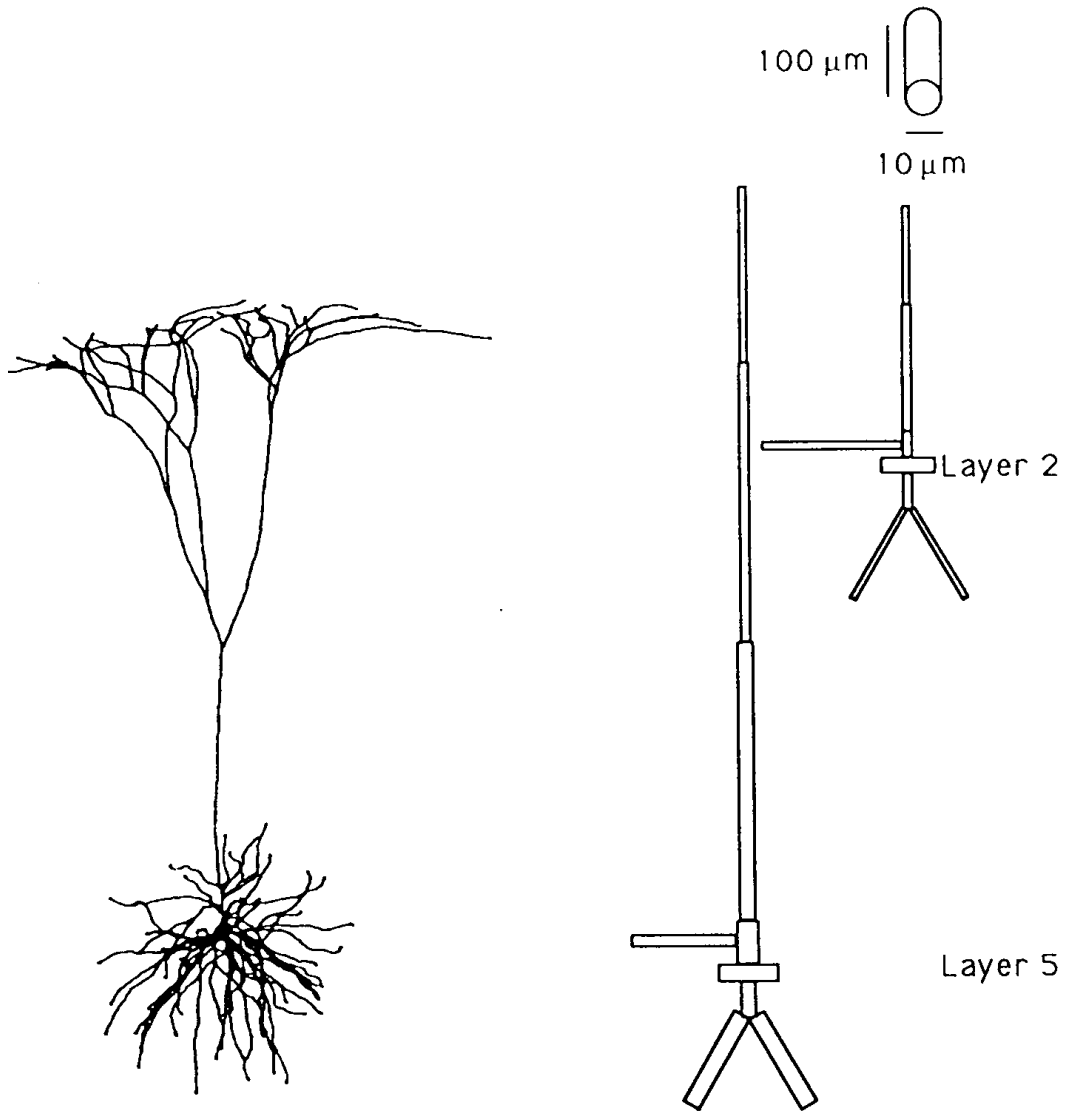
FIG. 1. A) Drawings of reconstructed HRP-filled layer 2 (right) and layer 5 (left) pyramidal cells. B) Geometries of reduced pyramidal cell models (see Table 1 for lengths and diameters of each compartment).
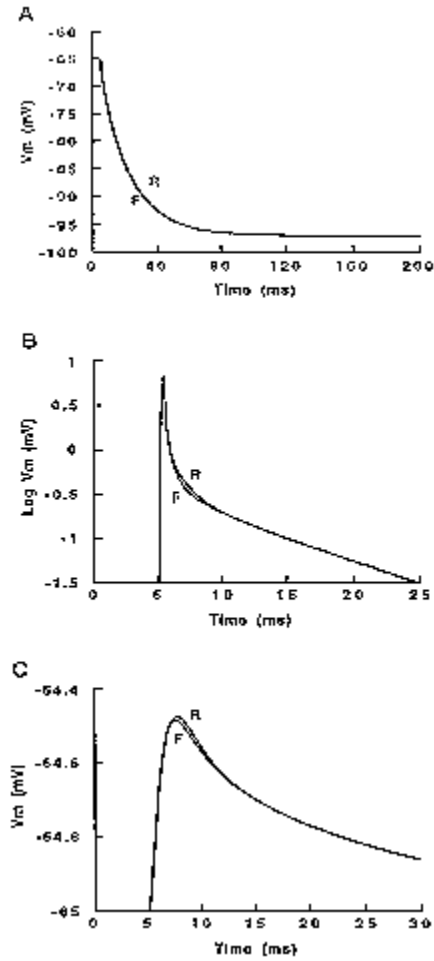
FIG. 2. Comparison of the response of the reduced (R) and full (F) models to somatic input. A) Voltage response at the soma of reduced and full layer 5 pyramid models to constant current injection of -0.7 nA. The superposition of the two traces indicates that both models have the same R_{in} and τ_m. B) Semi-log plot of voltage response of reduced and full layer 2 models to a 0.44 ms 0.3 nA somatic current injection at t = 5 ms. C) Voltage response of both layer 2 models to a 0.5 nS somatic EPSP. The close fit of the reduced model with the full model to these transient inputs indicates that the dendrites conduct charge away from the soma at the same rate in both models.
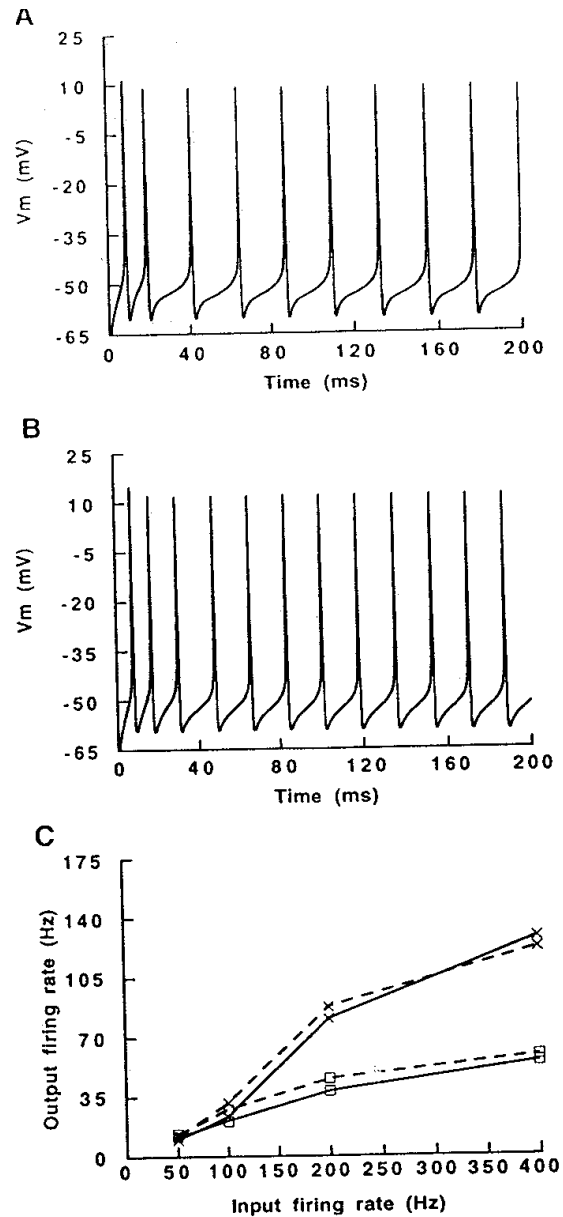
FIG. 3. Comparison of firing responses of reduced and full model layer 5 pyramidal cell. The somata of both models contain active conductances with exactly the same kinetics and densities. A) Adapting spike train of full model in response to constant 1 nA somatic current pulse. B) Spike train of reduced model in response to same stimulus. The response of the reduced model is of the same form as that of the full cell, but the firing frequency is slightly higher. C) Firing rate of full (solid traces) and reduced (dashed traces) models as a function of the firing rate of their 140 excitatory inputs. Each model also receives 45 inhibitory synapses, active at twice the rate of the excitatory ones. I = Initial, peak firing rate. G = Steady, adapted firing rate. The close fit of the two models demonstrates that the reduced model integrates excitatory and inhibitory synaptic input in the same manner as the full model.

TABLE 1 Dimensions of reduced models

	Layer 5 pyramid		Layer 2 pyramid	
	length(um)	diameter(um)	length(um)	diameter(um)
soma	23	17	21	15.3
apical trunk	60	6	35	2.5
obliques	150	3	200	2.3
apical #1	400	4.4	180	2.4
apical #2	400	2.9	-	-
apical tuft	250	2	140	2
basal trunk	50	4	50	2.5
basals (2)	150	5	150	1.6

CHAPTER IV

Synchronization of bursting action potential discharge in a model network of neocortical neurons

Abstract

We have used the morphology derived from single horse radish peroxidase-labelled neurons, known membrane conductance properties and microanatomy to construct a model neocortical network that exhibits synchronized bursting. The network was composed of interconnected pyramidal (excitatory) neurons with different intrinsic burst frequencies, and smooth (inhibitory) neurons that provided global feedback inhibition to all of the pyramids. When the network was activated by geniculocortical afferents the burst discharges of the pyramids quickly became synchronized with zero average phase-shift. The synchronization was strongly dependent on global feedback inhibition, which acted to group the co-activated bursts generated by intracortical re-excitation. Our results suggest that the synchronized bursting observed between cortical neurons responding to coherent visual stimuli is a simple consequence of the principles of intra-cortical connectivity.

Introduction

Recently there have been a number of reports that neurons in the visual cortex that respond to related features in the visual scene tend to synchronize their action potential discharge (Gray and Singer, 1989; Gray et al., 1990; Engel et al., 1990). This finding has attracted considerable attention because it may reflect a process whereby the cortex binds coherent visual features into objects (Crick, 1984; von der Malsburg and Schneider, 1986). Typically, the synchronization is observed between neurons that have Complex receptive field responses, and that have bursting rather than regular (Connors et al., 1982) discharge patterns. Theoretical analyses (Kammen et al., 1990) and simulations of connectionist networks (Sporns et al., 1989) have examined the conditions required for coherent neural activity but the detailed neuronal mechanism of synchronization has not been studied. In this paper we address this problem using a network of cortical neurons with realistic morphology and excitability.

Model Cortical Network

The network was composed of model pyramidal and smooth cortical neurons. Each neuron was represented by a compartmental model that consisted of a series of cylindrical dendritic segments and an ellipsoidal soma (Figure 1a,b). The dimensions of these compartments were obtained by simplification of the detailed morphology of a pyramidal neuron and a basket neuron that had been intracellularly labelled with horseradish peroxidase (Douglas and Martin, 1990a). Each of the compartments contained an appropriate profile of passive, voltage-dependent, calcium-dependent, and synaptic

conductances. Active conductances had Hodgkin-Huxley-like dynamics, except that time constants were independent of voltage. Passive properties of the model cell were obtained from intracellular recordings made in the real cell. The magnitudes and dynamics of the conductances, and the implementation of the compartmental simulation were similar to that described elsewhere in the literature (Traub et al., 1987; Getting, 1989; Douglas and Martin 1990a). The relevant parameters are listed in Table 1.

The cortical network consisted of ten bursting pyramidal neurons and one basket neuron (Figure 1c). The bursting behaviour of the pyramids was dependent on a small, transient delayed rectifier (g_{Kd}) and a large calcium-dependent potassium conductance (g_{KCa}). The reduced spike afterhyperpolarization that resulted from a small fast g_{Kd} encouraged a high frequency burst of action potentials and rapid accumulation of intracellular calcium. The burst was terminated by the hyperpolarization induced by g_{KCa}. The inter-burst interval depended on the rate of calcium removal (buffering) from the intracellular compartment. Each of the ten pyramidal cells was assigned a slightly different intracellular calcium decay rate so that their natural burst frequencies ranged between 18 and 37Hz for a 1nA intra-somatic current injection. The active conductances were located in the somatic compartment. Smooth cells have shorter spike durations, higher discharge rates, and show less adaptation than regular firing pyramidal cells (Connors et al., 1982). These characteristics were achieved in the model smooth cell by retaining only the spike conductances, g_{Na} and g_{Kd}, both of which were large and fast.

Each neuron represented the activity of a population of neurons of that type. The activities of these populations were measured as their average action potential discharge rates. The individual spikes of the representative neurons were used to estimate the average discharge rates of their respective populations. This was done by convolving each of the spikes of the representative neuron with a gamma interspike interval distribution. The shape parameter of the distribution was held constant ($\alpha=2$). The mean interspike

interval of the distribution was defined as the previous interspike interval of the representative neuron. Thus the interspike interval distribution became more compact at higher discharge frequencies. The lateral geniculate input to the pyramidal cells was modelled as a continuous discharge rate. The form of the input was a step-like function, and in some cases a noise component was added (Figure 4b).

The synaptic effect of a given population on its target neuron was computed from the average population discharge rate, maximum synaptic conductance, and synaptic conductance time-constants (Table 1). The distributions of inputs from various sources onto visual cortical cells are not accurately known. However, both asymmetric and symmetric synapses tend to cluster on the proximal dendrites of cortical neurons (White, 1989), and so in this simplified model we assigned all contacts to the proximal basal dendrites. We assumed that one excitatory synaptic input would contribute a somatic epsp with a peak amplitude of about 100µV. Thus, roughly 200 synchronous inputs are required to drive the post-synaptic cell to threshold, and about 600 to reach maximum discharge. In preliminary simulations we confirmed that this range of inputs could effectively drive a postsynaptic neuron if the maximum single synapse excitatory conductance was set to about 0.5nS. This and all other maximum synaptic conductances were determined at a presynaptic discharge rate of 300spikes/s. Anatomical studies indicate (for review of neocortical circuitry see Martin, 1988; Douglas and Martin, 1990b) that any particular cortical pyramid makes only about 1 contact with its post-synaptic target. This means that a reasonable size for the co-activating population is about 600 pyramids, which is about 10% of the total excitatory input to a typical pyramidal cell. In the final simulations the population of 600 pyramidal cells comprised 10 subpopulations of 60 neurons, each population having a different characteristic burst frequency.

Each single thalamic afferent supplies only about 1 synapse to any single post-synaptic neuron. We found that the input of about 40-80 such LGN afferents was suitable

for activating the network, if the maximum single thalamic synaptic conductance was also set to about 0.5nS. This number of cells represents roughly 10% of the total number of LGN contacts received by a pyramidal neuron.

The inhibitory population consisted of 100 neurons, each of which made 5 synapses onto each pyramidal target. The maximum single inhibitory synaptic conductance was 1nS.

The model network was simulated using the program CANON (written in TurboPascal by RJD, Douglas and Martin, 1990a), which executes on an AT-type microcomputer running under DOS. Simulation of 1 second of model time required about 3 hours of computation on a 16MHz 286AT.

Results and Discussion

Our initial simulations examined the bursting behaviour of pyramidal populations in the absence of either excitatory or inhibitory intracortical connections (Figure 2a,b). All of the pyramidal populations received the same constant thalamic input (Figure 4b, half amplitude of dashed trace). As anticipated, each of the pyramidal populations displayed bursting activity, and their burst frequencies differed according to their intrinsic characteristics. For example, the characteristic burst frequencies of the two cells shown in Figure 2a,b were 22Hz and 37Hz respectively when they were stimulated directly using an 1nA intra-somatic current injection. The same two pyramids displayed burst frequencies of 9Hz and 15Hz when activated by this particular geniculate input, and these frequencies are reflected in their power spectra (Figure 2a,b adjacent to voltage traces). The cross-correlation between these two cells (Figure 2e, upper trace) has very little power near zero time, confirming the lack of burst synchronization apparent from the time traces.

Introduction of excitatory intracortical connections between the pyramidal populations did not improve synchronization. On the contrary, the intracortical re-excitation implicit in these connections drove all of the pyramids to very high discharge rates (Compare time traces and power spectra of Figure 2a,b with c,d). The higher frequency intrinsic bursters fired continuously (Figure 2d). The cross-correlations between pyramids confirmed the lack of synchronization (Figure 2e, lower trace; no zero peak).

Introduction of a common inhibitory population (Figure 1c) led to a marked improvement in synchronization of pyramidal burst discharges (compare Figure 3a,b with Figure 2a-d). This is reflected in the marked increase in the zero peak of the cross-correlation (Figure 3d). Comparison of the power spectra of the synchronized cells (Figure 3 a,b) with their uncoupled, un-inhibited counterparts (Figure 2 a,b) shows that the synchronization process forces neurons with quite different burst frequencies (9Hz and 15Hz in these examples) towards a common burst frequency (averaging 17Hz in this example). The excitatory connections between the pyramidal populations provide a strong intra-cortical excitatory component that combines with the geniculate input (Douglas and Martin, 1990a). This enhanced average excitation rapidly initiates global bursting, while the common inhibitory feedback truncates the bursts that occur in each population and so improves the synchronization of subsequent burst cycles.

The synchronization of bursts is more robust than the periodicity of the bursts (Figure 3,4). This explains why the cross-correlations have a prominent zero peak, but relatively small side lobes. The inter-burst interval is dependent on both the post-burst hyperpolarization, and the strength of inhibition from the inhibitory population. The latter is in turn dependent on the average size of the previous burst in all the pyramids. This complex interdependence between events in many cells causes the interburst interval within a particular population to vary chaotically, even in the presence of constant thalamic input. This behaviour is very similar to that seen in real cortical neurons. For

example, compare the response of the model pyramids (Figure 3a,b 4a,c) with the intracellular signal derived from a real Complex cell during presentation of a preferred visual stimulus (Figure 3c). This *in vivo* recording was made in a layer 3 neuron of cat primary visual cortex (Douglas and Martin, unpublished).

Figure 4 shows the results of a simulation in which noise was added to the output of the geniculate populations. Comparison of Figure 4a,c with Figure 3a,b and the presence of a strong peak at zero time in the cross-correlation (Figure 4e, upper trace) indicate that burst synchronization was remarkably resistant to the noise superimposed on the geniculate input. The higher average burst frequency (23Hz) compared with the noise-free case (17Hz) (Figure 3a,b) is due to a larger geniculate signal.

The synchronization evolved rapidly, and was well established within about 100ms (2 bursts) of the onset of the pyramidal response. No particular population lead the bursting of the network. Instead the phase relations between any two populations changed chaotically from cycle to cycle so that the average phase between the cells remained zero (Figure 4, cross-correlation), as is seen *in vivo* (Engel et al., 1990). The onset of discharge in the inhibitory population necessarily lags behind the onset of the earliest bursts in pyramidal populations. However, the onset of inhibitory discharge occurred within about 5ms of the onset of the earliest pyramidal bursts and before the onset of the latest burst. Thus, we do not expect that the phase shift of inhibitory cells with respect to pyramidal cells will be easy to detect experimentally.

We found that the performance of the model was rather insensitive to the detailed cellular organization of the network as specified by the number of cells per population, number of synaptic contacts and magnitude of synaptic effect. The crucial organizational principle was the presence of cortical re-excitation and adequate global feedback inhibition. Evidence for these circuits has been found in intracellular recordings from cat visual cortex (Douglas and Martin, 1990a). This finding is consistent with the

mathematical proof of Kammen et al. (1990) that a number of oscillatory units driving a common feedback comparator can converge to a common oscillatory solution. However, our results indicate that synchronization occurs even in the presence of chaotic bursting discharge, when oscillation is not a prominent feature. Our results bear a qualitative similarity to those of Traub et al. (1987). The main difference is that in the case presented here fast, concentrated inhibition produces tightly coherent, high frequency (20Hz rather than 2-3Hz) bursting across the pyramidal populations.

Much has been written recently concerning *oscillations* in the neocortex. However, burst *synchronization* is the most compelling feature of our model cortical network. The inter-burst intervals were not regular, instead they varied chaotically. Consequently the power spectra of the discharges were broad, as has been noted *in vivo* (Freeman and van Dijk, 1987). Synchronous bursts from large populations converging on a postsynaptic target cell will produce very large transient depolarizations, which would be optimal for activating NMDA receptors. This suggests the possibility that learning occurs at times of synchronization. Coherent bursting may permit selective enhancement of synapses of common target neurons. If all inputs to the target cell are bursting rather than constant the chances of false correlations between different coherent populations are reduced. Moreover, varied interburst intervals could help to avoid phase locking between different sets of rhythmic signals impinging on the common target.

Conclusion

Our results suggest that the synchronized bursting observed *in vivo* between cortical neurons responding to coherent visual stimuli is a simple consequence of the known principles of intra-cortical connectivity. Two principles are involved. Firstly, intra-

cortical re-excitation by pyramidal collaterals amplifies the geniculate input signal and drives the co-activating pyramidal cells into strong coherent discharge. Secondly, global feedback inhibition converts the integrated burst discharges into a global reset signal that synchronizes the onset of the subsequent cycle in all the bursting pyramidal cells. Future work must investigate the processes that dynamically connect and disconnect populations of neurons to form coherent networks, the elements of which are then synchronized by the mechanisms outlined in this paper.

References

Connors, B.W., Gutnick, M.J., and Prince, D.A. 1982. Electrophysiological properties of neocortical neurons in vitro. *J. Neurophysiol*. **62**, 1149-1162.

Crick, F. 1984. Function of the thalamic reticular complex: the searchlight hypothesis. *Proc. Natl. Acad. Sci. USA*. **81**, 4586-4590.

Douglas, R.J., and Martin, K.A.C. 1990a. A functional microcircuit for cat visual cortex. *J. Physiol*. Submitted.

Douglas, R.J., and Martin, K.A.C. 1990b. Neocortex. In *The synaptic organization of the brain*. G.M. Shepherd, ed., pp. 389-438. Oxford University Press, New York.

Engel, A.K., Konig, P., Gray, C.M., and Singer, W. 1990. Stimulus-dependent neuronal oscillations in cat visual cortex: Inter-columnar interaction as determined by cross-correlation analysis. *Eur. J. Neurosci*. **2**, 586-606.

Freeman, W.J., and Dijk, B.W.v. 1987. Spatial patterns of visual cortical fast EEG during conditioned reflex in a rhesus monkey. *Brain Res*. **422**, 267-276.

Getting, P.A. 1989. Reconstruction of small neural networks. In *Methods in Neuronal modelling*. C. Koch and I. Segev, eds., pp. 171-194, MIT Press/Bradford books, Cambridge, Massachusetts.

Gray, C.M., and Singer, W. 1989. Stimulus-specific neuronal oscillations in orientation columns of cat visual cortex. *Proc. Natl. Acad. Sci. USA*. **86**, 1698-1702.

Gray, C.M., Engel, A.K., Konig, P., and Singer, W. 1990. Stimulus-dependent neuronal oscillations in cat visual cortex: Receptive field properties and feature dependence. *Eur. J. Neurosci*. **2**, 607-619.

Kammen , D., Holmes, P., and Koch, C. 1990. Collective oscillations in neuronal networks. In *Advances in neural information processing systems*. vol 2. D. Touretzky, ed., pp. 76-83. Morgan and Kaufman.

Malsburg, C.v.d., and Schneider, W. 1986. A neural cocktail-party processor. *Biol. Cybern*. **54**, 29-40.

Martin, K.A.C. 1988. The Welcome Prize Lecture: From single cells to simple circuits in the cerebral cortex. *Q. J. Exp. Physiol*. **73**, 637-702.

Sporns, O., Gally, J.A., Reeke, G.N. Jnr., and Edelman, G.M. 1989. Reentrant signalling among simulated neuronal groups leads to coherency in their oscillatory activity. *Proc. Natl. Acad. Sci. USA*. **86**, 7265-7269.

Traub, R.D., Miles, R., Wong, R.K.S. Schulman, L.S., and Schneiderman, J.H. 1987. Models of synchronized hippocampal bursts in the presence of inhibition. II. Ongoing spontaneous population events. *J. Neurophysiol*. **58**, 752-764.

White, E.L. 1989. Cortical Circuits: Synaptic Organization of the Cerebral Cortex - Structure, Function and Theory. Birkhauser, Boston.
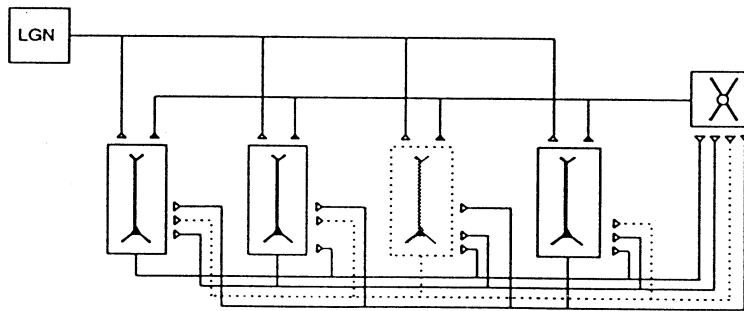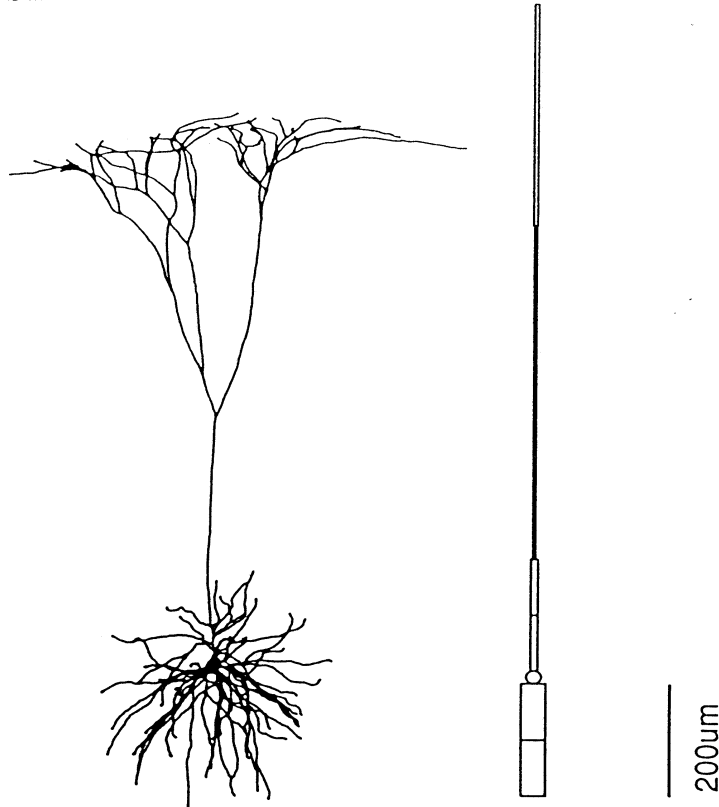
XSCHEM DRW

200um

Figure 1: (a) Layer 5 pyramidal cell from cat primary visual cortex intracellularly labelled with HRP and reconstructed in 3 dimensions (Douglas and Martin, 1990a). (b) Simplified compartmental model of the pyramidal cell. (c) Cortical network composed of model neurons. Each of ten populations (4 shown as rectangular boxes) composed of pyramidal cells (filled shapes) receives input from the LGN. Each pyramidal population sends afferents to all nine other pyramidal populations, and also to the common smooth cell population (box containing open stellate shape). The smooth cell population feeds back to all ten pyramidal populations.
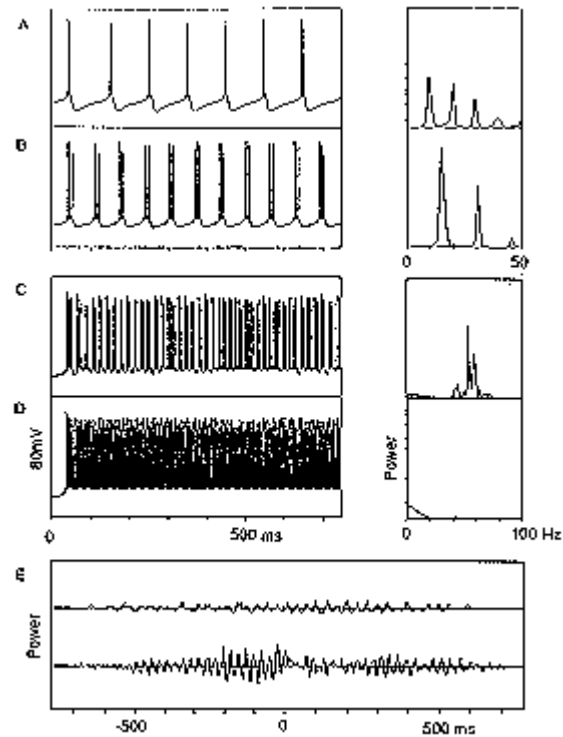
Figure 2: Response of partially connected model network to constant thalamic input (half amplitude of dashed trace in Figure 4b). In this and following Figures : power spectra are shown to the right of time traces; cross-correlations are shown at the foot of the figure; the amplitudes of the cortical power spectra are all to the same arbitrary scale, the LGN spectra (Figure 4b,d) are to a separate scale. (a) Pyramidal cell with no intra-cortical connections bursts rhythmically at 9Hz (fundamental frequency in adjacent power spectrum of voltage trace). (b) A different cell oscillates at 15Hz to same input. Cross-correlation of the output of these two cells (e, upper trace) exhibits no peak at zero time, indicating no correlation between these two signals. (c) Response of the same model cell as in a, but now including reciprocal excitatory connections to all 9 other populations. The consequent enhanced excitation results in higher frequency discharge (50-60Hz, see adjacent power spectrum). (d) Enhanced excitation causes the intrinsically higher frequency cell shown in b to latch up into continuous discharge. In this example all the power is at 200-300Hz, which is off-scale. Cross correlation of latter two traces (lower trace in e) indicates that their discharge is not synchronized.
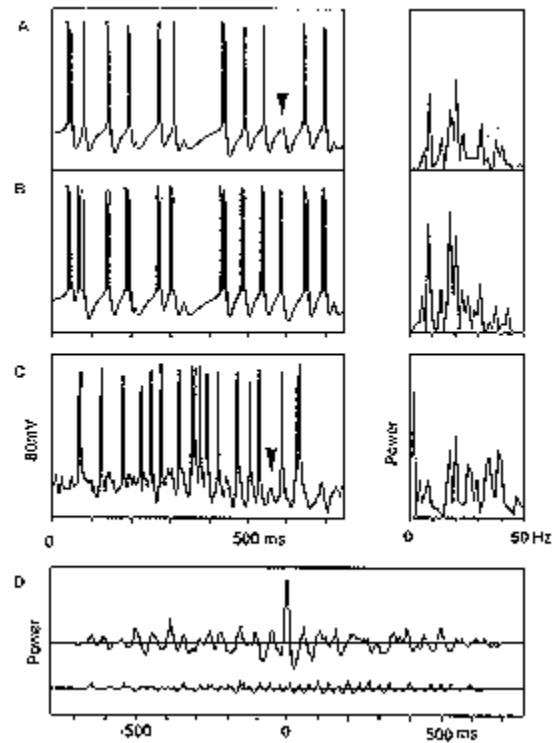
Figure 3: Response of fully connected model network to constant thalamic input (half amplitude of dashed trace in 4b). (a,b) Response of same cells shown in Figure 2a,c, but now incorporating common feedback inhibition (Figure 1c). The bursts in the two populations are synchronized, as indicated by the prominent zero peak in their cross-correlation (upper trace in d, for comparison lower trace is same as Figure 1e). Their common inter-burst frequency (17Hz) is reflected in their power spectra. Notice that each cell fires only in synchrony with the others. If a cell misses a burst (arrowed in b) then it fires again only on the next cycle. (c) Response of real complex cell in cat primary visual cortex to optimally orientated moving bar (Douglas and Martin, unpublished). Compare with model responses in Figure 3b,c and Figure 4a,c. Note missed burst (arrowed).
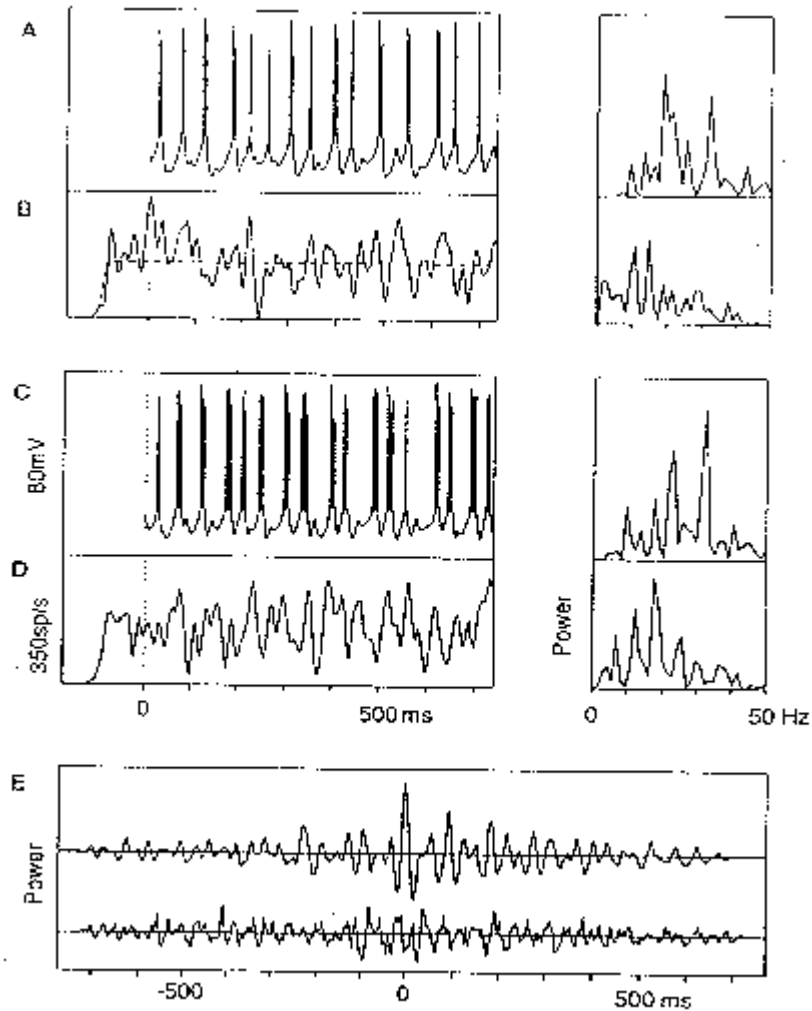
Figure 4:   Synchronization is not dependent on identical, constant thalamic input. In this example five pyramidal populations were driven by LGN input shown in b, the other five by input shown in d. Inputs are the sum of a constant signal (dashed trace in b) plus noise with 24% power of signal. Comparison of the outputs of the highest and lowest intrinsic frequency cells (a and c) show that the burst synchronization is not diminished by this procedure. As in Figure 3, superposition of peaks of power spectra and prominent zero peak on cross-corellogram (e, upper trace) confirm synchronization of pyramidal population discharges. The synchronization is lost if intracortical connections are removed (e, lower trace). Notice that the peaks of power spectra of LGN input (b and d) do not coincide with those of the model output (a and c), indicating that the cortical interburst frequency (averaging 23Hz) is insensitive to the spectral characteristics of the LGN input.

Table 1. Model parameters

Pyramidal Cells:
resting potential	-66mV
axial resistance	200ohmcm
specific membrane capacitance	$2\mu F/cm^2$
leak conductance	$0.1\ mS/cm^2$
calcium decay time constant	7-20ms
spike Na conductance	$400ms/cm^2$
τ_m	0.05ms
τ_h	0.5ms
delayed rectifier K conductance	$80mS/cm^2$
τ_m	0.5ms
persistent Na conductance	$2mS/cm^2$
τ_m	2ms
calcium-dependent K conductance	$15mS/cm^2$
τ_m	2ms
'A-current' K conductance	$2mS/cm^2$
τ_m	20ms
τ_h	100ms
calcium conductance	$0.5mS/cm^2$
τ_m	2ms
EPSP synaptic conductance (300s/s)	0.5nS
EPSP τ_m	5ms
EPSP τ_h	10ms
IPSP synaptic conductance (300s/s)	1nS
IPSP τ_m	2ms
IPSP τ_h	3ms

Smooth Cells:
resting potential	-66mV
axial resistance	100ohmcm
specific membrane capacitance	$2\mu F/cm^2$
leak conductance	$0.1\ mS/cm^2$

spike Na conductance	700mS/cm^2
τ_m	0.05ms
τ_h	0.5ms
delayed rectifier K conductance	400mS/cm^2
τ_m	0.2ms
EPSP synaptic conductance (300s/s)	0.5nS
EPSP τ_m	0.1ms
EPSP τ_h	0.1ms
axon conduction delay + synaptic delay	2ms

CHAPTER V

Inhibition Synchronizes Sparsely Connected Cortical Neurons Within and Between Columns in Realistic Network Models.

Abstract

Networks of compartmental model neurons were used to investigate the biophysical basis of the synchronization observed between sparsely-connected neurons in neocortex. A model of a single column in layer 5 consisted of 100 model neurons: 80 pyramidal and 20 inhibitory. The pyramidal cells had conductances that caused intrinsic repetitive bursting at different frequencies when driven with the same input. When connected randomly with a connection density of 10%, a single model column displayed synchronous oscillatory action potentials in response to stationary, uncorrelated Poisson spike-train inputs. Synchrony required a high ratio of inhibitory to excitatory synaptic strength; the optimal ratio was 4:1, within the range observed in cortex. The synchrony was insensitive to variation in amplitudes of postsynaptic potentials and synaptic delay times, even when the mean synaptic delay times were varied over the range 1 to 7 ms. Synchrony was found to be sensitive to the strength of reciprocal inhibition between the

inhibitory neurons in one column: Too weak or too strong reciprocal inhibition degraded intra-columnar synchrony. The only parameter that affected the oscillation frequency of the network was the strength of the external driving input which could shift the frequency between 35 to 60 Hz. The same results were obtained using a model column of 1000 neurons with a connection density of 5%, except that the oscillation became more regular.

Synchronization between cortical columns was studied in a model consisting of two columns with 100 model neurons each. When connections were made with a density of 3% between the pyramidal cells of each column there was no inter-columnar synchrony and in some cases the columns oscillated 180º out of phase with each other. Only when connections from the pyramidal cells in each column to the inhibitory cells in the other column were added was synchrony between the columns observed. This synchrony was established within one or two cycles of the oscillation and there was on average zero ms phase difference between the two columns. Unlike the intra-columnar synchronization, the inter-columnar synchronization was found to be sensitive to the synaptic delay: A mean delay of greater than 5 ms virtually abolished synchronization between columns.

Introduction

Although the traditional role for inhibition has been to regulate the level of excitation, recent experimental and modeling studies suggest an additional function for inhibition in cortex: Regulating the timing of action potential occurrence (Gray et al., 1992; Lytton & Sejnowski, 1991; Bush & Sejnowski, 1994). In this study, we explore the influence of inhibition on the temporal pattern of spike firing both within and between columns consisting of small networks of sparsely connected model neurons.

Synchronous oscillatory firing of populations of cortical neurons at frequencies around 40 Hz has been observed within and between many different cortical areas in primates and cats both awake and anaesthetized (for recent review see Singer (1993)). It has been proposed that this synchronous activity is used to group separated parts of single objects (Engel et al., 1991a; Sporns et al., 1991) and even signal visual awareness (Crick & Koch, 1990). Although there is still much debate as to the role and significance of synchrony, it is generally agreed that many cortical neurons can fire synchronously under some conditions. Therefore, it is worthwhile to discover exactly how cortical tissue generates and sustains synchronized oscillatory firing of its component neurons, both within a single column and between columns that may be located in different hemispheres (Engel et al., 1991b). For simplicity, we have restricted our model to a single layer of cortex (layer 5). Slice experiments have shown that isolated layer 5 is capable of intrinsic generation of oscillatory activity, although at lower frequencies than those discussed here (Silva et al., 1991). It is possible that intrinsic bursting cells *in vivo* have significantly higher bursting frequencies than those *in vitro*, and it is also possible that there are other populations of intrinsic bursting cells with different intrinsic frequencies (McCormick et al., 1993).

A number of other studies have modeled synchronized oscillations in cortex at a simpler level of physiological realism, many of them focusing on how such activity might be useful, for example in perceptual grouping (Koenig & Schillen, 1991; Sporns et al., 1989). This study does not address the function of synchronization; instead we have constructed a physiologically realistic network model based on ionic currents and conductances, with every parameter directly representing a physiological variable. We intended to determine whether the presently available data on the physiology and microanatomy of cortex are sufficient to explain how synchronized oscillatory firing occurs and how certain physiological variables affect this activity. We found both intra-

and inter-columnar synchronization to be robust to changes in parameters known to have a wide degree of variation in cortex. Some parameters did affect synchronization, such as the degree of connectivity and the involvement and interaction of inhibitory interneurons.

A previous pilot study (Bush & Douglas, 1991), using a simplified biophysical model of a cortical column, established a basic mechanism for cortical synchronization to arise. This model included a number of simplifications: It consisted of only 11 fully connected cells and each synapse had to be spread out in time as well as increased in amplitude to compensate. One of the simplifications led to an artifactual phenomenon explained in the Discussion. The present model is a much more faithful simulation of a piece of cortical tissue, incorporating a more realistic model reduced cell, many more cells, sparse connectivity and connections between as well as within columns. This more accurate model not only produced results that were better fits to the experimental data, but also allowed us to determine systematically how and in what way each physiological variable affected synchronization, which was not possible with the simpler model.

We have also modeled the interactions that occur between columns. When long-range horizontal connections between columns were first discovered in neocortex they seemed to imply a paradox: These connections extended far beyond the receptive fields of single cells, yet stimulating the surrounding area outside the receptive fields of undriven cells was not effective in driving them (Gilbert et al., 1990). This suggested that perhaps these connections were relatively weak, and indeed the density of synaptic connectivity is much higher within a column than between columns (Kisvarday & Eysel, 1992; Martin, 1988). Although excitatory postsynaptic potentials (EPSPs) can be generated in neurons when long range horizontal afferents are stimulated, it is not possible to generate action potentials by stimulating these fibers alone (Hirsch & Gilbert, 1991). This suggests that these connections might have more of a modulatory role. We have used our model to simulate inter-columnar connectivity to explore this possibility.

Methods

Model neurons

Simulations were performed using standard techniques for compartmental models of branching dendritic trees (Rall, 1964). The primary neuron used in our networks was a layer 5 pyramidal neuron modeled by 9 compartments. This model neuron was reduced from a 400 compartment model of a reconstructed cat visual cortex pyramidal cell (Koch et al., 1990) using a method that preserves essential electrotonic parameters (Bush & Sejnowski, 1993). The reduced model pyramidal cell had a specific membrane resistance $R_m = 7042$ Ωcm^2 and a specific capacitance $C_m = 2.84$ μ F/cm^2 which produced an input resistance $R_{in} = 45$ MΩ and a membrane time constant $\tau_m = 20$ ms. Since approximately 20% of neocortical cells are inhibitory (Douglas & Martin, 1990) 20% of our cells were 7 compartment inhibitory (basket) neurons (not based on a reconstructed cell) with $C_m = 2.21$ μ F/cm^2 and $R_m = 6800$ Ωcm^2 giving an $R_{in} = 164$ MΩ and $\tau_m = 15$ ms. The values of C_m and R_m for the reduced cells are respectively larger and smaller than for the full cells to compensate for the reduction in surface area (Bush & Sejnowski, 1993). For all model cells the axial resistivity was 200 Ωcm and the resting membrane potential was -55 mV ('resting' assumes background synaptic activity producing a steady depolarization). The values chosen for these passive parameters are within the typical range observed in neocortical cells *in vivo* and are have been discussed elsewhere (Bush & Sejnowski, 1994).

Each model neuron had Hodgkin-Huxley-type active conductances at the soma only. These conductances were implemented exactly as described in Bush & Sejnowski

(1994), using a kinetic scheme developed by Borg-Graham (1987). The pyramidal cells had fast sodium and potassium conductances (g_{Na} + g_{Kd}) to produce action potentials, a fast high-threshold calcium conductance (g_{Ca}) to introduce calcium into the cell during each spike, and a calcium-dependent potassium conductance (g_{Kca}) to produce hyperpolarizations that terminated bursts of spikes. Intracellular calcium accumulated in the soma compartment and decayed exponentially to its resting value with a time constant that was different for each cell, between 10-50 ms. The different calcium decay rates gave each pyramidal cell a different intrinsic bursting frequency. The basket cells had only fast sodium and potassium conductances and fired continuous trains of high-frequency spikes to constant current input. Fig. 1 shows the intrinsic firing properties of the model pyramidal and baskets cells.

During network simulations noise was injected into the soma of every model neuron in the form of a current that changed every time step to a random number uniformly distributed between positive and negative 1 nA for pyramidal cells and 0.3 nA for basket cells. This method produced a varying resting membrane potential similar to that seen *in vivo* due to background synaptic inputs, without changing R_{in} and τ_m. This background noise made synchronization more difficult and produced a background resting firing rate of a few Hz.

Synaptic connectivity

Synaptic conductances were modeled using an alpha function conductance change (1 ms to peak) activated on the postsynaptic dendrite with some delay after the presynaptic spike (Bernander et al., 1991). Peak amplitudes and synaptic delays for each connection were randomly assigned according to a gaussian distribution with a standard deviation equal to half the mean. This reproduced the large range of delays and

postsynaptic potential (PSP) amplitudes observed experimentally. The mean synaptic delay time was 1.2 ms with a fixed minimum of 0.5 ms (Mason et al., 1991; Nicoll & Blakemore, 1990). Mean peak PSP amplitudes were varied but were typically 1-2 nS except for inhibitory synapses on pyramidal cells, which were typically 4-8 nS. This reflects the observations of (Komatsu et al., 1988) who found that single inhibitory conductance changes were significantly larger than single excitatory ones. This may reflect the fact that basket cells typically make multiple synaptic contacts on the proximal dendrites of a target pyramidal cell while pyramidal cells only make one or a few contacts per target (Somogyi et al., 1983; Gabbot et al., 1987). The reversal potential for EPSPs was 0 mV and that for inhibitory postsynaptic potentials (IPSPs) was -65 mV (10 mV below the resting potential) (Connors et al., 1988).

Excitatory synapses on model pyramidal cells were made on the terminal basal and oblique dendritic compartments, whereas inhibitory synapses were made onto the soma and proximal dendrites. Excitatory and inhibitory synapses were made onto all compartments of the basket cells (Douglas & Martin, 1990). Pyramidal cells received external driving input from uncorrelated Poisson spike trains. Typically each cell received four 20 nS excitatory synapses active at a mean rate of 200 Hz. This is equivalent to a larger number of inputs active at a lower rate.

Connectivity within a single column, at the scale of 100-200 μ m, appears to be random in the sense that axons make contacts on all potential targets within their zone of arborization (White, 1989). Thus, there was no spatial topography within our model columns: Every cell had an equal chance of contacting every other cell (but no self-connections were allowed). The density of connectivity within a column has been estimated by dual intracellular impalement and spike-triggered averaging to be 5-15% (Mason et al., 1991; Thomson et al., 1988; Komatsu et al., 1988), although it may be lower in the deeper layers (Nicoll & Blakemore, 1990; Nicoll & Blakemore, 1993;

Thomson et al., 1993). We explored a range of different connection densities: For the 100 neuron columns presented here we used a connectivity of 10%. Thus each model cell received input from exactly 8 pyramidal cells and 2 baskets cells, randomly chosen. Since each neuron received input from only 10 other neurons in the column, it was necessary to add a scaling factor to the peak synaptic strengths. For a 100 neuron column with 10% connectivity all synaptic strengths were multiplied by 10. For a 1000 neuron column with 10% connectivity no scaling factor was necessary.

In order to view rapidly and easily the average activity of the whole network an analog of the local field potential (LFP) was calculated for each simulation, called the local averaged potential (LAP). This was a running average of all the membrane potentials of all the pyramidal cell somas. The presence of oscillations in this LFP analog was an indicator of synchronized activity in the pyramidal cell population. Our LAP is not directly equivalent to a real LFP, which is a sum of all the local currents, both voltage- and ligand-gated, weighted by the distance of the sources from the electrode. However, our LAP is a direct measure of the average neuronal activity and for the task of showing synchronous oscillations it is actually better suited than the real LFP.

A quantitative measure of the degree of synchronization between two columns is provided by the correlation amplitude (CA), ranging from -1 to +1, which is the height of the peak closest to zero in the cross-correlation of the two network LAPs (Gray et al., 1992). The phase shift of this peak from zero provides a measure of the tightness of the synchronization. For single columns the CA is measured for the first peak away from zero in the auto-correlation of the LAP. This number reflects the regularity and amplitude of the oscillatory discharges of the synchronized column. The phase shift of this peak gives the period of the oscillation.

For some data the power and phase spectra were calculated using the software package ACE/gr (Paul Turner, Oregon Graduate Institute of Science and Technology) which calculates the spectrum by

$$Power(\omega) = \sqrt{x^2(\omega) + y^2(\omega)}$$

where $x(\omega)$ and $y(\omega)$ are the real and imaginary frequency coefficients computed by the FFT. The phase was calculated by

$$Phase(\omega) = \tan^{-1}\left(\frac{y(\omega)}{x(\omega)}\right)$$

Simulations

All simulations were carried out on a MIPS Magnum 3000/33 using a modified version of CABLE (Hines, 1989). We used a time step of 0.1 ms with 2nd order correct numerical integration. A simulation with 100 neurons and 10% connectivity took 9 minutes of computer time to simulate 500 ms of real time.

Results

Synchronization within a single column

Fig. 2 shows a simulation of a 100 neuron column (80 pyramidal cells, 20 basket cells) without synaptic connections. The pyramidal cells were all driven by uncorrelated Poisson spike train inputs at a mean frequency of 200 Hz, but they had different intrinsic bursting frequencies because of different internal calcium elimination rates (see Methods). The bursting was less regular than in Fig. 1 due to the injection of noise into each pyramidal cell soma. The basket cells received no driving input and only fired a few spontaneous spikes due to background noise. Because there were no synaptic connections, there were no correlations between the neurons and the LAP was flat after the initial transient burst.

Fig. 3 shows the output of the same network when the neurons were randomly connected at a density of 10%. Oscillations were visible in the LAP indicating synchronized firing of the pyramidal cells (CA = 0.56 and the period of oscillation was 22.2 ms, giving a frequency of 45 Hz). The basket cells showed evidence for bursting at the same frequency as the pyramidal cells even thought they have no intrinsic oscillatory properties; they are directly driven by the pyramidal cells, so the fact that they fired in bursts is further evidence of synchronized population discharge. The mechanism of synchronization is detailed in the Discussion.

As observed in experimental recordings *in vivo* (Gray et al., 1992), the synchronization sometimes spontaneously ceased (in this case at 100 and 350 ms) and then reappeared. The basket cell bursts in the model became less clumped at these times. Since the driving input to the network was stationary throughout, these changes were not due to changes in the nature of the external input. The synchronization was a statistical phenomenon, as observed in the experimental recordings; it was often difficult to see a regular oscillation in the spike train of a single cell, especially if it did not fire many spikes, and of course it was impossible to see synchronization. When examining all 7 single-cell traces, one observes moments when the spikes all 'lined up', but even in these cases there

was significant jitter in individual spike times. Comparing two traces spike by spike, such as the top two pyramidal cell traces in Fig. 3, we often found few instances of simultaneous firing, although on average both cells were locked to the underlying oscillation of the population (shown by the LAP). In other cases (such as the 3rd and 4th trace) the synchronization of spike firing was clearer. It is important to have an averaged measure of the activity of the whole population (such as the LAP shown here) to determine if the component cells are collectively oscillating in synchrony.

In networks with 100 neurons we could not obtain good synchrony with connection densities of less than 10%, but lower connection densities were effective when simulating networks with more neurons. In Fig. 4, 1000 neurons were connected at a density of 5%, with a synaptic strength scaling factor of 2 (see Methods). We obtained the same results with a connectivity of 10% and no scaling factor; i.e. the synapses had same strengths as in real cortex. The oscillation and synchronization in a network of 1000 neurons was highly regular, as a consequence of the law of large numbers, although there was still a significant amount of jitter in spike times at the level of single cell traces (CA = 0.58 and the period was 19.8 ms, giving a frequency of 50.5 Hz, slightly higher than the 100 cell network). Even though in terms of numbers this simulation may be more realistic than the 100 neuron simulations, the output of the smaller network appears more realistic (less regular). This is considered further in the Discussion.

The membrane potential trace of the 4th pyramidal cell in Fig. 4 is shown at a higher temporal resolution in Fig. 5. The large compound EPSP present on each cycle of the population oscillation is clearly visible. Spikes only arise from the top of these compound EPSPs, but not every compound EPSP causes a spike. This figure can be compared to Fig. 6, an intracellular recording from a cat visual cortex neuron firing oscillatory bursts during optimal stimulation. There is a rhythmic series of large compound

EPSPs, some of which cause spiking. There are no spikes at other times in the phase of the oscillation.

Sensitivity to varying parameters

The distributions of synaptic conductances and time delays in all of our simulations had large standard deviations, so that synaptic connections with an overall mean of 1 nS often had values as small as 0 nS and as large as 3 nS and time delays with a mean of 1.2 ms had values from 0.5 ms up to as high as 4 ms. The synchronized firing of the network was not affected by this variability, and was in general a robust phenomenon: We repeated all of our simulations with a noise level 4 times higher than that shown here (peak current 4 nA for pyramids, 1.2 nA for basket cells - see Methods) and with a resting membrane potential of -65 mV instead of -55 mV, but synchronized oscillation was still present. With some sets of parameters (such as higher connectivity, stronger inhibitory synapses and lower resting membrane potentials) we were able to obtain even stronger synchronization, but the values of parameters used for the simulations presented in this paper are probably closer to those in the real cortex.

We found that increasing the mean synaptic delay within a column did not disrupt synchronization, even when the mean delay was as large as 7.2 ms rather than 1.2 ms (not shown). In this case, the oscillation became more regular, with every cell firing on every cycle and the cells with the highest intrinsic bursting frequency always leading the others. The frequency of oscillation of the network was also decreased due to the long duration of each burst. The only other way we found to alter the frequency of oscillation of the network was to vary the strength of the external driving input. By changing this parameter it was possible to vary the oscillation frequency of the network in the range 35-60 Hz.

Network synchronization was generally resistant to variations in synaptic strengths. However, inhibitory synapses had to be stronger than excitatory ones. We found that a ratio of approximately 4:1, the value initially chosen on the basis of physiological results (see Methods), was optimal for realistic synchronization. In networks without inhibition, simulating the effect of bicuculine, excitatory feedback operates unconstrained producing large paroxysmal burst discharges, with the membrane potentials of the highest intrinsic frequency cells latching up past spike threshold (not shown). The only inhibitory/hyperpolarizing force in these networks was the intrinsic potassium conductance of the pyramidal cells, which was not strong enough to control the excitatory feedback.

The network was also somewhat sensitive to the strength of reciprocal inhibition between the basket cells. Although it is known from anatomical studies that local inhibitory interneurons make synaptic connections on each other (Douglas & Martin, 1990), very little is known about the function of these connections beyond the vague concept of 'disinhibition'. Fig. 7B shows the same network LAP as in Fig. 3 (CA = 0.56) and one of the basket cell traces. Fig. 7A is the LAP from the same network with inhibitory contacts between basket cells removed. Synchrony was slightly weaker (CA = 0.50) because the basket cell bursts were no longer terminated by inhibitory feedback and as a result became less discrete, sometimes continuing into the next cycle. This produced a lower frequency of oscillation (38 Hz compared to 45 Hz in Fig. 7B). This higher level of inhibitory activity also resulted in less activity in the pyramidal cell population (not shown). When synapses between baskets cells were made very strong (Fig. 7C) synchronization was severely disrupted (CA = 0.04) . In this case basket cells were inhibited before they could provide effective inhibition to the pyramidal cell population so the pyramidal cells began to fire continuously instead of in synchronous bursts. Thus, mutual inhibition between inhibitory interneurons within a single column is important for

producing synchronized population oscillations, but the strength of this inhibition should not be as great as that between inhibitory cells and their pyramidal targets.

Synchronization between columns

Since synchronization has been observed between different cortical columns and even different cortical areas (Eckhorn et al., 1988; Gray et al., 1989; Engel et al., 1991b; Kreiter & Singer, 1992; Koenig et al., 1995) we performed simulations to examine how synchronization arises between two columns, both internally synchronized. Two columns of 100 neurons each were simulated, each column connected as in Fig. 3. Connections between the columns were then added to see if synchronization between them could be established. Long-range connections in cortex are mediated by pyramidal cell axons, and these axons make most of their synapses on other pyramidal cells, although at a significantly lower density than within their own column (Hirsch & Gilbert, 1991; Martin, 1988; Kisvarday & Eysel, 1992). Therefore, we started by connecting the pyramidal cells between the two columns with a density of 2.5% (each pyramidal cell received a synapse from 2 pyramidal cells in the other column). In this case and all other simulations using pyramidal-pyramidal connections only, we were not able to obtain good synchronization between the two columns (not shown). The internal synchrony of each column appeared to be degraded and the only clear tendency we noted was for the columns to sometimes oscillate 180 degrees out-of-phase with each other. With some parameter choices this was a very strong effect, but in no case did clear synchronization with zero phase lag develop between the columns.

Long-range pyramidal cell axons make some of their synapses on dendritic shafts, many presumably belonging to inhibitory neurons (Douglas & Martin, 1990; White, 1989). Thus we added intercolumnar connections from pyramidal cells to basket cells to see if

this would synchronize the two columns. Fig. 8 shows the results of a simulation with two columns connected together at a density of 4% (each pyramidal cell received 3 synapses and each basket cell received 4 synapses from pyramidal cells in the other column). When the intercolumnar connections were turned on at 100 ms, the two columns immediately began to synchronize (CA = 0.61) and maintained near zero average phase difference (1.2 ms) for the duration of the simulation. When one column spontaneously desynchronized (eg at 350 ms) the other did too, then both rapidly resynchronized. Intercolumnar synchronization could not be obtained by simply increasing the number of pyramidal-pyramidal connections. Thus the pyramidal-basket intercolumnar connection, while numerically small, was vital for intercolumnar synchronization.

Fig. 9A shows the cross correlation of two LAPs from the simulation shown in Fig. 8. The central peak is at -1.2 ms indicating tight synchronization between the two populations. For comparison Fig. 9B shows the cross correlation between two LAPs from a simulation in which the two columns were not connected (CA = 0.17). In this case there was a peak at some random non-zero position indicating that the two populations were not synchronized with each other.

The simulation of the synchronization between the two columns in Fig. 8 was extended for 6.5 sec. Fig. 10B shows the averaged power spectra of the two LAPs, with a clear peak at 44 Hz, the frequency of the population oscillation. There may be a smaller peak near 22 Hz, a subharmonic of the main peak. Fig. 10A shows the difference between the phase spectra of the two LAPs over the same frequency range as the power spectra. This phase difference has large, random fluctuations at all frequencies except around the frequency of the population oscillation. In this region the phase difference was consistently small, and at 44 Hz it was almost zero. This is evidence that the two populations were oscillating at 44 Hz in phase with each other.

Fig. 10C,D shows the same results for the two unconnected columns. Although there was significant power in both spectra around 40 Hz, a single peak was not as clear. The phase difference did not decrease around 40 Hz, indicating that the two columns were oscillating at random phase with respect to each other.

Increasing synaptic time delays between neurons within a column did not disrupt synchronization. However, increasing the synaptic delay of the intercolumnar connections adversely affected the synchronization of the two columns. As the delay was increased to 3-4 ms a phase shift of a few ms developed between the two populations. When the intercolumnar delay was greater than 5 ms synchronization was severely disrupted. Fig. 11 shows two columns connected with a mean delay of 7.2 ms. The synchronization of the two columns was weak (CA = 0.39) because the internal synchrony of each column was weak and sporadic. We conclude that to maintain effective synchronization two columns must be connected with a delay of approximately 5 ms or less. The implications of this result will be considered in the Discussion.

Effectiveness of long-range horizontal axons

The results of our model suggest that intercolumnar connections mediated by long-range horizontal axons are modulatory in function rather than directly excitatory, primarily because of inhibition directly evoked by long-range axonal stimulation. In order to test the validity of this result we have compared our model with an *in vitro* experiment directly testing the effects of long-range axonal stimulation. Fig. 12 shows a simulation of an experiment performed in a cat cortical slice preparation (Fig. 7 of Hirsch & Gilbert (1991)). In the experiment, shocks of increasing strength were applied to lateral fibers in the upper layers, presumably stimulating horizontal pyramidal axons connecting distant columns. Synaptic responses were recorded from target pyramidal and presumed

inhibitory interneurons. Our simulation produced the same results as the experiment: At low stimulus strengths EPSPs were observed in both pyramidal and basket cells. Due to the lower threshold of the basket cells, spikes were sometimes produced. As the stimulus strength increased the basket cells fired more spikes in response; in contrast, the pyramidal cells were inhibited by stronger shocks. This inhibition was a direct result of the response of the basket cells. Thus, due to the relatively low numbers of inter-columnar axons and the lower threshold of the target basket cells, the excitatory inter-columnar fibers do not necessarily have a strong excitatory effect on their target columns.

Fig. 13 shows the output of two connected columns, the bottom one driven normally by external input, the top receiving no external input until 350 ms. Although the top column received input from the bottom one that was sufficient to synchronize the two populations when they were both being driven (after 350 ms), this input was not strong enough to cause significant firing before 350 ms. The low firing rate in the top column was not significantly higher than the spontaneous rate due to noise.

Discussion

Synchronized oscillations have been demonstrated in a wide variety of models of interacting neurons ranging from models based on coupled intrinsic oscillators (Winfree, 1967; Schuster & Wagner, 1990; Sompolinsky et al., 1990; Williams, 1992) to more realistic models incorporating the characteristics of real neurons (Wilson & Cowan, 1972; Wilson & Bower, 1991; Sporns et al., 1989; Bush & Douglas, 1991). The former allow analysis while the latter allow detailed comparisons to be made to recordings from cortical neurons. In particular, our realistic model was highly constrained by the morphology and physiology of cortical neurons and the patterns of connectivity observed in primary

sensory cortices. Parameters that were not fully constrained were varied over a wide range to find values that led to a match with physiological recordings. Our main results concern the essential role of inhibitory neurons in synchronizing collective oscillations within and between sparsely connected columns of cortical neurons.

Synchronization in a single column

The mechanism of synchronization is similar to that described previously (Bush & Douglas, 1991): Pyramidal cell burst discharges rapidly excite other pyramidal cells, producing a large compound EPSP in all cells in the network, including the inhibitory basket cells. The basket cells are driven to fire simultaneously, their feedback inhibition onto the pyramidal cells then terminates the population burst and, together with intrinsic potassium conductances, produces a post-burst hyperpolarization. Since the input resistance of the pyramidal cells is greatly reduced during this hyperpolarization (Bush & Sejnowski, 1994), there is less chance of the cell spiking during this time (out of phase with the oscillation). Cells with intrinsic bursting frequencies that vary over an octave (15 - 30 Hz) can be made to synchronize together at one frequency (eg. 45 Hz) by this mechanism. Cells with lower intrinsic frequencies tend to 'miss' cycles of the oscillation rather than fire out of phase and they tend to fire single spikes instead of bursts.

This mechanism also produced synchronization in networks of regular firing pyramidal cells that do not fire in bursts (not shown). The population EPSPs were smaller and shorter in duration without bursting and of course the pyramidal cells fired less spikes; thus, bursting improves but is not necessary for synchronization. A combination of bursting and regular firing cells also produced synchronization (not shown).

The synchronized oscillations demonstrated by the network shown in Fig. 3 display a number of features in common with experimental recordings (Engel et al., 1990): The

similarity of the form of single cell traces from simulation and experiment (Figs. 5 and 6) suggests that the model has captured some of the most basic characteristics of the biophysical mechanism of synchronous oscillatory firing in cortex. Intracellular recordings from cat striate cortex demonstrate oscillations that are stimulus dependent (absent during spontaneous activity) and increase in amplitude during stimulation while the cell is hyperpolarized (Jagadeesh et al., 1992; Bringuier et al., 1992). This suggests that the oscillations arose from rhythmic intracortical excitatory synaptic input. Of course other mechanisms may produce the same type of behavior (Llinas et al., 1991); (McCormick et al., 1993), and several mechanisms may be involved.

Another feature observed in the network simulations is the variability of synchronization. In the model, as in the experimental data (Gray et al., 1992), periods of synchrony generally lasted a few hundred ms, with rapid spontaneous transitions into and out of the synchronized state. In addition, the presence of synchrony varied from trial to trial (using a different seed for the random number generator for noise and Poisson input). Throughout each trial the external driving input was a stationary Poisson process; thus, this variability cannot be due to changes in the statistics of the input and the complex internal dynamics of the network must be responsible for the rapid switching between synchronous and asynchronous firing. However, in the 1000 neuron simulation the variability in the LAP was reduced (although individual cell traces still showed marked variability) (Fig. 4). Therefore, one possibility is that synchronized oscillations in neocortex are mediated by cell groups composed of about a hundred neurons. Synaptic strengths would have to be very large in a 100 neuron network (scaling factor of 10, giving EPSPs of 10 nS - see Methods). There is recent evidence that some single EPSPs could be this large, producing quantal depolarizations of a few mV instead of a few hundred μV (Thomson et al., 1993).

With 1000 neurons we were able to use synaptic strengths without a scaling factor, evidence that oscillating neuronal groups are made up of on the order of 1000 neurons. This would fit better with a consideration of the number of cells involved: Given approximately 100,000 neurons/mm^3 and a column 100-200 μ m in diameter there are on the order of 1000 neurons in one layer of one column. If this is the case then the variability described above must be due to some source not included in the model. There are many potential candidates, including low probabilities of quantal release, use- and time-dependent potentiation and/or depression of synaptic strengths, the action of neuromodulators or some extrinsic cortical or subcortical signal. In a few 1000 neuron simulations the probability of an EPSP/IPSP given a presynaptic action potential was reduced to 0.5 or lower (not shown): The amplitude and regularity of the LAP oscillation was significantly reduced. If this is not the case and instead 100 neurons is the minimal size of an oscillating group, then a single layer in a single column could contain many such groups, which would seem unlikely in primary visual cortex, although association areas such as entorhinal cortex may support such smaller groups.

Experimental recordings also show a frequency variability of synchronized activity within and between trials ranging from 40-60 Hz (Gray et al., 1992). The model of Bush and Douglas (1991) displayed frequency variability within a single trial, but this was an artifact of having only one inhibitory neuron in their model: A single extra spike from this neuron would significantly delay the onset of the next population burst. We could obtain different frequencies of oscillation in our more realistic simulations only by changing the strength of the external driving input. In this way the frequency could be changed in the range 35-60 Hz. The external input was kept constant within a trial and a change in oscillation frequency was never observed. Therefore, we suggest that the frequency variability observed in experimental recordings is due to a concomitant variability in the strength of the external input. External here means external to the synchronized group,

coming from the thalamus or other areas of cortex. For a pyramidal cell in one of our simulations, approximately half of its excitatory input was external stationary Poisson spike trains and half was excitatory feedback from other pyramidal cells in the network, the sole source of synchronized inputs.

There was no external input onto the basket cells in our model. If we included such input network synchrony was degraded. Thus, although external inputs to a cortical column do contact inhibitory cells as well as pyramidal cells (Douglas & Martin, 1990), our results suggest that the vast majority of input to the inhibitory interneurons in a synchronized oscillating cell group comes from excitatory (pyramidal) cells in that same group. Alternatively strong external inputs to inhibitory cells may be correlated, either from the thalamus or other cortical regions, as long as they are synchronized with that column.

Synchronization between columns

Zero-phase lag synchrony between two populations was established within one or two cycles of the intercolumnar connections being activated (Figs. 8 and 13). Often the oscillation in one column would continue unperturbed while a cycle in the other would be suppressed or a new one prematurely initiated to get the two columns in phase. Connections from the pyramidal cells in a column to both the pyramidal cells and the basket cells in the other column were required. The greater effectiveness of inhibitory input in producing synchronization (Lytton & Sejnowski, 1991) may explain the need for pyramidal-basket intercolumnar connections. Reciprocal connections were not strictly necessary: Two columns could be synchronized with uni-directional connections from one to the other (not shown), although the synchrony obtained with this connectivity was not as strong as with reciprocal connections between the columns.

One parameter that did have a large effect on synchrony between columns was the delay time (Fig. 11). Our model predicts that two cortical areas cannot be synchronized by direct connections if the delay in those connections is significantly greater than 5 ms (~1/4 period), in agreement with previous models based on coupled oscillators (Schuster & Wagner, 1989; Sompolinsky et al., 1990). Interestingly, in the cat this does not appear to exclude any areas of cortex directly connected to each other, even if they are in opposite hemispheres. Time delays between cells in the same column, separated by 10s of μ m, are 1-2 ms due to conduction along thin, unmyelinated axons (Mason et al., 1991; Thomson et al., 1988). Time delays between cells in opposite hemispheres, separated by several cm, have been recorded at or below 5 ms due to conduction along thick, myelinated axons (McCourt et al., 1990). It would appear that the axons are organized to put cortical cells functionally next to each other. Thus, cells coupled by synchronization throughout the extent of the visual system can work on the same task simultaneously.

However, the same is not true for the cortex of the rabbit, where callosal conduction times are 10s of ms (Swadlow, 1991), too long for synchronization to work by direct connections. Thus, for this animal either there is some other mechanism of synchronization, or it does without synchronized 40 Hz activity of its two hemispheres.

The results shown in Figs. 12 and 13 are consistent with the hypothesis that the horizontal connections in neocortex serve a modulatory role; in this case they serve to synchronize cortical columns. The strong effect of surround stimulation on a neuron that is also receiving direct stimulation of its receptive field (Gilbert & Wiesel, 1990) is also consistent with a modulatory role for the long-range horizontal connections. It should be noted that recent work has suggested that these connections can be strengthened under some conditions (perhaps by sprouting of extra axon collaterals) to the point where they can indeed drive cells in the absence of other input (Pettet & Gilbert, 1992; Darian-Smith & Gilbert, 1994).

Conclusion

Synchronization in model cortical networks is a robust phenomenon resistant to variation in parameters that are known to show a wide degree of variation in cortex. As long as time delays are short enough, which in the cat seems to hold even across hemispheres, cells in any number of directly connected cortical regions could fire in synchrony with each other regardless of where they are located physically. Our model is incomplete in some respects, but the central role of inhibition in promoting synchronous activity is likely to be robust; indeed, inhibition has been shown to be crucial for synchronization in other related models (van Vreeswijk et al., 1994; Kopell & LeMasson, 1994).

References

Bernander, O., Douglas, R. J., Martin, K. A. C., & Koch, C. (1991). Synaptic background activity influences spatiotemporal integration in single pyramidal cells. *Proc. Nat. Acad. Sci.*, **88**, 11569-11573.

Borg-Graham, L. J. (1987). *Modeling the somatic electrical response of hippocampal pyramidal neurons*. M.S., MIT.

Bringuier, V., Fregnac, Y., Debanne, D., Shulz, D., & Baranyi, A. (1992). Synaptic origin of rhythmic visually evoked activity in kitten area 17 neurones. *Neuroreport.*, **3**(12), 1065-8.

Bush, P. C., & Douglas, R. J. (1991). Synchronization of bursting action potential discharge in a model network of neocortical neurons. *Neural Comp.*, **3**, 19-30.

Bush, P. C., & Sejnowski, T. J. (1993). Reduced compartmental models of neocortical pyramidal cells. *J. Neurosci. Methods*, **46**, 159-166.

Bush, P. C., & Sejnowski, T. J. (1994). Effects of inhibition and dendritic saturation in simulated neocortical pyramidal cells. *J. Neurophysiol.*, **71**(6), 2183-2193.

Connors, B. W., Malenka, R. C., & Silva, L. R. (1988). Two inhibitory postsynaptic potentials, and GABAa and GABAb receptor-mediated responses in neocortex of rat and cat. *J. Physiol.*, **406**, 443-468.

Crick, F., & Koch, C. (1990). Towards a neurobiological theory of consciousness. *Sem. Neurosci.*, **2**, 263-275.

Darian-Smith, C., & Gilbert, C. D. (1994). Axonal sprouting accompanies functional reorganization in adult cat striate cortex. *Nature*, **368**, 737-740.

Douglas, R. J., & Martin, K. A. C. (1990). Neocortex. In G. Shepherd (Ed.), *Synaptic Organization of the Brain* (pp. 220-248). New York: Oxford University Press.

Eckhorn, R., Bauer, R., Jordan, W., Brosch, M., & Kruse, W. (1988). Coherent oscillations: A mechanism for feature linking in the visual cortex. *Biol. Cybern.*, **60**, 121-30.

Engel, A. K., Koenig, P., & Singer, W. (1991a). Direct physiological evidence for scene segmentation by temporal coding. *Proc. Natl. Acad. Sci. USA*, **88**, 9136-9140.

Engel, A. K., Konig, P., Gray, C. M., & Singer, W. (1990). Stimulus-dependent neuronal oscillations in cat visual cortex: Inter-columnar interaction as determined by cross-correlation analysis. *Eur. J. Neurosci.*, **2**, 588-606.

Engel, A. K., Konig, P., Kreiter, A. K., & Singer, W. (1991b). Interhemisphric synchronization of oscillatory neuronal responses in cat visual cortex. *Science.*, **252**, 11177-79.

Gabbot, P. L. A., Martin, K. A. C., & Whitteridge, D. (1987). Connections between pyramidal neurons in layer 5 of cat visual cortex (area 17). *J. Comp. Neurol.*, **259**, 364-381.

Gilbert, C. D., Hirsch, J. A., & Wiesel, T. N. (1990). Lateral interactions in visual cortex. *Cold Spring Harbor Symposia on Quantitative Biology*, **55**, 663-677.

Gilbert, C. D., & Wiesel, T. N. (1990). The influence of contextual stimuli on the orientation selectivity of cells in primary visual cortex of the cat. *Vis. Res.*, **30**(11), 1689-1701.

Gray, C. M., Engel, A. K., Koenig, P., & Singer, W. (1992). Synchronization of oscillatory neuronal responses in cat striate cortex: Temporal properties. *Vis. Neurosci.*, **8**, 337-347.

Gray, C. M., Konig, P., Engel, A. K., & Singer, W. (1989). Oscillatory responses in cat visual cortex exhibit inter-columnar synchronization which reflects global stimulus properties. *Nature*, **338**, 334-37.

Hines, M. L. (1989). A program for simulation of nerve equations with branching geometries. *Int. J. Biomed. Comp.*, **24**, 55-68.

Hirsch, J. A., & Gilbert, C. D. (1991). Synaptic physiology of horizontal connections in the cat's visual cortex. *J. Neurosci.*, **11**(6), 1800-1809.

Jagadeesh, B., Gray, C. M., & Ferster, D. (1992). Visually evoked oscillations of membrane potential in cells of cat visual cortex. *Science.*, **257**, 552-4.

Kisvarday, Z. F., & Eysel, U. T. (1992). Cellular organization of reciprocal patchy networks in layer III of cat visual cortex (area 17). *Neurosci.*, **46**(2), 275-286.

Koch, C., Douglas, R., & Wehmeier, U. (1990). Visibility of synaptically induced conductance changes: theory and simulations of anatomically characterized cortical pyramidal cells. *J. Neurosci.*, **10**, 1728-1744.

Koenig, P., Engel, A. K., & Singer, W. (1995). Relation between oscillatory activity and long-range synchronization in cat visual cortex. *Proc. Natl. Acad. Sci. USA.*, **92**, 290-294.

Koenig, P., & Schillen, T. B. (1991). Stimulus-dependent assembly formation of oscillatory responses: I. synchronization. *Neural Comp.*, **3**, 155-166.

Komatsu, Y., Nakajima, S., Toyama, K., & Fetz, E. E. (1988). Intracortical connectivity revealed by spike-triggered averaging in slice preparations of cat visual cortex. *Brain Res.*, **442**, 359-362.

Kopell, N., & LeMasson, G. (1994). Rhythmogenesis, amplitude modulation, and multiplexing in a cortical architecture. *Proc. Natl. Acad. Sci. USA*, **91**, 10586-10590.

Kreiter, A. K., & Singer, W. (1992). Oscillatory neuronal responses in the visual cortex of the awake macaque monkey. *Eur. J. Neurosci.*, **4**, 369-75.

Llinas, R. R., Grace, A. A., & Yarom, Y. (1991). In vitro neurons in mammalian cortical layer 4 exhibit intrinsic oscillatory activity in the 10- to 50-Hz frequency range. *Proc. Natl. Acad. Sci. USA*, **88**(3), 897-901.

Lytton, W. W., & Sejnowski, T. J. (1991). Simulations of cortical pyramidal neurons synchronized by inhibitory interneurons. *J. Neurophysiol.*, **66**, 1059-1079.

Martin, K. A. C. (1988). From single cells to simple circuits in the cerebral cortex. *Q. J. Exp. Physiol.*, **73**, 637-702.

Mason, A., Nicoll, A., & Stratford, K. (1991). Synaptic transmission between individual pyramidal neurons of the rat visual cortex *in vitro*. *J. Neurosci.*, **11**(1), 72-84.

McCormick, D. A., Gray, C., & Wang, Z. (1993). Chattering cells: A new physiological subtype which may contribute to 20-60 Hz oscillations in cat visual cortex. *Soc. Neurosci. Abst.*, **19**, 359.9.

McCourt, M. E., Thalluri, G., & Henry, G. H. (1990). Properties of area 17/18 border neurons contributing to the visual transcallosal pathway in the cat. *Vis. Neurosci.*, **5**(1), 83-98.

Nicoll, A., & Blakemore, C. (1990). Dual intracellular impalement *in vitro* reveals excitatory synaptic connections between pyramidal neurons in rat visual cortex. *J. Physiol.*, 15P.

Nicoll, A., & Blakemore, C. (1993). Patterns of local connectivity in the neocortex. *Neural Comp.*, **5**, 665-680.

Pettet, M. W., & Gilbert, C. D. (1992). Dynamic changes in receptive-field size in cat primary visual cortex. *Proc. Natl. Acad. Sci. USA*, **89**, 8366-8370.

Rall, W. (1964). Theoretical significance of dendritic trees for neuronal input-output relations. In R. Reiss (Ed.), *Neural Theory and Modeling* (pp. 73-97). Stanford: Stanford University Press.

Schuster, H. G., & Wagner, P. (1989). Mutual entrainment of two limit cycle oscillators with time delayed coupling. *Prog. Theor. Phys.*, **81**(5), 939-45.

Schuster, H. G., & Wagner, P. (1990). A model for neuronal oscillations in the visual cortex. 1. Mean-field theory and derivation of the phase equations. *Biol. Cybernet.*, **64**(1), 77-82.

Silva, L. R., Amitai, Y., & Connors, B. W. (1991). Intrinsic oscillations of neocortex generated by layer 5 pyramidal neurons. *Science*, **251**, 432-435.

Singer, W. (1993). Synchronization of cortical activity and its putative role in information processing and learning. *Ann. Rev. Physiol.*, **55**, 349-374.

Somogyi, P., Kisvardy, Z. F., Martin, K. A. C., & Whitteridge, D. (1983). Synaptic connections of morphologically identified and physiologically characterized large basket cells in the striate cortex of cat. *Neurosci.*, **10**(2), 261-294.

Sompolinsky, H., Golomb, D., & Kleinfeld, D. (1990). Global processing of visual stimuli in a neural network of coupled oscillators. *Proc. Natl. Acad. Sci. USA.*, **87**(18), 7200-4.

Sporns, O., Gally, J. A., Reeke, G. N., & Edelman, G. M. (1989). Reentrant signalling among simulated neuronal groups leds to coherency in their oscillatory activity. *Proc. Natl. Acad. Sci. USA*, **86**, 7265-7269.

Sporns, O., Tononi, G., & Edelman, G. M. (1991). Modeling perceptual grouping and figure-ground separation by means of active reentrant connections. *Proc. Natl. Acad. Sci. USA*, **88**, 129-33.

Swadlow, H. A. (1991). Efferent neurons and suspected interneurons in second somatosensory cortex of the awake rabbit: Receptive fields and axonal properties. *J. Neurophysiol.*, **66**(4), 1392-1408.

Thomson, A. M., Deuchars, J., & West, D. C. (1993). Large, deep layer pyramid-pyramid single axon EPSPs in slices of rat motor cortex display paired pulse and frequency-dependent depression, mediated presynaptically and self-facilitation, mediated postsynaptically. *J. Neurophysiol.*, **70**(6), 2354-2369.

Thomson, A. M., Girdlestone, D., & West, D. C. (1988). Voltage-dependent currents prolong single-axon postsynaptic potentials in layer III pyramidal neurons in rat neocortical slices. *J. Neurophysiol.*, **60**, 1896-1907.

van Vreeswijk, C., Abbott, L. F., & Ermentrout, G. B. (1994). When inhibition not excitation synchronizes neural firing. *J. Comp. Neurosci.*, **1**(4).

White, E. L. (1989). *Cortical Circuits*. Boston: Birkhauser.

Williams, T. L. (1992). Phase coupling by synaptic spread in chains of coupled neuronal oscillators. *Science*, **258**, 662-5.

Wilson, H. R., & Cowan, J. D. (1972). Excitatory and inhibitory interactions in localized populations of model neurons. *Biophys. J.*, **12**, 1-24.

Wilson, W. A., & Bower, J. A. (1991). A computer simulation of oscillatory behavior in primary visual cortex. *Neural Comp.*, **3**, 498-509.

Winfree, A. T. (1967). Biological rhythms and the behavior of populations of coupled oscillators. *J. Theor. Biol.*, **16**, 15-42.
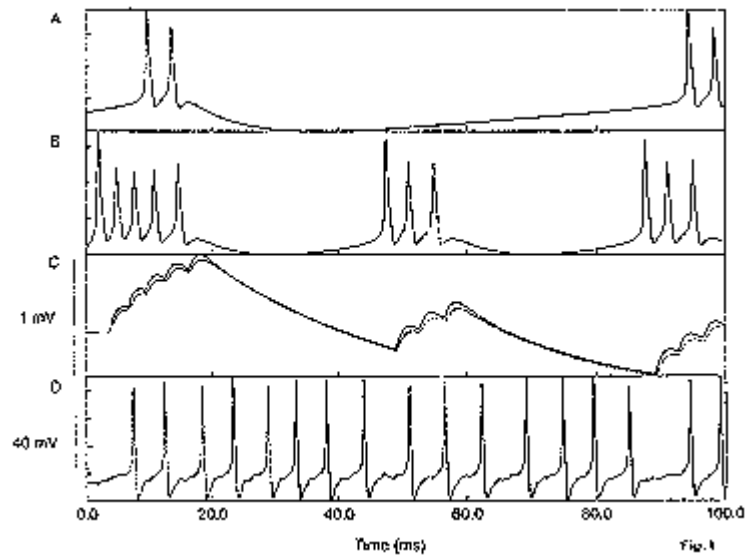
FIG. 1. Intrinsic firing properties of isolated model neurons. A) Bursting response of a pyramidal cell when injected with constant 0.2 nA depolarizing current at the soma. B) Higher frequency response to a 1 nA current. The stronger input also produces more spikes per burst. C) Postsynaptic response of a second pyramidal cell connected with a 0.5 nS synapse to the cell shown in (A). Top trace is the dendritic potential, bottom trace is the somatic potential. D) Spike train from a basket cell injected with 0.05 nA depolarizing current and +/- 0.3 nA noise (see Methods).
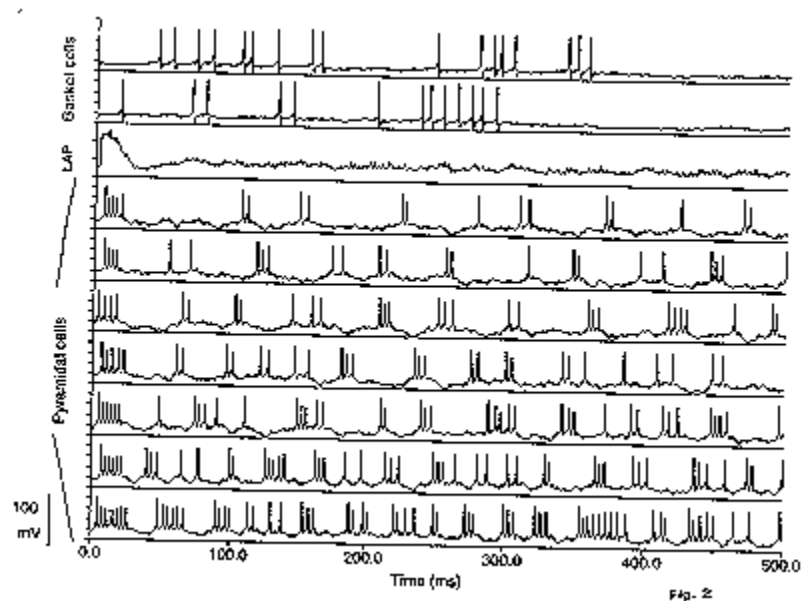
FIG. 2. Activity in models of 100 isolated layer 5 cortical neurons. The top 2 traces show the somatic membrane potential of 2 basket cells from a population of 20 making up one column. Since the driving input to the network goes only to the pyramidal cells the basket cells do not fire many spikes. The next trace is an analog of the local field potential, called the local averaged potential (LAP), to show the global synchronization of the whole column (see Methods). The flat trace shown here indicates that the neurons were not firing synchronously. The bottom 7 traces show the somatic membrane potential of 7 sample pyramidal cells from the total population of 80. In this example the intrinsic bursting frequency of the cells increases towards the bottom.
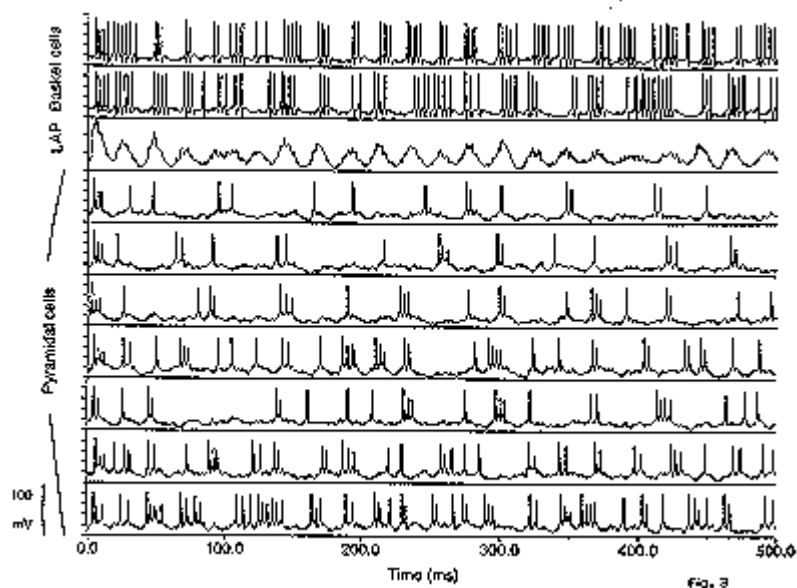
FIG. 3. Intracolumnar synchronization in a model network of neurons connected with a probability of 10%. The oscillations in the LAP shown here indicate that the neurons in the column fired synchronously. This is confirmed by the firing of the basket cells, which have no intrinsic bursting dynamics and only fire bursts in response to synchronized input from the pyramidal cells. There is considerable 'jitter' in an individual pyramidal cell's output; the network oscillation is a statistical property of the population and not at all 'clock-like'. The synchrony spontaneously disappears and reappears at 100 and 350 ms. This rapid shift has been seen in real experimental data.
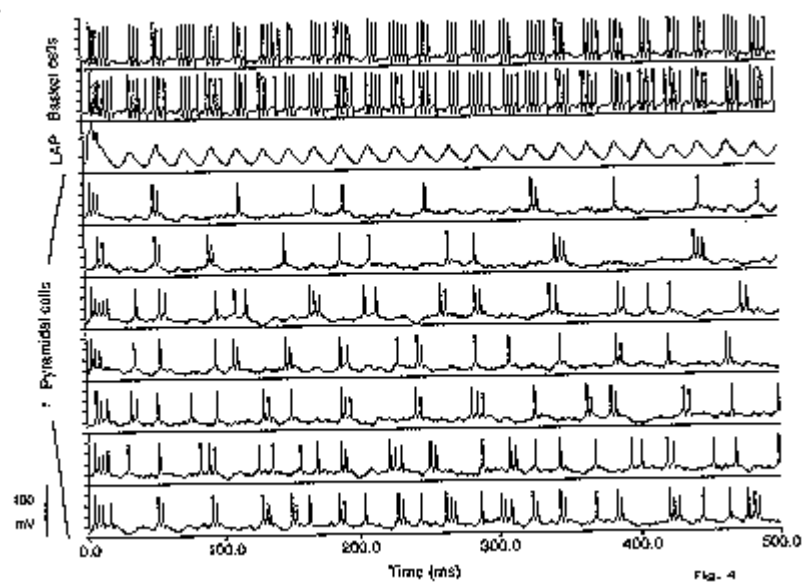
FIG. 4. Synchronization of a 1000 neuron network connected at a density of 5%. The oscillation in this network, apparent in the LAP and rhythmic bursting of the basket cells, is much more regular than that of the 100 neuron network shown in Fig. 3, although there is still significant 'jitter' in the individual pyramidal spike trains.
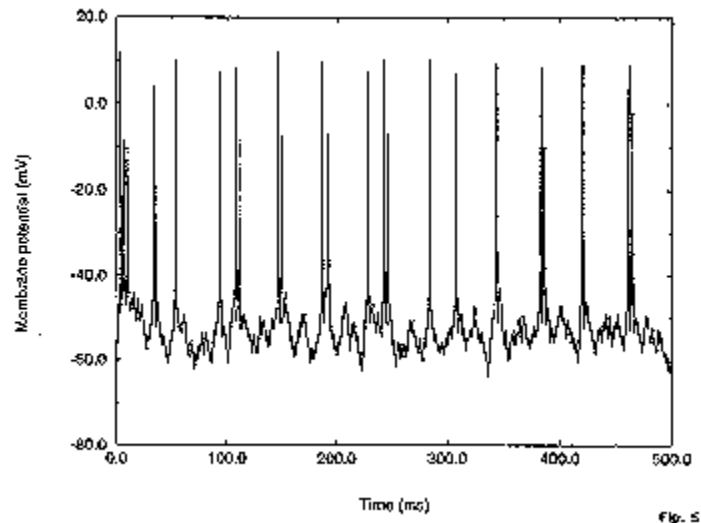
FIG. 5. Higher resolution plot of the membrane potential of the 4th pyramidal cell from Fig.4. There are a series of rhythmic compound EPSPs, some of which have spikes arising from them. Spikes do not occur at other times (in the 'troughs') because the membrane resistance is substantially reduced by a combination of inhibitory feedback and intrinsic potassium currents.

25 mV

400 msec
50 msec
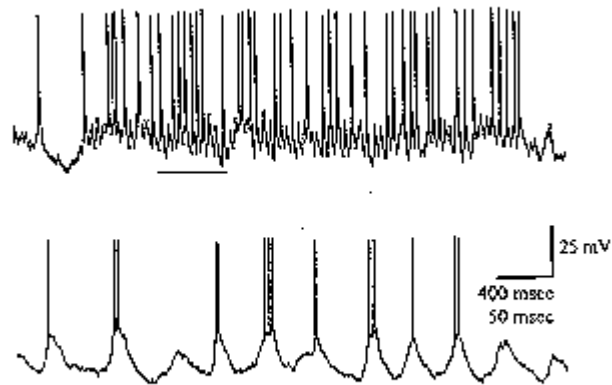
Fig. 6

FIG. 6. The response of a simple cell recorded intracellularly in area 17 of the cat to a square wave grating (1 c/deg) presented to the left eye at the optimal orientation and velocity. The data in the lower trace at higher time resolution was taken from the epoch in the upper trace that is marked by a horizontal line. The cell was tightly tuned for orientation and showed a monocular preference for the left eye. V_m = -80 mV, R_{in} = 57 MΩ. This trace shows a similar series of compound EPSPs sometimes topped by spikes as the trace in Fig. 5. It is not known whether this neuron was an intrinsically bursting cell as assumed in the model. Cell recorded by CM Gray and DA McCormick.
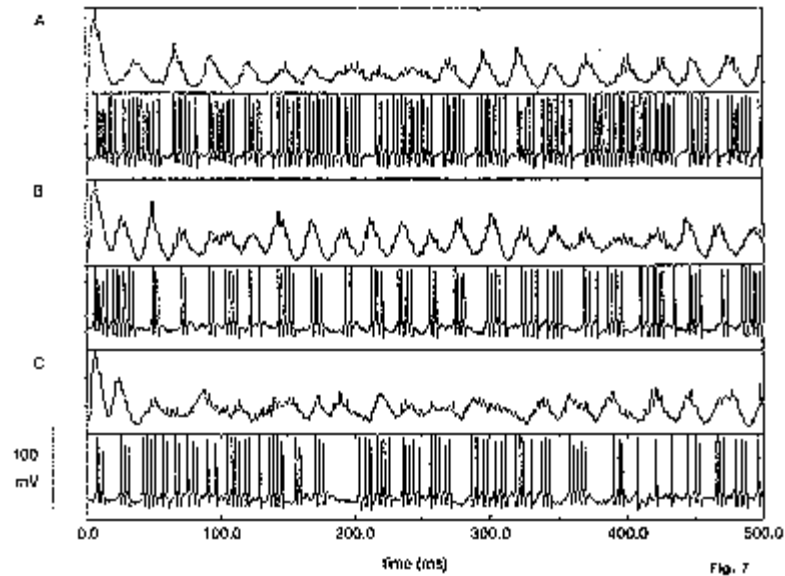
FIG. 7. Effect of increasing the strength of reciprocal inhibition between the basket cells in a 100 neuron network. Inhibition increases from top to bottom. Each trace shows the population LAP and a sample basket cell trace. A) No inhibition between basket cells. Synchronization can still occur, but is not optimal because the discharges of the basket cells on each cycle perseverate, sometimes running into the next cycle. B) Basket cells connected by 1 nS synapses. These traces are taken from Fig. 3. This is the optimal amount of mutual inhibition between basket cells in our model column. C) Basket cells connected by 2 nS synapses. Synchronization is degraded because the basket cells inhibit each other too strongly before they can fire a coherent burst and effectively terminate the burst of firing in the pyramidal cell population.

FIG. 8. Zero phase lag synchrony between two columns of 100 neurons connected with pyramidal to pyramidal and basket cell synapses at a probability of 4%. For each column a basket cell trace, 3 pyramidal cell traces and the LAP of all the pyramidal cells in that column are shown. Synchrony is rapidly established when the inter-columnar connections turn on at 100 ms and remains for the duration of the simulation. When the columns temporarily desynchronize and then resynchronize (eg. at 375 ms), they do so together.
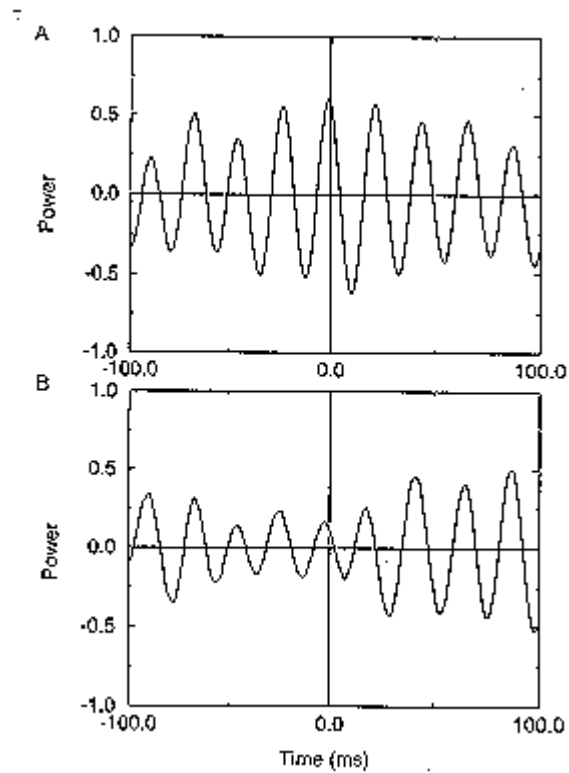
FIG. 9. Cross-correlations of the LAPs of two-column simulations. A) Results from network shown in Fig. 8. There is a large central peak centered on -2.6 ms which indicates that the two columns were oscillating in phase. B) Cross-correlation from two unconnected columns. The largest peak is at some random non-zero position indicating that these two columns were not oscillating in phase with each other.
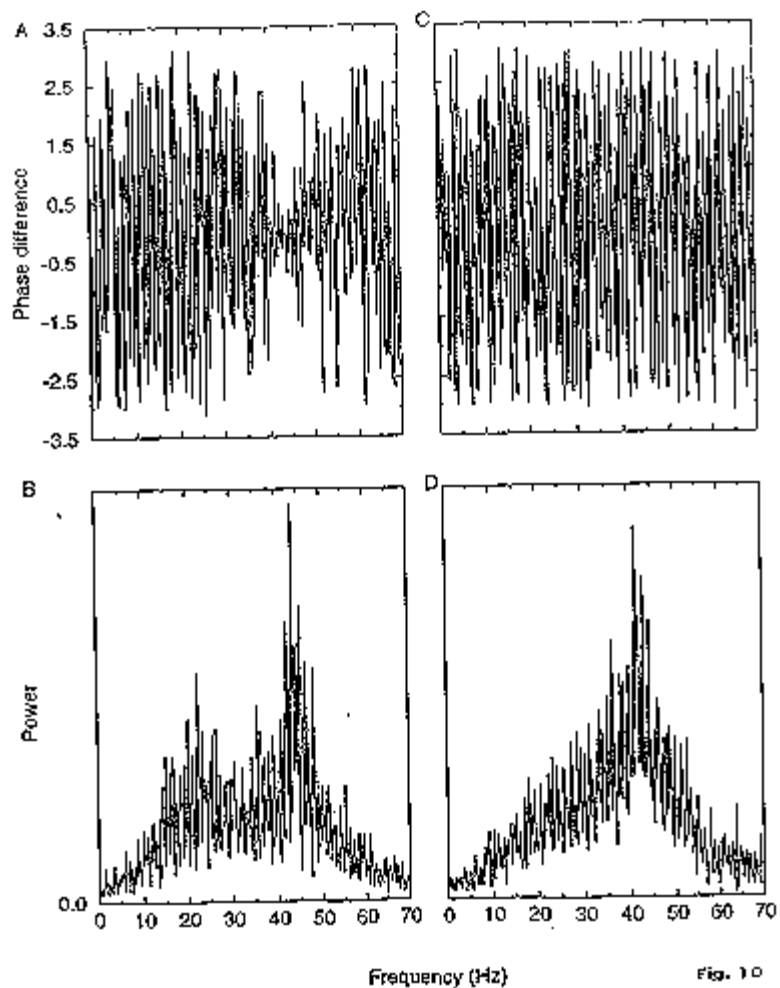
FIG. 10. Phase difference between LAPs from two-column simulations. A) Difference between the phase spectra of the LAPs over the same frequency range as in (B). The phase difference decreases to zero at 44 Hz, the oscillation frequency of the network, indicating zero-lag synchronization of the two columns. B) Averaged power spectra of the two LAPs of Fig. 8 (simulation continued for 6.5 secs). There is a large peak at 44 Hz. C) Phase difference between two LAPs from two unconnected columns. There is no decrease in the phase difference around the oscillation frequency of the two columns confirming that they are not synchronized together. D) Averaged power spectra of the two LAPs.
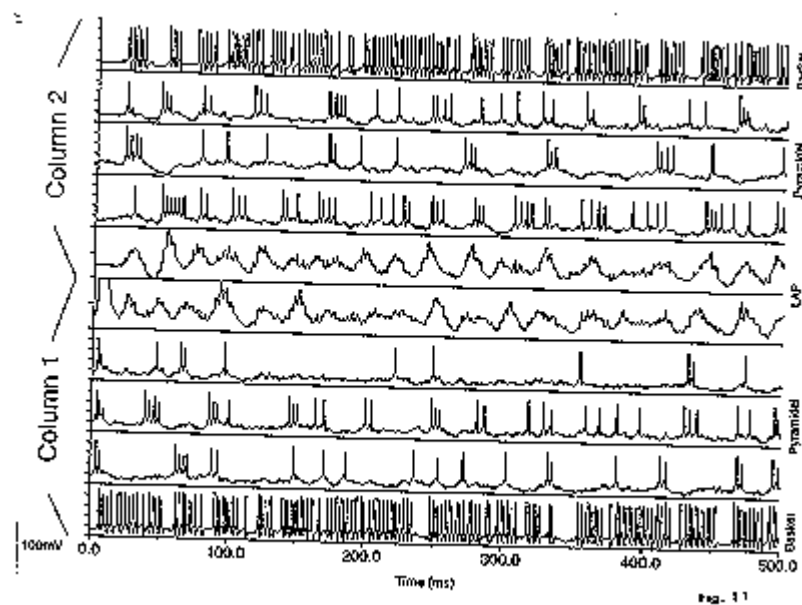
FIG. 11. Synchrony between columns is severely degraded by increasing the inter-columnar time delay. These two columns were connected by synapses that had a mean delay of 7.2 ms and turned on at 100 ms. Not only was the synchrony between the columns degraded by long time delays, but the internal synchrony within each column was also disrupted.
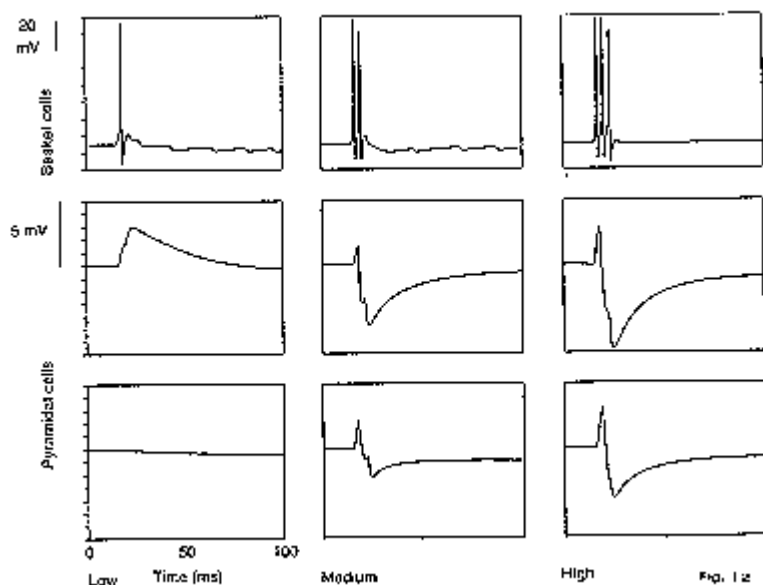
FIG. 12. Response of a sample basket cell and two representative pyramidal cells to stimulation of inter-columnar connections. Increasing from left to right, 10, 50 or 80 pyramidal cells in one column were stimulated with 0.5 nA current for 8 ms. Postsynaptic responses were recorded in the other column. Synaptic scaling factor of intercolumnar connections was reduced from 10 to 3 to allow the simulation of stimulating a small number of fibers. Weak stimuli produce an EPSP in one the pyramidal cells and a single spike in the basket cell. Stronger stimuli produce more spikes in the basket cells which cause IPSPs in the pyramidal cells, shutting off the excitatory response.
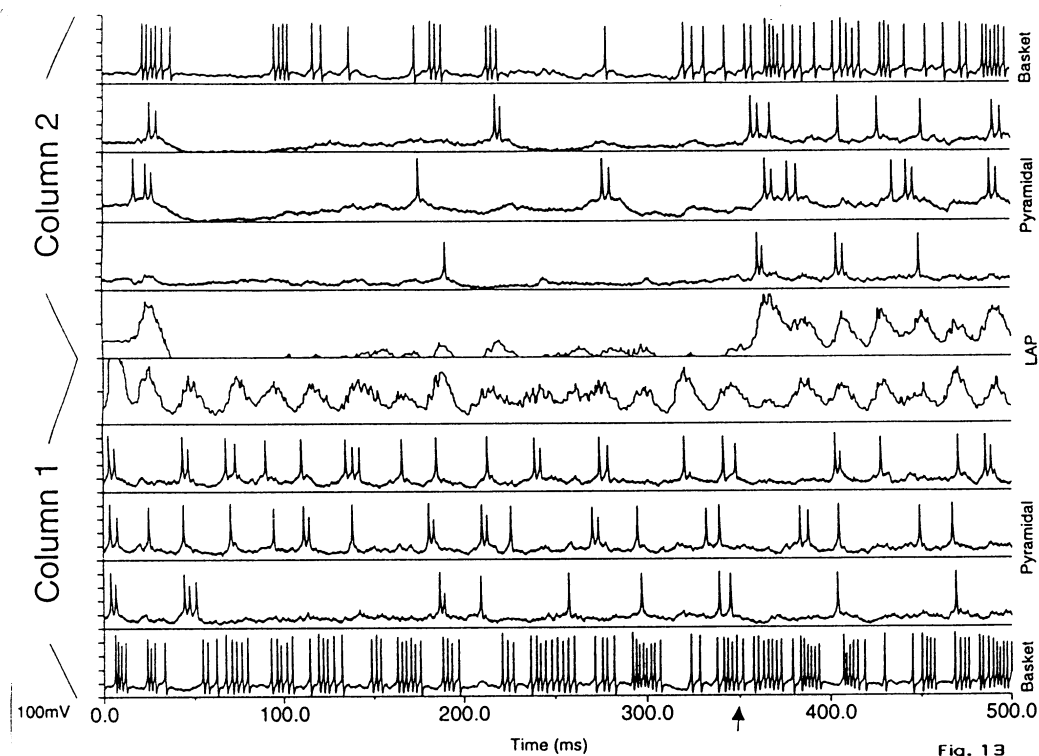
FIG. 13. Inter-columnar connections have little effect on an undriven column. The two columns shown here are connected as in Fig. 8, with the inter-columnar connections turned on at zero ms. The upper column receives no external driving input until 350 ms (arrow). After this time the two columns are synchronized by the inter-columnar connections, but before this they have very little effect on the undriven column, producing a few subthreshold depolarizations but few spikes. The basket cells have a lower threshold and fire a few spikes, which helps to suppress the pyramidal cells (see Fig. 12).